Staphylococcal Biofilms: Microstructure, Mechanics,

Self-assembly, and Multispecies Communities

by

Elizabeth Jeanne Stewart

A dissertation submitted in partial fulfillment
of the requirements for the degree of
Doctor of Philosophy
(Chemical Engineering)
in the University of Michigan
2015

Doctoral Committee:

Professor Michael J. Solomon, Co-Chair
Professor Mark A. Burns
Professor Ronald G. Larson
Professor John G. Younger

Dedication

In loving memory of my grandparents, John C. Ballow and Martha Jeanne Ballow

who celebrated love of life, family, and lifelong learning.

Acknowledgements

I would like to take the time to thank the people who have supported and encouraged me throughout the duration of my PhD. The journey to my doctorate has been filled with both highs and lows and the people who have been by my side in this journey have made all the difference.

First, I would like to thank my advisor, Mike Solomon. It is hard to put into words how grateful I am to have had the privilege to work with Mike. I joined the Solomon lab a year and a half into my PhD and it was a real turning point in my experience at University of Michigan. Mike is a diligent researcher and caring advisor who values teaching and mentoring his students. His research approach is thorough and he values the lessons learned from both expected and unexpected results. He holds us to high standards and always emphasizes the integrity of the work. He gave me the freedom to explore problems that were outside of the main skillset of the lab, which included pursuing engineering education research. He has given me countless hours of advice related to both my research and my career aspirations. He serves as a mentor and a role model. I am constantly impressed with his ability to prioritize research, teaching, advising, and his family.

John Younger, my co-advisor, is one of the most energetic and enthusiastic researchers I know. John brought a clinical perspective to the work that was extremely valuable and allowed me to begin to think about aspects of my work that may be valued in clinical practice. His

enthusiasm for projects is contagious. He is always willing to pursue collaborations, eager to recognize and thank people for their contributions, and ready to try new things. He recently took a leap in his career and became involved in a start-up company. I am encouraged by his ever-changing pursuit of new challenges. He is intentional about keeping his work interesting and exciting and that is a lesson I hope to take with me into my career. I thank John for his guidance, support and enthusiasm throughout the last five years.

Mark Burns is one of my committee members, and has served as a mentor since my first year of graduate school. I would like to thank Mark for serving on my committee and for making time for me to sit in his office to discuss my career trajectory on so many occasions. He has always been a supportive and friendly voice of reason to discuss decisions related to both my graduate school experience and career, from helping me think about choosing an advisor my first year to discussing when to begin my search for faculty positions or offering his assistance with my postdoc search. I am sure he will continue to be a mentor in years to come.

I would like to thank Ron Larson for serving on my committee and his encouragement and support over the years. Ron is an extremely bright and humble man. I first met Ron when I was taking his fluid mechanics course. Ron is a thorough researcher and seeks to understand my research to enable the best work possible. His questions have always provided me with a new perspective and helped me to clarify complex or complicated areas of my research. Ron's kind words of encouragement over the years have always been memorable to me, and carry a lot of weight. I look forward to continuing to learn from him in the future as his questions at conferences are always thought provoking and well-received by the research community.

My dissertation research has included many collaborators. First, I would like to thank Mahesh Ganesan. Mahesh and I have sat next to each other for five years, and bounced

countless ideas off one another. He and I actively co-authored one research project and I value the time we spent conducting this research together. Thank you for your thoughts and wisdom over the years, but more importantly thank you for your friendship. I would also like to thank Ashley Satorius and Prannda Sharma of the Younger lab for their valued discussions about the microbiological aspects of my projects. Jason Hammond and David Bortz at the University of Colorado helped me to understand the applicability of my research to modeling biofilms. David Payne and Blaise Boles were instrumental in helping me to create a system for investigating the multispecies behavior of *S. aureus* and *S. epidermidis* biofilms. Asish Misra of the Lahann lab was particularly helpful in instructing me in the techniques and methods of the confocal Raman microscope, and I thank him his patience, assistance and friendship.

During graduate school, I became involved with the Engineering Teaching Consultant program at the Center for Research on Learning and Teaching—Engineering (CRLT-Engin). I have learned so much about engineering education through this experience. I would like to thank Shanna Daly, Tershia Pinder-Grover, and Cindy Finelli of CRLT-Engin for the lessons that will help me become a better educator in the future. In particular, I would like to extend additional thanks to Shanna. Her help was instrumental in the success of the engineering education research included in this dissertation.

I extend my gratitude to the members of the Solomon lab for their friendship during the past five years, specifically, Aayush Shah, Mahesh Ganesan, Youngri Kim, Megan Szakasits, Ona Shemi, Joe Ferrar, Laura Colón-Meléndez, Leo Pavlovsky, and Lilian Hsiao. Thanks for your laughter and smiles to lighten up the office, mid-day walks down to get coffee, thoughts on science, assistance in the lab, moral support when research was challenging, and friendship. This would have been a very different experience without all of you.

I would like to thank my Ann Arbor friends who have become like family and made Ann Arbor feel like home. Youngri Kim is the best roommate, lab mate, and friend anyone could ask for, thank you for being your kind, caring and intelligent self. Thank you to Huanan Zhang, Chad Huelsman, Aaron Shinkle, Matt Morabito and Bobby Levine from my first year chemical engineering class. Thank you to Christine Andres, Adam Holewinski, Michael Hoepfner, Jake Dickinson, Nick Cilfone, Alex Thompson, and Mike Nelson for all the fun adventures. My Grace Ann Arbor community has brought support to my life in so many ways in the past 6 1/2 years. Thank you to Andrea Lawson for being my running partner, confidant and friend. Thank you to Min Kim, Katie Liu, Sandra Truitt, Alex Bryan, Anne Jaskot, Bryan Hogle, Nick Babij, Elizabeth Garrett, Alicia Benevides, and Pam Munson for your friendship.

Vincent Kan, thank you for loving me, sharing your life with me, and supporting me to pursue my dreams. Even though we were miles apart you were never far from my thoughts. To my grandparents, Charlotte and Hank, thank you for always loving me, supporting my education, and inspiring my love for reading and learning since my childhood. To my extended family, thank you for your love and support. To my brother, Andrew, and my sister-in-law, Hailey, thank you for your unconditional love, encouragement and friendship. To my parents, thank you for everything. There are not words that could express my gratitude for all you have given to me. I love you.

Table of Contents

List of Tables

List of Figures

Abstract

In this dissertation, we find that *Staphylococcal* biofilm microstructure is highly dependent on growth environment. Biofilms consist of structured communities of cells encapsulated in matrix materials, and are frequently responsible for clinical infections. We found that *Staphylococcus epidermidis* biofilm microstructure is heterogeneous in both unstressed and stressed (NaCl and sub-lethal vancomycin) conditions. Unstressed biofilms contained high-, medium-, and low-density phenotypes, and stressed biofilms had medium- and low-density phenotypes. High-density biofilms contained densely packed, disordered structures, while low-density biofilms contained open, porous structures.

We used our understanding of microstructure to create bacterial-chitosan constructs with high- and low-density phenotypes and creep compliances matching natural biofilms through self-assembly of cells and chitosan at pH > 7. The phase instability of chitosan controlled the mechanical behavior of these constructs. We compared the phase instability of chitosan to that of *S. epidermidis* biofilm matrix materials. Chitosan was unstable at pH > 7, while matrix materials were unstable at pH < 7. We increased the pH of a *S. epidermidis* biofilm and found that the biofilm softened at pH > 7. *S. aureus* biofilms also softened at pH > 7.

We extended our work on biofilm structure by investigating structure of multispecies biofilms of *S. aureus* and *S. epidermidis*. In multispecies biofilms, *S. aureus* is the dominant species in unstressed conditions (pH 7, 37°C), at high pH (8, 9) and at high temperature (45°C). *S. epidermidis* is the dominant species when multispecies biofilms are grown at low pH (5) and in 1.0 μg/mL vancomycin. We also investigated a label-free method for imaging *S. epidermidis* biofilm microstructure. We found that cellular microstructure was revealed using confocal Raman microscopy when samples were thin.

Overall, our understanding of biofilm microstructure aids in understanding their mechanical properties and provides ground for development of biofilm control strategies or theoretical models of biofilms. In addition to this fundamental understanding of biofilm microstructure, we investigated interdisciplinary learning in a graduate elective course on biofilms. We found that student self-perception of interdisciplinary learning outcomes related to recognizing disciplinary perspectives and teamwork skills, and interdisciplinary fluency increased over the course of the semester.

Chapter 1

Introduction

Bacterial biofilms are multicellular, surface-adherent, structured communities of cells encapsulated in matrix materials consisting of polysaccharides, proteins and DNA[1,2]. In naturally occurring environments, microbial life is commonly found in these surface-adherent structured communities of cells [2]. When biofilms form on a surface, the bacteria typically undergo a lifecycle with four steps: adhesion of the bacteria to the surface, accumulation of the bacteria and matrix components on the surface, maturation of the biofilm into a structured community, and, finally, the disassembly and dispersal of the bacteria from the biofilm [3].

Biofilms are prevalent in a variety of environments [2,4]. They form in riverbeds and streams [2] as well as in soil [5]. Industrially relevant biofilms can be problematic for operations and are frequently found within fouled pipelines [6], water distribution systems [7], and on the hulls of ships [8]. Within wastewater treatment systems, biofilms are beneficial and used to digest waste products [9].

Of particular interest is the prevalence of biofilms that live on or in the human body[2]. Bacteria frequently form biofilms on the surfaces of implanted medical devices or catheters[10]. These device-associated biofilm infections are responsible for chronic or systemic infections in

patients. The plaque on teeth also consists of microbial biofilms[11]. Dental plaques made up of biofilms cause periodontal diseases [12]. Because of the involvement of biofilms in a variety of infections and diseases, research on clinically relevant species of biofilm-forming bacteria is common.

Due to the ubiquity of biofilms on surfaces in a broad range of natural and manmade environments, biofilm research has increased in the past few decades[1]. Biofilm research in the laboratory has primarily focused on single-species communities of bacteria[13]. These research studies on individual species are used to advance both the general understanding of biofilm development as well as the behavior of a particular species. However, it is important to consider that biofilms in many natural environments grow in highly structured multispecies communities[14,15]. Thus, in addition to continuing to understand single-species communities, it is necessary to consider interactions of multiple species of bacteria when studying biofilms.

1.1 Staphylococcal biofilms

Species within the genus *Staphylococcus* are the most frequent cause of biofilm-associated infections due to the frequency that staphylococci inhabit skin and mucous surfaces[16]. In addition to the high frequency of staphylococcal infections, staphylococcal species have gained attention lately due to the development of single or multidrug resistance to antibiotics[17,18]. Vancomycin—an antibiotic that interferes with peptidoglycan synthesis in gram-positive bacteria and inhibits the formation of the bacterial cell wall[19]—is commonly used to treat *S. epidermidis* and *S. aureus* infections, including in methicillin-resistant *S. aureus* (MRSA) infections.

S. epidermidis is a gram-positive, non-motile, prominent member of the human skin flora[3,20]. It belongs to coagulase-negative staphylococci, which are distinguished from coagulase-positive staphylococci, such as *S. aureus* by their lack of the enzyme coagulase[3].

Biofilm formation is the primary virulence factor of *S. epidermidis* [21]. Since *S. epidermidis* is found within the skin microbiome, it frequently contaminates medical devices when the device is being inserted into the body. *S. epidermidis* is one of the most frequent causes of bloodstream infections in the United States[22]. When *S. epidermidis* forms biofilms in the bloodstream, they experience a wide variety of environmental conditions, including shear stresses due to blood flow ranging from 0.076-0.76 Pa[23].

Another prominent staphylococcal species is *S. aureus*. *S. aureus* is a gram positive bacteria that colonizes the nasal cavities and throats of 20-25% of the human population and 75-80% of the population is occasionally or never colonized by *S. aureus*[24]. There is a strong casual relationship between *S. aureus* nasal carriage and risk of nosocomial (hospital-acquired) infections[24]. Nasal carriage allows for *S. aureus* to spread to other areas of the body if the *S. aureus* comes into contact with the bloodstream. *S. aureus* cells invading the bloodstream are then capable of forming biofilms on tissues within the body or on medical-devices[24].

The polysaccharide portion of the biofilm matrix in both *S. epidermidis* and *S. aureus* is made up of polysaccharide intercellular adhesion (PIA)[25]. PIA is a linear homoglycan of β-1,6-linked N-acetylglucosamine[26]. The production of PIA is regulated through the *ica* operon[25]. The environmental conditions surrounding the bacteria impact the regulation of the production of PIA. One study showed that supplementing *S. epidermidis* growth media with 1-5% NaCl stimulated *ica* expression and upregulated the production of PIA[27].

S. aureus and S. epidermidis are responsible for 66% of orthopedic-associated implants[28]. Though *S. epidermidis* and *S. aureus* are typically studied as single-species biofilms, there is the

potential for *S. epidermidis* and *S. aureus* to form multispecies communities with each other at these orthopedic infection sites or on other medical devices.

1.2 Biofilm structure

Biofilm structural heterogeneity governs the microbial distribution, transport properties, local microenvironment, and mechanical properties of biofilms[29, 30]. Confocal laser scanning microscopy (CLSM) is a technique that allows for the 3D visualization of fluorescently tagged microscale features through the compilation of 2D optical sections obtained at different depths within an unaltered sample. CLSM is particularly beneficial to biofilm research, because it provides a noninvasive method to reconstruct a 3D image volume representation of the fluorescently labeled cells within a hydrated biofilm[31]. CLSM has been used in biofilm research to observe large-scale structural features, such as biovolumes, porosity, and mean thicknesses of the biofilm[32,33]. These large-scale morphological features were studied to investigate biofilm development and adaptation to change in response to environmental factors[33,34,35]. Because a large field of view has been used to observe these gross morphological features (~ 250 x 250 μm^2 or greater), the resulting images are low magnification and can not be used to investigate intercellular microstructural features of the biofilm that are 5 μm or smaller. These intercellular features are important for relating the biofilm microstructural properties to bulk mechanical properties. An additional limitation of the current method for imaging structural features of biofilms is that it requires the fluorescent labeling of the biofilm sample. Label-free imaging techniques, such as confocal Raman microscopy, may prove useful for probing biofilm structure without being dependent on the use of fluorescent stains.

1.3 Biofilms as complex fluids

Biofilms are viscoelastic materials[36-39] that can be considered analogous to colloidal composite materials[30]. Bacterial cells, which are ~ 500 nm, can be considered to be similar to colloidal particles, which are typically on the order of 1 μm, and matrix materials can be considered as similar to a viscoelastic hydrogel. In biofilms, the mechanical and transport properties of the material are dependent on the interactions between the components of the system, as is the case with attractive colloids, whose interactions produce heterogeneous, viscoelastic structures [30,40]. Thus, to understand the viscoelastic behavior of these structurally heterogeneous communities, it is necessary to determine bacterial intercellular microstructure to understand the contributions of the bacteria to the viscoelasticity of biofilms.

1.4 Techniques for assessing colloidal microstructure and dynamics

Though biofilm intercellular microstructure has not been investigated prior to the work within this dissertation, many techniques have been developed within the colloidal sciences for investigating the microstructure of colloidal systems.

CLSM images can be coupled with 3D image processing techniques to determine the location of all centroids within an image volume. Image processing in colloidal science is frequently performed using techniques based on the Crocker and Grier algorithm[41], which was developed for colloid and soft matter material characterization to determine the location of the particle centroids within an image volume. The Crocker and Grier algorithm inputs raw image data, filters out noise through the use of a Gaussian mask and a boxcar average, identifies the brightest pixel in a local region of width, *w,* and then corrects for particle location error. Using the individual particle locations, parameters can be determined such as the local number densities, radial distribution functions or cluster sizes of the particles within the volume.

In addition to static measurements performed on 3D CLSM image volumes, dynamic measurements can be made to determine the trajectories of colloidal particles within a system[42]. Using the trajectories from a dynamic time series of images, the mean squared displacement (MSD) of the particles can be computed. The MSD can be used to compute the diffusivity of the particles within the system[43]. Additionally, the MSD can be used to compute the creep compliance or the modulus of the material that the colloidal particles are embedded in[44].

1.5 Interdisciplinary learning in graduate education

To understand bacterial biofilms a research approach that incorporates skills from both engineering and microbiology produces a clearer understanding of the area. In this introduction to the field, we have already raised approaches that are at the interface of these two fields. Thus, understanding the role of interdisciplinary learning in this area is necessary for instructing graduate students or other researchers who are entering this field.

Bacterial biofilm research is just one example of interdisciplinary research. The prevalence of interdisciplinary research opportunities, and interdisciplinary programs for graduate students is increasing as research challenges begin to fall at the interface of multiple disciplines. Interdisciplinary graduate programs frequently depend on interdisciplinary coursework, seminars, retreats or workshops to provide interdisciplinary learning opportunities for students[45]. Interdisciplinarity can be defined as a way of solving problems that integrates knowledge from two or more disciplines to provide a more complete understanding of a problem that would be unlikely using methods from a single discipline alone [46-48]. While faculty may agree that interdisciplinary training for approaching problems is helpful, much of the university is structured around departments or colleges, and faculty are rarely encouraged to develop pedagogies or assessment methods related to interdisciplinary learning[49]. Therefore, assessment

methods should be implemented to determine the effect interdisciplinary components of graduate programs are having on student learning.

1.6 Research goals and organization of the dissertation

The overarching goal of this dissertation is to determine the microstructural behavior of *S. epidermidis* biofilms in unstressed and stressed growth environments and apply this knowledge to investigate the role of self-assembly in determining biofilm mechanics, the structural changes that occur in multispecies communities of *S. epidermidis* and *S. aureus,* and the effectiveness of label-free methods for imaging *S. epidermidis* biofilm microstructure. Ultimately, this microstructural understanding of biofilms will aid in the understanding of the origins of the mechanical properties of biofilms. This work can also be used to develop biofilm control strategies that could be used in clinical treatments of biofilms, or to create models of biofilm behavior including biofilm fracture and disassembly in fluid flow. In addition to the fundamental understanding of biofilm microstructure developed in this dissertation, engineering education research on interdisciplinary student learning in a graduate elective course on bacterial biofilms is reported.

In Chapter 2, we determined the typical variation in *S. epidermidis* biofilm architecture at the microscale and investigated the effect of treatment with environmental stressors (NaCl and sub-lethal vancomycin) on the spatial organization of bacteria within a biofilm. To do this, we grew biofilms in flow cells and collected high-resolution CLSM image volumes of the biofilms. After performing image processing to extract the centroids of the bacteria, we computed the local number densities, radial distribution functions, and cluster distributions of the biofilms and evaluated how these measures changed in different growth environments.

In Chapter 3, we created bacterial-chitosan constructs with microstructures and mechanics matching those of naturally grown biofilms and used these constructs to establish the role of physical self-assembly in biofilm formation. Bacterial-chitosan constructs were created from different concentrations of cells and chitosan and in different pH environments. The creep compliance of the constructs was assessed in the different pH environments. The creep compliance was found using the MSD obtained from image processing of 2D CLSM time series images. The solution properties of chitosan and biofilm matrix materials at different pH values were evaluated and compared. Using our understanding of the stability of the biofilm matrix at low and high pH, we changed the pH environment of *S. epidermidis* and *S. aureus* biofilms to alter their mechanical properties.

In Chapter 4, we extended our work on biofilm structure to determine the effect of antibiotic and physical treatments on the structural behavior of *S. epidermidis* and *S. aureus* in multispecies biofilm communities. We first considered the kinetic growth of bacteria within single and multispecies communities. Then we evaluated the effect of sub-lethal vancomycin, pH and temperature treatments on the structural behavior of each species within the multispecies communities.

The work in Chapters 2-4 was dependent on the use of CLSM to evaluate the microstructural behavior of *Staphylococcal* bacterial biofilms. In Chapter 5, we investigate a label-free method for probing biofilm structure in *S. epidermidis* biofilms. We image biofilms of various thicknesses to determine the applicability of confocal raman microscopy for investigating *S. epidermidis* biofilm microstructure.

The approach that was taken in Chapters 2-5 was interdisciplinary in that it combined tools and knowledge from both the physical sciences and microbiology to investigate biofilm microstructure. In Chapter 6, we use a graduate elective course on bacterial biofilms to assess changes in interdisciplinary learning during a single semester interdisciplinary course. Specifically, we assess student self-perception of learning outcomes related to interdisciplinarity through surveys distributed at three time points during the course and changes in interdisciplinary fluency through the coding of language related to microbiology and engineering in open-ended assignments administered at two time points during the course.

Finally, we discuss the overall conclusions and future work that could be investigated as a result of the body of work included in this dissertation.

1.7 References

(1) Costerton, J. W.; Stewart, P. S.; Greenberg, E. P. *Science* **1999**, *284*, 1318-1322.

(2) Hall-Stoodley, L.; Costerton, J. W.; Stoodley, P. *Nature Reviews Microbiology* **2004**, *2*, 95-108.

(3) Otto, M. *Nature Reviews Microbiology* **2009**, *7*, 555-567.

(4) Costerton, J. W.; Cheng, K. J.; Geesey, G. G.; Ladd, T. I.; Nickel, J. C.; Dasgupta, M.; Marrie, T. J. *Annual Reviews in Microbiology* **1987**, *41*, 435-464.

(5) Davey, M. E.; O'toole, G. A. *Microbiology and molecular biology reviews* **2000**, *64*, 847-867.

(6) Barton, A. F.; Wallis, M. R.; Sargison, J. E.; Buia, A.; Walker, G. J. *Journal of Hydraulic Engineering* **2008**, *134*, 852-857.

(7) Donlan, R. M.; Pipes, W. O.; Yohe, T. L. *Water Research* **1994**, *28*, 1497-1503.

(8) Schultz, M. P.; Bendick, J. A.; Holm, E. R.; Hertel, W. M. *Biofouling* **2011**, *27*, 87-98.

(9) Nicolella, C.; Van Loosdrecht, M. C. M.; Heijnen, J. J. *Journal of biotechnology* **2000**, *80*, 1-33.

(10) Costerton, J. W.; Montanaro, L.; Arciola, C. R. *The International journal of artificial organs* **2005**, *28*, 1062-1068.

(11) Marsh, P. D. *Journal of Clinical Periodontology* **2005**, *32*, 7-15.

(12) Pihlstrom, B. L.; Michalowicz, B. S.; Johnson, N. W. *The Lancet* **2005**, *366*, 1809-1820.

(13) Kolter, R.; Greenberg, E. P. *Nature* **2006**, *441*, 300-302.

(14) O'Toole, G.; Kaplan, H. B.; Kolter, R. *Annual Reviews in Microbiology* **2000**, *54*, 49-79.

(15) Stoodley, P.; Sauer, K.; Davies, D. G.; Costerton, J. W. *Annual Reviews in Microbiology* **2002**, *56*, 187-209.

(16) Otto, M. *Curr Top Microbiol Immunol* **2008**, *322*, 207-228.

(17) Enright, M. C.; Robinson, D. A.; Randle, G.; Feil, E. J.; Grundmann, H.; Spratt, B. G. *Proceedings of the National Academy of Sciences* **2002**, *99*, 7687-7692.

(18) Raad, I.; Alrahwan, A.; Rolston, K. *Clinical infectious diseases* **1998**, *26*, 1182-1187.

(19) Gbejuade, H. O.; Lovering, A. M.; Webb, J. C. *Acta orthopaedica* **2014**, *85*.

(20) Ziebuhr, W.; Hennig, S.; Eckart, M.; Kränzler, H.; Batzilla, C.; Kozitskaya, S. *International journal of antimicrobial agents* **2006**, *28*, 14-20.

(21) Fey, P. D.; Olson, M. E. *Future microbiology* **2010**, *5*, 917-933.

(22) Wisplinghoff, H.; Bischoff, T.; Tallent, S. M.; Seifert, H.; Wenzel, R. P.; Edmond, M. B. *Clinical Infectious Diseases* **2004**, *39*, 309-317.

(23) Loscalzo, J.; Schafer, A. I. *Thrombosis and hemorrhage*; Williams & Wilkins: 1998.

(24) Archer, N. K.; Mazaitis, M. J.; Costerton, J. W.; Leid, J. G.; Powers, M. E.; Shirtliff, M. E.

Virulence **2011**, *2*, 445-459.

(25) O'Gara, J. P. *FEMS microbiology letters* **2007**, *270*, 179-188.

(26) Ganesan, M.; Stewart, E. J.; Szafranski, J.; Satorius, A. E.; Younger, J. G.; Solomon, M. J. *Biomacromolecules* **2013**, *14*, 1474-1481.

(27) Rachid, S.; Ohlsen, K.; Witte, W.; Hacker, J.; Ziebuhr, W. *Antimicrobial agents and chemotherapy* **2000**, *44*, 3357-3363.

(28) Campoccia, D.; Montanaro, L.; Arciola, C. R. *Biomaterials* **2006**, *27*, 2331-2339.

(29) Renslow, R.; Lewandowski, Z.; Beyenal, H. *Biotechnology and bioengineering* **2011**, *108*, 1383-1394.

(30) Wilking, J. N.; Angelini, T. E.; Seminara, A.; Brenner, M. P.; Weitz, D. A. *MRS bulletin* **2011**, *36*, 385-391.

(31) Dunne, W. M. *Clinical microbiology reviews* **2002**, *15*, 155-166.

(32) Xavier, J. B.; White, D. C.; Almeida, J. S. *Water Science & Technology* **2003**, *47*, 31-37.

(33) Beyenal, H.; Donovan, C.; Lewandowski, Z.; Harkin, G. *Journal of microbiological methods* **2004**, *59*, 395-413.

(34) Heydorn, A.; Nielsen, A. T.; Hentzer, M.; Sternberg, C.; Givskov, M.; Ersbøll, B. K.; Molin, S. *Microbiology* **2000**, *146*, 2395-2407.

(35) McLean, J. S.; Ona, O. N.; Majors, P. D. *The ISME journal* **2007**, *2*, 121-131.

(36) Stoodley, P.; Lewandowski, Z.; Boyle, J. D.; Lappin‐Scott, H. M. *Biotechnology and Bioengineering* **1999**, *65*, 83-92.

(37) Towler, B. W.; Rupp, C. J.; Cunningham, A. L. B.; Stoodley, P. *Biofouling* **2003**, *19*, 279-285.

(38) Hohne, D. N.; Younger, J. G.; Solomon, M. J. *Langmuir* **2009**, *25*, 7743-7751.

(39) Pavlovsky, L.; Younger, J. G.; Solomon, M. J. *Soft Matter* **2013**, *9*, 122-131.

(40) Zaccarelli, E. *Journal of Physics: Condensed Matter* **2007**, *19*, 323101.

(41) Crocker, J. C.; Grier, D. G. *Journal of colloid and interface science* **1996**, *179*, 298-310.

(42) Dibble, C. J.; Kogan, M.; Solomon, M. J. *Physical Review E* **2006**, *74*, 041403.

(43) Berg, H. C. *Random walks in biology*; Princeton University Press: 1993.

(44) Squires, T. M.; Mason, T. G. *Annual Review of Fluid Mechanics* **2009**, *42*, 413.

(45) Borrego, M.; Cutler, S. *Journal of Engineering Education* **2010**, *99*, 355-369.

(46) Mansilla, V. B. *Change: The Magazine of Higher Learning* **2005**, *37*, 14-21.

(47) Borrego, M.; Newswander, L. K. *The Review of Higher Education* **2010**, *34*, 61-84.

(48) Lattuca, L. R.; Trautvetter, L. C.; Codd, S.; Knight, D. B. *Proceedings of the 118th Annual Conference of the American Society for Engineering Education, Vancouver, BC, Canada*. **2011**.

(49) McNair, L. D.; Newswander, C.; Boden, D.; Borrego, M. *Journal of Engineering Education* **2011**, *100*, 374-396.

Chapter 2

Role of Environmental and Antibiotic Stress on *Staphylococcus epidermidis* Biofilm Microstructure*

2.1 Abstract

Cellular clustering and separation of *Staphylococcus epidermidis* surface adherent biofilms were found to depend significantly on both antibiotic and environmental stress present during growth under steady flow. Image analysis techniques common to colloidal science were applied to image volumes acquired with high-resolution confocal laser scanning microscopy to extract spatial positions of individual bacteria in volumes of size ~ 30 x 30 x 15 μm^3. The local number density, cluster distribution, and radial distribution function were determined at each condition by analyzing the statistics of the bacterial spatial positions. Environmental stressors of high osmotic pressure (776 mM NaCl) and sub-lethal antibiotic dose (1.9 μg/mL vancomycin) decreased the average bacterial local number density 10-fold. Device-associated bacterial

* The text in this chapter was originally published in [E.J. Stewart, A.E. Satorius, J.G. Younger, & M.J. Solomon, *Langmuir* **2013**, *29,* 7017-7024].

biofilms are frequently exposed to these environmental and antibiotic stressors while undergoing flow in the bloodstream. Characteristic density phenotypes associated with low, medium and high local number densities were identified in unstressed *S. epidermidis* biofilms, while stressed biofilms contained medium- and low-density phenotypes. All biofilms exhibited clustering at length scales commensurate with cell division (~1.0 μm). However, density phenotypes differed in cellular connectivity at the scale of ~ 6 μm. On this scale, nearly all cells in the high- and medium-density phenotypes were connected into a single cluster with a structure characteristic of a densely packed disordered fluid. However, in the low-density phenotype, the number of clusters was greater, equal to 4% of the total number of cells, and structures were fractal in nature with $d_f = 1.7 \pm 0.1$. The work advances the understanding of biofilm growth, informs the development of predictive models of transport and mechanical properties of biofilms, and provides a method for quantifying the kinetics of bacterial surface colonization as well as biofilm fracture and fragmentation.

2.2 Introduction

Bacterial biofilms are multi-cellular, surface-adherent, structured communities of cells encapsulated in a polysaccharide matrix. Biofilm formation occurs when bacteria shift from a planktonic phenotype to a sessile phenotype—an observable trait resulting from an organism's gene regulation, environmental factors, and interactions between the two. These bacterial communities are known to be structurally heterogeneous [1, 2, 3], and are found in a variety of clinical, industrial, and environmental settings. Biofilms can be viewed as a biocolloidal composite material consisting of bacterial cells as the colloidal particles, and matrix materials such as polyintercellular adhesion (PIA), proteins and DNA as the viscoelastic hydrogel [4]. The interactions at the interface of these components determine the mechanical properties and

behavior of the composite material, similar to the way in which the elasticity of attractive colloidal systems such as gels, networks and glasses is determined by the statistical configuration of particles [5]. There is also evidence suggesting that the mechanical properties of biofilms are strongly dependent on the intercellular microstructure, primarily due to the heterogeneity of the biofilm structure [6, 7]. Such mechanical properties and how they vary in different environments plays an important role in the accumulation, maturation, and dispersion stages of the biofilm life cycle [4,8, 9, 10].

Confocal laser scanning microscopy (CLSM) is a useful tool for quantifying the microstructure of biofilms because it provides a nondestructive method to image a 3D volume of cells within a mature, hydrated biofilm [11]. CLSM has previously been used to observe heterogeneity of gross morphological features during biofilm development and adaptation [12, 13, 14, 15]. Because a large field of view (~ 250 x 250 μm^2 or greater) is used to observe such gross morphology, the resulting images are low magnification. This low magnification does not resolve the intercellular features of the biofilm microstructure that are displayed at 5 μm scales and smaller, and which are important to the aforementioned questions of biofilm rheology and permeability.

More recently, high-resolution CLSM methods have been identified as valuable tools to address fundamental questions about the intercellular microstructure of biofilms and their components [16, 17]. Here, we define the intercellular microstructure as the spatial organization of biofilm cells on length scales from ~ 0.5 μm up to 5.0 μm. This scale is observable by means of high resolution CLSM imaging, which can resolve submicron features of biofilms. Moreover, analyzing biofilms at this resolution potentially quantifies morphological features mediated by

the effects of cell division, extracellular matrix synthesis, and diffusive transport (e.g., of oxygen, nutrients, antibiotics, quorum sensing molecules) [2].

When equipped with high numerical aperture objectives, CLSM yields sub-micron resolution for characterizing the many body interactions at the 0.5 – 5.0 μm scale. However, quantitative analysis of the CLSM images requires image analysis methods that determine the intercellular microstructure of biofilms by characterizing cellular locations. These strategies can be adapted from work in colloidal and materials science [18, 19, 20]. These techniques describe structural features by determining statistical measures such as: the number of bacteria per unit volume (i.e., the number density); the variation in spacing between cells; the probability of finding a bacterium at some distance from a reference bacterium (i.e., the radial distribution function); the spatial clustering (or clumpiness) of a collection of individual cells (i.e., the cluster distribution). These measures quantify, in a statistically well-defined way, the phenotypic differences that arise among strains, species, and environmental conditions in biofilms. They also connect to a large collection of theories, tools, and techniques in the physical sciences that already exist to study materials at a microscopic level [21].

Bacterial biofilm infection and surface colonization is a major complication of medical device procedures. *Staphylococcus epidermidis*—a prominent member of normal human skin flora, and a primary cause of complications for patients with medical implants [22]— was chosen as the model organism for our studies. As with other biofilm-associated infections, *S. epidermidis* causes disease and device failure by establishing a surface-adherent viscoelastic composite of cells and secreted polymers that resist treatment with antibiotics. As such, these living structures share much in common with other colloidal systems, a fact underscored by recent application of such methodologies to understand single cell properties [23, 24], and the

interactions of cells with surfaces [25, 26, 27]. Our work extends this approach to include the multi-cellular properties of bacterial communities. This multicellular perspective is critical to understanding how these short-range physical and chemical properties contribute to the gross mechanical behavior of bacterial biofilms that many groups have characterized [28, 29, 30].

Here, we combine CLSM with image analysis methods to locate individual bacteria with submicron resolution and, thereby, statistically characterize the microscopic structure of *S. epidermidis* biofilms. These measures specifically address the following two questions: First, what is the typical variation in *S. epidermidis* biofilm architecture at the microscale as quantified by the colloidal measures of number density, radial distribution function, and cluster distribution? Second, does treatment with environmental stressors, such as increased salinity or sub-lethal antibiotic dosage, affect the soft matter organization of biofilms at this short length scale through a general or stress-specific response?

2.3 Materials and Methods

2.3.1 Bacterial biofilm growth conditions

S. epidermidis RP62A was obtained from American Type Culture Collection (ATCC 35984). Each experiment began with an overnight culture grown in tryptic soy broth (TSB). 1 mL of the overnight culture with 9 mL of TSB with 1% glucose was injected into one channel of a 40 mm x 4 mm x 1 mm flow cell with the inlet and outlet located on opposite ends of the 4 mm flow cell width (Stovall Life Sciences, Peosta, IA), and allowed to incubate without flow at 37°C for one hour. Flow cells were then perfused with media at 37ºC at 0.5 mL/min, Re = 4,which induced a shear stress of 0.01 Pa along the floor of the flow cell. These conditions were chosen to represent

common non-turbulent flow regimes (e.g., venous blood, cerebral spinal fluid, urine) within the human body [31, 32, 33].

Each biofilm was grown within a flow cell for 24 hours with TSB and 1% glucose in the unstressed condition (86 mM NaCl) and TSB and 1% glucose with either 136 mM NaCl, 776 mM NaCl, or 1.9 μg/mL vancomycin growth media in the stressed conditions. 24 hours was chosen as the period for growth because after 24 hours bacteria have colonized the surface and biofilms have developed well beyond the initial period of attachment [34]. 1% glucose was added to all growth media, because glucose supplemented media has been shown to induce the expression of the biofilm positive phenotype of *S. epidermidis* [35, 36]. Unadjusted TSB contains 86 mM NaCl. To induce osmotic stress, we increased TSB salinity to 136 mM NaCl (representative of human extracellular fluid), and 776 mM NaCl (4% NaCl, a concentration of NaCl known to increase the production of PIA [37, 38]). To evaluate vancomycin-associated stress, 1.9 μg/mL vancomycin was used, which our preliminary results and published reports confirmed was 95% of the minimum inhibitory concentration (MIC) for RP62A [39]. Four different flow cell biofilms were grown for each experimental condition in separate experimental runs.

2.3.2 Confocal Laser Scanning Microscopy

After 24-hour growth, biofilms were stained with 10 μM Syto9 (Invitrogen, Carlsbad, CA) for 60 minutes. From each flow cell experiment, five CLSM image volumes were obtained using a Leica SP2 CLSM with a 100x, 1.4 NA, oil immersion objective lens. The excitation wavelength was 488 nm. Image volumes were of size 30 μm x 30 μm in the objective plane parallel to the shearing surface, and 6 to 25 μm in the direction perpendicular to the shearing surface. The latter dimension was varied to accommodate differences in the biofilm thickness. The shear surface was always the lower bound of the image volume. All image voxels were 60

nm x 60 nm x 60 nm. The five image volumes were collected in the shape of a cross, centered across the width of the flow cell. The spacing between each imaged volume was 100 μm and all measurements were taken in the 10 mm nearest the flow cell inlet. We image near the center of the inlet to ensure nutrient depletion has not occurred as flow traverses the length of the flow cell and to require that we have minimal effects of flow instabilities that commonly exist at the corners of the expansion flow into the cell.

2.3.3 Image Analysis

Image analysis of raw CLSM image stacks was performed to determine the collective structure of the biofilm. Our image processing resolves the spatial position of all bacteria within each image volume with sub-100 nm resolution. The method, based on the work of Crocker and Grier [18], resolves the location of all bacterium geometric centroids within an image volume to within ±35 nm in the object plane and ±45 nm in the axial plane [19]. The error of statistical measures from the image analysis, such as the number density, is less than 3% [40]. This method inputs raw image data, filters out noise through the use of a Gaussian mask, identifies the brightest voxel in a local region of width, *w,* and then corrects for bacterium location error. The performance on the method was verified by confirming that all bacteria were correctly identified within sub-regions of an image volume. Results for one such sub-region are reported in Figure 2-1. The 3D coordinates of all the bacteria in the image volume were rendered in POV-Ray, a ray-tracing program (POV-Ray, Persistence of Vision Raytracer [http://www.povray.org]).

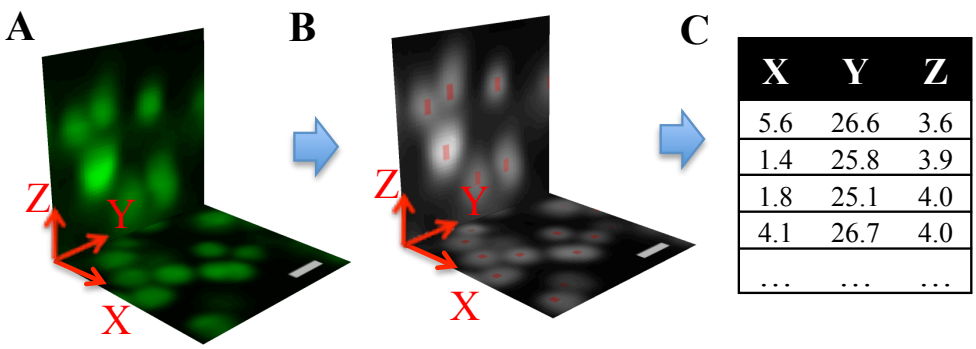

X	Y	Z
5.6	26.6	3.6
1.4	25.8	3.9
1.8	25.1	4.0
4.1	26.7	4.0
…	…	…

Figure 2-1: Determination of bacterium centroid locations using CLSM coupled with image analysis. (A) Two perpendicular image sections taken from the 3D CLSM image volume. (B) Bacterium centroid locations identified within the two perpendicular image slices by image processing. Centroids are indicated in red. (C) List of centroid coordinates (in µm) identified in B. Scale bars: 1 µm. This figure was originally published in [E.J. Stewart, A.E. Satorius, J.G. Younger, & M.J. Solomon, *Langmuir* 2013, *29*, 7017-7024].

2.3.4 Quantification of spatial organization

The local number density, the cluster distribution, the radial distribution function, and the dimensionality of fractal structures were determined from the coordinates of the identified bacteria. The local number density is the number of bacteria per unit volume within the imaged region of the biofilm.

To quantify spatial clustering, all cells in an imaged volume were grouped according to the following definition: (i) all members of a group were separated from at least one other member of the group by no more than a critical distance r_c, the cluster cutoff distance; (ii) each member of a group was separated from all other members of all other groups by at least that same critical distance r_c. That is, all bacteria in a cluster share at least one link with another bacteria within the same cluster, and no links with bacteria in other clusters. The definition is shown figuratively in Figure 2-5a. Clusters were identified according to the method of Lu et al.

[41]. The cluster distribution was reported as the ratio of the number of clusters for a given r_c to the total number of bacteria within the image volume.[†]

The radial distribution function, a common structural measure from statistical mechanics, is defined as the probability of finding a bacterium at a distance, r, from a reference bacterium at the origin. It is computed as in Allen and Tildesley [42].

For phenotypes with fractal structure, the fractal dimension, d_f, was determined by a power-law fit of the average radial distribution function from $2R < r < 10R$, where R is 320 nm, the average radius of *S. epidermidis* RP62A [43]. In this region, the radial distribution function is related to the fractal dimension through the relationship, $g(r) \sim r^{df-3}$ [44, 45].

2.3.5 Statistical analysis

Bacterial number density results were analyzed with one-way ANOVA when examining differences between different levels of osmotic stress. Vancomycin effects were compared to the 86 mM NaCl condition with unpaired two-tailed t-tests. Comparison of the clustering and radial distribution functions between experimental groups was carried out using spline-based general additive models as used previously for spatial characterization of bacterial aggregate geometry [16], and as outlined in the *mgcv* package in R 2.15.1 (Wood, S., R Foundation for Statistical Computing [http://www.r-project.org/index.html]).

2.4 Results

Unstressed *S. epidermidis* biofilms grown in flow cells exhibited heterogeneous structure on multiple length scales, as reported in Figure 2-2. Figure 2-2A shows the heterogeneity across

[†] R. Newman and L. C. Hsiao developed the cluster distribution program used in this analysis.

the width of the flow cell at the millimeter length scale, as indicated by stereoscopic imaging. Figure 2-2B shows the spatial heterogeneity observed when using a 10x, 0.3 NA objective; Figure 2-2C shows the spatial heterogeneity when using a 40x, 0.95 NA objective. The images indicate that these biofilms, consistent with the literature [12, 13, 14, 15], display a hierarchy of structures of dimension 200 microns and smaller. Using 10x microscopy and COMSTAT [14], we find that the unstressed biofilm thickness is ~ 200 microns and that the available biovolume is ~ 90 $\mu m^3/\mu m^2$.

Here we probe a finer length scale, and thereby show that *S. epidermidis* biofilm architecture is heterogeneous at scales <5 μm, as shown in Figure 2-2D. This length scale of our 3D imaging is an order of magnitude smaller than those typically reported for biofilm images. Figure 2-2C is a single image slice from an image volume used for image processing. Figure 2-2E shows renderings of all bacterial centroids identified within the entire CLSM volume that the slice in Figure 2-2D was taken from. These centroids were used to quantify intercellular biofilm structural heterogeneity. CLSM, as these short length scales (<5 μm) revealed highly varied cellular density in healthy, unstressed S. *epidermidis* biofilms. The range of local number densities varied significantly with local number densities varying from 0.02-0.41 cells/μm^3, and with a mean of 0.19 ± 0.03 cells/μm^3.

Bacterial local number densities decreased with increased osmotic stress, an environmental stress added to the growth environment of the bacteria. The average local number density decreased to 0.09 ± 0.01 cells/μm^3 for biofilms grown in 136 mM NaCl, and further decreased to 0.020 ± 0.003 cells/μm^3 for biofilms grown in 776 mM NaCl. Thus, high osmotic stress decreased average bacteria local number density 10-fold.

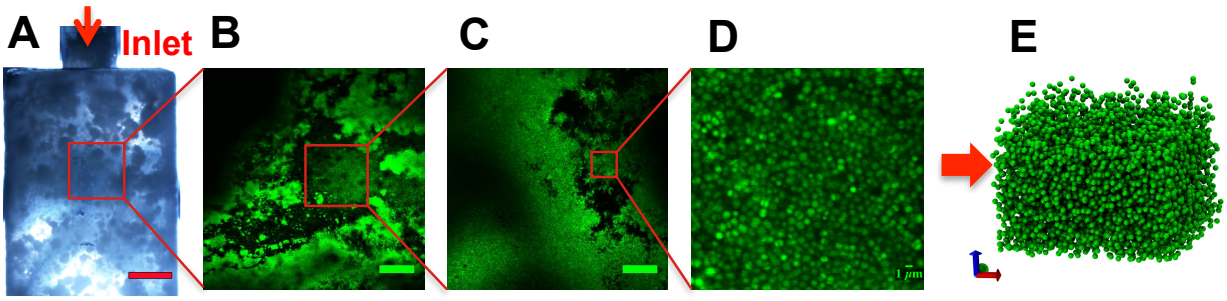

Figure 2-2: Multi-scale structure of *S. epidermidis* biofilms. A) Stereoscope image of heterogeneous biofilm structure across flow cell inlet. Flow through the device results in a wall shear stress of 0.01 Pa. Scale bar: 1 mm. B) Single slice of a large microscale, 1270 µm x 1270 µm x 224 µm CLSM image volume taken with a 10x, 0.3 NA objective. Scale Bar: 200 µm. C) Single image of a 317 µm x 317 µm x 26 µm CLSM volume at a length scale typical for gross structural studies taken with a 40x, 0.95 NA objective. Scale Bar: 50 µm. D) Single CLSM slice from 3D image volume of *S. epidermidis* biofilm rendered in panel E. Scale Bar: 1 µm. E) 3D rendering of bacterial coordinates representing the 3D intercellular microstructure of the entire volume from image section of D. This figure was originally published in [E.J. Stewart, A.E. Satorius, J.G. Younger, & M.J. Solomon, *Langmuir* 2013, *29*, 7017-7024].

The variability of the range of local number densities also decreased as osmotic stress increased. Plotting histograms of the data reveals this decrease in variability, as reported in Figure 2-3. As demonstrated by the variation in these plots, heterogeneity in local number density is apparent within all osmotic stress conditions; however, high-density regions of growth are excluded as stress is increased as represented by the decrease in number of bins. Although high cellular densities are not achieved with added stressors, biofilm growth is still present. This observation indicates that PIA or other matrix components contribute significantly to biofilm formation when environmental stressors are present. Therefore, the control variable of osmotic stress is able to induce differences in biofilm cellular morphology. Numerical values of averages and ranges at the different stress conditions studied are reported in Table 2-1.

Table 2-1: Average local number density values and range of local number density values for each growth condition. This table was originally published in [E.J. Stewart, A.E. Satorius, J.G. Younger, & M.J. Solomon, *Langmuir* 2013, *29,* 7017-7024].

Environmental Condition	Average local number density (cells/μm^3)	Range of local number densities (cells/μm^3)
86 mM NaCl	0.19 ± 0.03	0.02-0.41
136 mM NaCl	0.09 ± 0.01	0.02-0.19
776 mM NaCl	0.02 ± 0.003*	0.005-0.04
1.9 μg/mL Vancomycin	0.02 ± 0.006**	0.003-0.11

* $p < 0.01$ for increasing salinity by one-way ANOVA.
** $p < 0.01$ for vancomycin versus 86 mM NaCl by unpaired t-test.

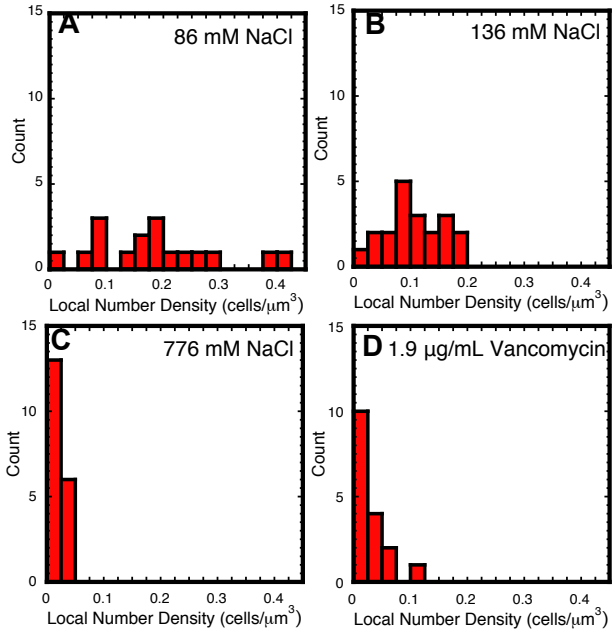

Figure 2-3: Heterogeneity of number densities decreases with increasing environmental stress. Histograms of local number density data for: A) 86 mM NaCl, B) 136 mM NaCl, C) 776 mM NaCl, and D) 1.9 μg/mL vancomycin. This figure was originally published in [E.J. Stewart, A.E. Satorius, J.G. Younger, & M.J. Solomon, *Langmuir* 2013, *29,* 7017-7024].

Bacterial local number densities decreased with vancomycin stress. With a sub-lethal vancomycin stress, the average local number density is 0.02 ± 0.01 cells/μm^3. However, and as indicated by the histograms in Figure 2-2D, the variability in local number densities decreased, compared to the unstressed growth condition, when stressed with vancomycin. Thus, we found that both osmotic and sub-lethal vancomycin stress decreased average local number density of cells within the biofilm, but did not eradicate biofilm growth.

Three general density phenotypes—low (Density Phenotype I), medium (Density Phenotype II) and high (Density Phenotype III) local number density phenotypes—were identified. Due to the variation in local number densities present in unstressed biofilms, we categorized the measured local number densities into three density phenotype regions: the low-density phenotype (I) is from 0-0.06 cells/μm^3; the medium density phenotype (II) is from 0.06-0.20 cells/μm^3; and the high-density phenotype (III) is from 0.20-0.41 cells/μm^3. We established the range of each phenotype by considering the entire range of local number densities that could be achieved by both unstressed and stressed biofilms and empirically determining two divisions within the data. The first division was the maximum density observed at the most stressed condition of 776 mM NaCl, which was about 0.06 cells/μm^3. This limit was taken as the upper bound of the low-density phenotype for all conditions. The second division was taken as the density range in which only the unstressed biofilms (86 mM NaCl) displayed biofilm growth. This limit (0.20 cells/μm^3) was taken as the lower limit of the high-density phenotype. The difference between these two limits was the medium density phenotype. These limits were applied uniformly to all four environmental growth conditions.

The density phenotype ranges are plotted on a per sample basis in Figure 2-4a. In Figure 2-4a, different symbols denote each of the three density phenotypes. Three-dimensional

projections of bacterial centroids extracted from representative CLSM image volumes from each condition for each phenotype are shown in Figure 2-4b. The low-density phenotype exhibits more clustering than the medium- and high-density phenotypes. The medium- and high-density phenotypes are qualitatively more close-packed and more uniform than the low-density phenotypes. As stress is increased within the system fewer phenotypes are present.

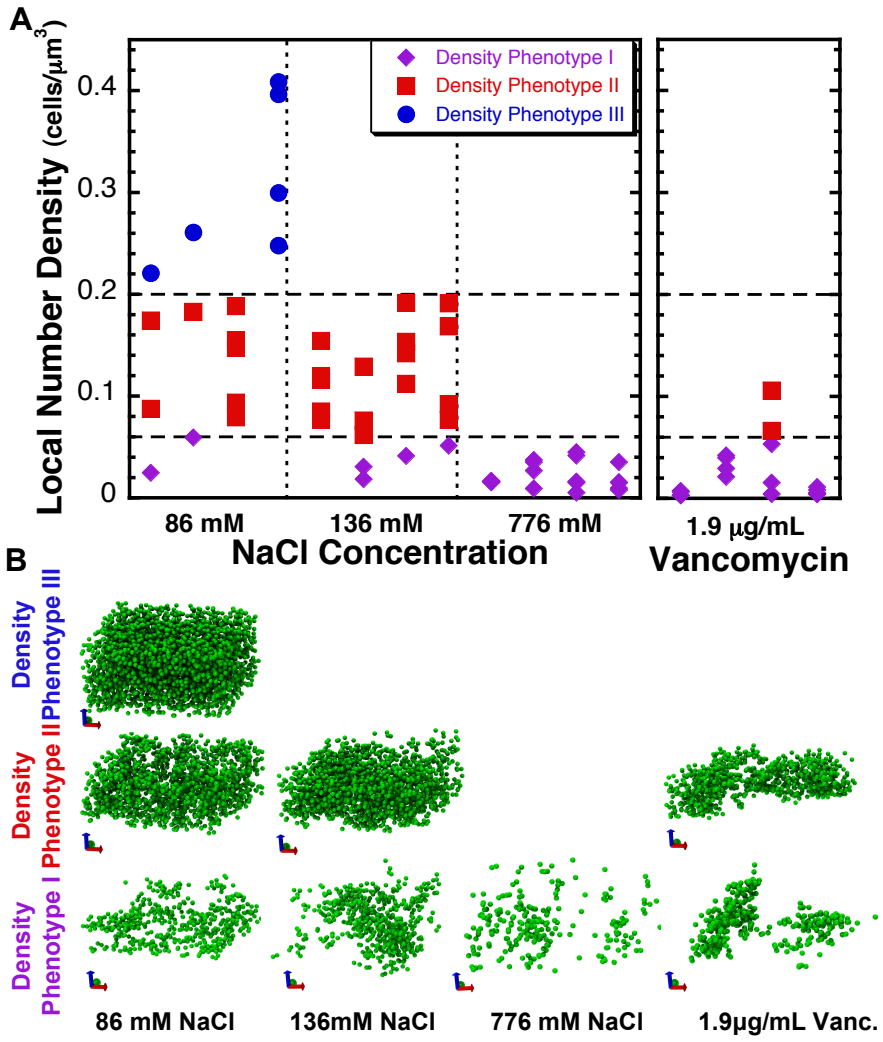

Figure 2-4: (A) Bacterial local number density varies according to environmental stress condition and can be described by identification of three density phenotypes. Within each condition, each column of data represents the results of one flow cell replicate. There were four replicates per experimental condition. (B) Representative 3D renderings of bacteria, organized by both environmental stress condition and low (I), medium (II), and high (III) density phenotypes. As

osmotic stress increased, the number of density phenotypes present decreased. This figure was originally published in [E.J. Stewart, A.E. Satorius, J.G. Younger, & M.J. Solomon, *Langmuir* 2013, *29,* 7017-7024].

Cluster distributions indicated that all *S. epidermidis* biofilm phenotypes contain close spatial association at short length scales, presumably due to daughter cells from cell division. The cluster distribution, plotted in Figure 2-5b, shows that similarities exist in *S. epidermidis* biofilm clustering for all density phenotypes at short length scales ($r_c < \sim 1.0$ μm). This conclusion is drawn from the fact that a sharp decrease in the ratio of number of clusters to total number of bacteria (the y-axis in Figure 2-5b) occurs at a cluster cutoff, r_c, of ~ 1 μm. This sharp decrease is at the same length scale as that expected for the effects of cell division. That is, at the separation distance of daughter cells (dimers) and pairs of daughter cells (tetramers), the number of clusters drops precipitously. This drop occurs because on the 1 μm scale bacteria are grouped together into dimers and tetramers. These dimer and tetramer groups suggest that the biofilm density phenotypes found have internal structure seemingly linked to cell division. Representative sections of CLSM images of dimers, trimers, and tetramers found in the biofilms are shown in Figure 2-5c.

Cluster distributions showed that cellular connectivity at $r_c = 6$ μm is a strong function of density phenotype. In the limit of $r_c > 2$ μm, the low-density phenotype contains significantly more clusters relative to that of the medium and high-density phenotypes, as shown on the right hand side of Figure 2-5b. Increased clustering of the low-density phenotype is indicated by the fact that the ratio of number of clusters to number of bacteria (N_{Cl}/N_B) only decreases to 0.04 at $r_c = 6$ μm, instead of dropping to nearly 0 ($<10^{-3}$) as in the medium and high density phenotypes.

N_{Cl}/N_B tending to zero indicates that all bacteria in the image volume have been grouped into either a single cluster, or a few very large clusters (typically >1000 bacteria/cluster).

Thus, in the low-density phenotype, biofilms are structured at ~ 6 μm scales into small clusters of abundance equal to about 4% of the total number of cells. In the medium- and high-density phenotypes cells on this scale are connected into large clusters that span the entire image volume.

The radial distribution function corroborates the short-range structural findings of the cluster analysis. The radial distribution function—g(r)—is the probability of finding a bacterium at a distance, r, given that a reference bacterium is located at the origin, relative to a uniform distribution of the same density. Thus, peaks in the radial distribution function represent an increased probability of finding a bacterium at a given location from the origin, while troughs represent a decrease in the probability of finding a bacterium at a given location from the origin. The radial distribution functions plotted in Figure 2-5d display two features that corroborate the cluster distribution findings.

First, the radial distribution function of each density phenotype displays a peak at short length scales (< 1.2 μm). This peak indicates an increased probability of finding bacteria separated by short distances relative to a uniform distribution of bacteria. These peaks support the evidence of a first coordination shell on the length scale of cell division in the biofilms.

Second, the magnitude of the radial distribution function of the low-density phenotype is significantly greater than the medium- and high-density phenotypes. The medium- and high-density phenotype measurements are consistent with results for disordered liquids and packings, such as those found in fluid and glassy suspensions of colloids [46]. By comparison, the large

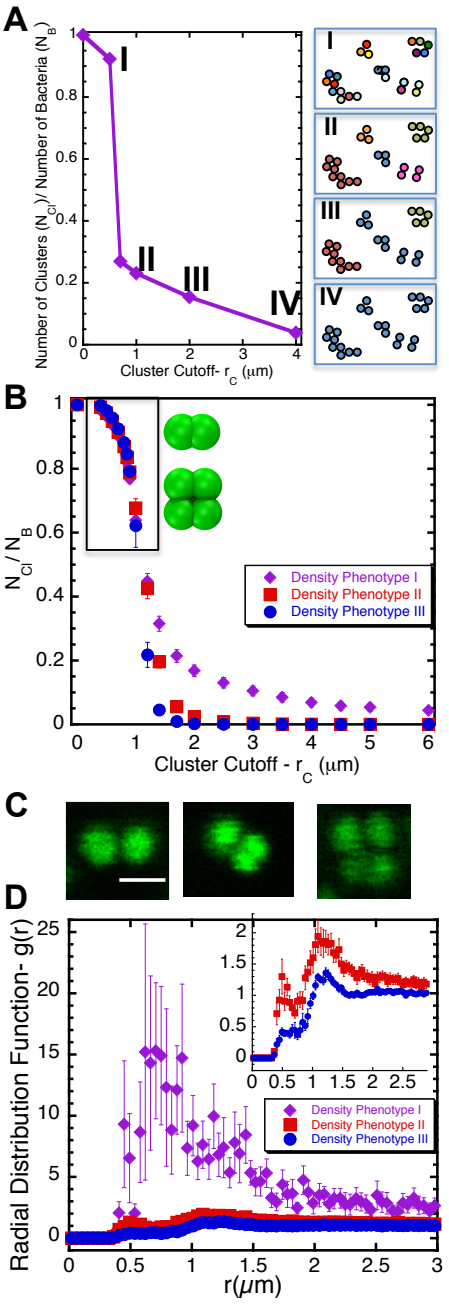

Figure 2-5: (A) Schematic representations of specific regions within the cluster distribution curve. When the cluster cutoff size, r_c, is low, the number of bacteria in each cluster is low. This decrease results from the close spatial association required by small r_c. Thus, many clusters are identified, each with few bacteria. Conversely, when r_c is high, bacteria are increasingly connected and the number of clusters is small. In the above figure each cluster is represented by a different color. (I) $r_c = 0.5$ μm shows that all cells other than the pair of cells in the middle that are directly touching are counted as individual clusters. (II) $r_c = 0.7$ μm yields 5 clusters. (III) $r_c = 1$ μm yields 3 clusters. (IV) $r_c = 4$ μm yields one cluster. (B) Cluster distribution of low (I), medium (II), and high (III) density phenotypes. Cluster distribution is plotted as Number of Clusters (N_{Cl})/ Number of Bacteria (N_B) verses Cluster Cutoff (r_C). All biofilms cluster at $r_c \sim 1$ μm indicating that all growth conditions and density phenotypes contain similar clustering on length scales of cell division (upper left hand box). This clustering consists of small clusters: dimers, trimers, and tetramers. In addition, cluster distributions for $r_c \sim 5$ μm differ in cellular connectivity between the low-density phenotypes and the medium- and high-density phenotypes. A greater number of clusters (equal to ~4% of the number of cells) are present within the low-density phenotype (I) compared to the medium(II)- and high(III)-density phenotypes, where only single clusters are present at ~6 μm for these two cases. The cluster distribution data analyzed include all data collected from both unstressed and stressed biofilms with the given phenotype. All curves for the three phenotypes were statistically distinct by general additive modeling ($p < 0.01$ for each). (C) CLSM evidence of clustering of dimers, trimers and tetramers, on length scales linked to cell division. Scale bar: 1 μm. (D) Radial distribution function of low (I), medium (II), and high (III) density phenotypes. The peaks at <1.2 μm indicate that bacteria are separated by short distances, consistent with the short-range clustering of panel A. Additionally, the significantly higher peak of the low(I)-density phenotype indicates fractal structure of the biofilm, whereas the peaks of the medium(II)- and high(III)-density phenotypes indicate dense, disordered packing of the biofilm. The g(r) data analyzed include all data collected from both unstressed and stressed biofilms with the given phenotype. All curves for the three phenotypes were statistically distinct by general additive modeling ($p < 0.01$ for each). This figure was originally published in [E.J. Stewart, A.E. Satorius, J.G. Younger, & M.J. Solomon, *Langmuir* 2013, *29,* 7017-7024].

magnitude of the radial distribution function of the low-density phenotype indicates substantial deviation in bacterial pair separation relative to that expected for a uniform distribution of bacteria. This heterogeneity is consistent with the both the greater clumpiness on ~6 μm length scales found in the cluster distribution of low-density phenotypes, and the colloidal clustering of structures with fractal distributions [47]. To further understand the low-density phenotype, we quantified the fractal behavior of these structures (over the range $2R < r < 10R$), and determined the average fractal dimension to be 1.7 ± 0.1. Although the mechanism of association is potentially very different, it is interesting that this value is similar to the Diffusion Limited Cluster Aggregation (DLCA) regime, for which $d_f = 1.8$ [48]. A plot of the data and fit used to determine the fractal dimension is shown in Figure 2-6.

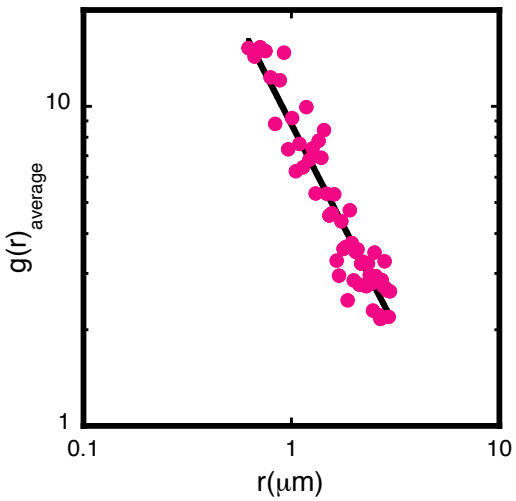

Figure 2-6: Fractal dimension calculation. The low-density phenotype radial distribution function was consistent with fractal scaling. We computed the fractal dimension, f_d, of the low-density phenotype through a power-law fit of the radial distribution function, g(r), from $2R < r < 10R$, where R is 320 nm, the average radius of *S. epidermidis* [43]. g(r) is related to f_d through $g(r) \sim r^{d_f - 3}$ [44,45]. The fit of the average radial distribution function was determined to be: $y=8.79 * x^{-1.2692}$, $R^2 = 0.95$. Thus, the fractal dimension was computed to be 1.7. To obtain the error, the fractal dimension was determined for each of the low-density phenotype samples and the standard error of the mean was computed to be ± 0.1. This figure was originally published in [E.J. Stewart, A.E. Satorius, J.G. Younger, & M.J. Solomon, *Langmuir* 2013, *29,* 7017-7024].

2.5 Discussion

This paper has applied high-resolution confocal laser scanning microscopy coupled with image analysis to evaluate the effect of environmental stress and antibiotics on biofilm architecture on the 0.5 – 5 μm scale of intercellular microstructure. Our findings indicate that unstressed *S. epidermidis* biofilm architecture is highly variable at short length scales, consisting of distinct phenotypes distributed across the biofilm. In unstressed biofilms, the cellular density of these phenotypes varies by a factor of 20. Osmotic stress decreased the variation in number density of *S. epidermidis* biofilms, as indicated by the uniformly low local number densities of these samples. Likewise, stress from vancomycin, an antibiotic commonly used to treat *Staphylococcal* infections, reduced the structural variation of the biofilms, as shown by an equivalent decrease in the range of the local number density phenotypes present.

We probed the internal structure of the high-, medium-, and low-density phenotypes through cluster distribution analysis. We found that low-density phenotypes consisted of small clusters of bacteria, whereas high-density phenotypes displayed continuous connectivity throughout the entire volume being sampled. We also found that all biofilms observed contained short-range structure on length scales commensurate with cell division.

This work demonstrates that clustering of low-density biofilms on scales of ~ 6 μm and below is a common feature of biofilms. We observed increased clustering of *S. epidermidis* in low-density phenotype biofilms on length scales <6 μm. This scale is similar to clustering observed by Berk et al. in *V. cholerae* biofilms [17]. The observation of such clustering in two different biofilm forming species suggests that the ~ 6 um scale is broadly relevant to understanding the morphology and architecture of bacterial biofilms. Moreover, as discussed in the next paragraphs, our work extends the understanding of this clustering by showing: (a)

unstressed biofilms have cellular connectivity across ~30 μm regions, while stressed biofilms only maintain cellular connectivity on ~ 6 μm size scales; (b) small scale clustering in biofilms is consistent with the effects of cell division; (c) low-density biofilms form fractal structures with fractal dimensions $d_f = 1.7 \pm 0.1$.

The long-range (~30 μm) cellular connectivity of unstressed biofilms with high- and medium density phenotypes and the short-range cellular connectivity of stressed biofilms (~6 μm) with low-density phenotypes have implications for the mechanism of biofilm connectivity in each of these systems. The cluster distribution characterization of Figure 2-4A distinguishes between cells that are directly connected to each other (because they are separated by distances < 5 μm and thus grouped into a single cluster), and cells that are not directly connected, and thus are associated indirectly through PIA and other components of the EPS (because the cells are separated by distances greater than 6 μm). This finding shows that cellular connectivity in stressed biofilms is decreased relative to unstressed biofilms. This difference in cellular contact and connectivity may have implications for the rheological (e.g. elastic modulus, yield strength) and transport properties (e.g. diffusion of oxygen, nutrients, antibiotics, quorum sensing molecules) of biofilms. For example, the bacterial contact interactions could deform with a rigid or soft response depending on the spacing and angles between bacteria. These two types of clusters would behave differently when subjected to deformation [49, 50].

Cell replication also appears to significantly impact biofilm microstructure. Both unstressed biofilms and biofilms grown in the presence of environmental stressors contained structure signatures suggestive of cell division on length scales of < 2 μm. This result suggests that progeny remain nearby original cells within biofilms.

Low-density phenotype *S. epidermidis* biofilms have an average fractal dimension (d_f = 1.7 ± 0.1) consistent with values found for other modes of aggregation, such as diffusion limited cluster aggregation [51]. This tenuous structure of the low-density phenotype biofilms is similar to that observed for number of of colloidal gels [52] formed through spinodal decomposition-type mechansims. The mechanism of bacteria clustering into fractal structures is likely more complex than such colloidal mechanisms of aggregation because of the potential contribution of cell division, matrix materials, and quorum sensing to the multicellular structure of bacterial communities. Nevertheless, the very low fractal dimension observed is consistent with the very open, low dimensionality structures for these loose biofilms. The fractal structure of gels has profound implications for rheological properties – for example, in colloidal systems, both the fractal structure and cluster dimension specify the hierarchy of fluctuating modes that determine the gel elasticity[53]. Identification of this structural feature in stressed biofilms suggests a potential avenue to model the contribution of their intercellular structure to their elastic rheology. In colloidal gels, fractal models of internal particle dynamics have been used to develop a scaling relationship among the volume fraction, fractal dimension, and elastic modulus [53]. Similar scaling relationships may be useful for determining the elastic moduli of biofilms.

More broadly, the experimental characterization of the spatial position of every bacterium in a local region of the biofilm, as pursued in the present study, is critical to advancing understanding of a number of biofilm transport and mechanical properties. For example, spatial coordinates can be used to further understand matrix behavior through allowing for calculations of the average extracellular concentration of PIA per cell present within the biofilm [43]. Moreover, the bacterial positions can be applied to initialize composite based predictive models of biofilm mechanical behavior, thereby better linking these models to real conditions in the

biofilms. These models have been applied to flow induced fragmentation models of biofilms [54]. Additionally, computer modeling of biofilms has shown how clustering behavior may change due to social evolution within single species and multi-species biofilms [55]. Consequently, the tools developed in the present study are immediately applicable for experimentally evaluating the behavior of each individual species in these simulations or could be expanded to multi-species biofilms for testing the structural behavior of each species as well.

2.6 Conclusions

Our work has identified that unstressed biofilms are comprised of multicellular structures representing the full range of high-, medium, and low-density phenotypes, while biofilms stressed by either osmotic pressure or an antibiotic contain only medium- and low-density phenotypes. Although it was expected that biofilms undergoing stress would not develop as extensively as unstressed biofilms, the short- and long-range structural behaviors that accompany these developmental differences were previously unknown. All *S. epidermidis* biofilms observed contained clustering commensurate with the length scale of cell division (~1 μm). However, biofilm connectivity differed on ~6 μm scales, where high- and medium- density phenotype biofilms contained longer range connectivity (>30 μm), and low-density phenotype biofilms clustered into fractal structures. Advancing the understanding of how bacteria organize at the intercellular level in unstressed and stressed conditions introduces a new perspective for understanding biofilm growth. The metrics used here could be applied to quantify and advance the understanding of the kinetics of bacterial surface colonization in both single species and multi-species biofilms, bacterial behavior at the biofilm-water interface or other regions within the biofilm, and biofilm dispersal, fracture and fragmentation.

2.7 References

(1) Costerton, J. W.; Stewart, P. S.; Greenberg, E. P. Bacterial biofilms: a common cause of persistent infections. *Science* **1999**, *284*, 1318.

(2) Stewart, P. S.; Franklin, M. J. Physiological heterogeneity in biofilms. *Nat Rev Micro* **2008**, *6*, 199-210.

(3) Fux, C. A.; Costerton, J. W.; Stewart, P. S.; Stoodley, P. Survival strategies of infectious biofilms. *Trends in Microbiology* **2005**, *13*, 34-40.

(4) Wilking, J. N.; Angelini, T. E.; Seminara, A.; Brenner, M. P.; Weitz, D. A. Biofilms as complex fluids. *MRS BULLETIN* **2011**, *36,* 385-391.

(5) Zaccarelli, E. Colloidal gels: Equilibrium and non-equilibrium routes. *Journal of Physics: Condensed Matter* **2007**, *19*, 323101.

(6) Hohne, D. N.; Younger, J. G.; Solomon, M. J. Flexible Microfluidic Device for Mechanical Property Characterization of Soft Viscoelastic Solids Such as Bacterial Biofilms. *Langmuir* **2009**, *25*, 7743-7751.

(7) Rogers, S. S.; van, d. W., C.; Waigh, T. A. Microrheology of Bacterial Biofilms In Vitro: Staphylococcus aureus and Pseudomonas aeruginosa. *Langmuir* **2008**, *24*, 13549-13555.

(8) Hall-Stoodley, L.; Costerton, J. W.; Stoodley, P. Bacterial biofilms: from the Natural environment to infectious diseases. *Nat Rev Micro* **2004**, *2*, 95-108.

(9) Lieleg, O.; Caldara, M.; Baumgärtel, R.; Ribbeck, K. Mechanical robustness of Pseudomonas aeruginosa biofilms. *Soft Matter* **2011**, *7*, 3307-3314.

(10) Aggarwal, S.; Poppele, E. H.; Hozalski, R. M. Development and testing of a novel microcantilever technique for measuring the cohesive strength of intact biofilms. *Biotechnology and Bioengineering* **2010**, *105*, 924–934.

(11) Dunne Jr, W. M. Bacterial adhesion: seen any good biofilms lately? *Clinical microbiology reviews* **2002**, *15*, 155.

(12) Xavier, J. B.; White, D. C.; Almeida, J. S. Automated biofilm morphology quantification from confocal laser scanning microscopy imaging. *Water Science & Technology* **2003**, *47*, 31-37.

(13) Beyenal, H.; Donovan, C.; Lewandowski, Z.; Harkin, G. Three-dimensional biofilm structure quantification. *Journal of microbiological methods* **2004**, *59*, 395-413.

(14) Heydorn, A.; Nielsen, A. T.; Hentzer, M.; Sternberg, C.; Givskov, M.; Ersbøll, B. K.; Molin, S. Quantification of biofilm structures by the novel computer program COMSTAT. *Microbiology* **2000**, *146*, 2395.

(15) McLean, J. S.; Ona, O. N.; Majors, P. D. Correlated biofilm imaging, transport and metabolism measurements via combined nuclear magnetic resonance and confocal microscopy. *The ISME journal* **2007**, *2*, 121-131.

(16) Dzul, S. P.; Thornton, M. M.; Hohne, D. N.; Stewart, E. J.; Shah, A. A.; Bortz, D. M.; Solomon, M. J.; Younger, J. G. Contribution of the Klebsiella pneumoniae Capsule to Bacterial Aggregate and Biofilm Microstructures. *Applied and Environmental Microbiology* **2011**, *77*, 1777-1782.

(17) Berk, V.; Fong, J. C. N.; Dempsey, G. T.; Develioglu, O. N.; Zhuang, X.; Liphardt, J.; Yildiz, F. H.; Chu, S. Molecular Architecture and Assembly Principles of Vibrio cholerae Biofilms. *Science* **2012**, *337*, 236-239.

(18) Crocker, J. C.; Grier, D. G. Methods of digital video microscopy for colloidal studies. *Journal of Colloid and Interface Science* **1996**, *179*, 298-310.

(19) Dibble, C. J.; Kogan, M.; Solomon, M. J. Structure and dynamics of colloidal depletion gels: Coincidence of transitions and heterogeneity. *Physical Review E* **2006**, *74*, 041403.

(20) Poon, W. C. K.; Weeks, E. R.; Royall, C. P. On measuring colloidal volume fractions. *Soft Matter* **2012**, *8*, 21-30.

(21) Dill, K. A.; Bromberg, S. *Molecular driving forces: statistical thermodynamics in chemistry and biology*; Garland Science: 2003.

(22) Uçkay, I.; Pittet, D.; Vaudaux, P.; Sax, H.; Lew, D.; Waldvogel, F. Foreign body infections due to Staphylococcus epidermidis. *Annals of medicine* **2009**, *41*, 109-119.

(23) Gaboriaud, F.; Gee, M. L.; Strugnell, R.; Duval, J. F. L. Coupled Electrostatic, Hydrodynamic, and Mechanical Properties of Bacterial Interfaces in Aqueous Media. *Langmuir* **2008**, *24*, 10988-10995.

(24) Camesano, T. A.; Natan, M. J.; Logan, B. E. Observation of Changes in Bacterial Cell Morphology Using Tapping Mode Atomic Force Microscopy. *Langmuir* **2000**, *16*, 4563-4572.

(25) Xu, H.; Murdaugh, A. E.; Chen, W.; Aidala, K. E.; Ferguson, M. A.; Spain, E. M.; Núñez, M. E. Characterizing Pilus-Mediated Adhesion of Biofilm-Forming E. coli to Chemically Diverse Surfaces Using Atomic Force Microscopy. *Langmuir* **2013**, *29*, 3000-3011.

(26) Emerson, Bergstrom, T. S.; Liu, Y.; Soto, E. R.; Brown, C. A.; McGimpsey, W. G.; Camesano, T. A. Microscale Correlation between Surface Chemistry, Texture, and the Adhesive Strength of Staphylococcus epidermidis. *Langmuir* **2006**, *22*, 11311-11321.

(27) Busscher, H. J.; van, d. B.-G., Betsy; Dijkstra, R. J. B.; Norde, W.; van, d. M., Henny C. Streptococcus mutans and Streptococcus intermedius Adhesion to Fibronectin Films Are Oppositely Influenced by Ionic Strength. *Langmuir* **2008**, *24*, 10968-10973.

(28) Pavlovsky, L.; Younger, J. G.; Solomon, M. J. In situ rheology of Staphylococcus epidermidis bacterial biofilms. *Soft Matter* **2013**, *9*, 122-131.

(29) Shaw, T.; Winston, M.; Rupp, C. J.; Klapper, I.; Stoodley, P. Commonality of Elastic Relaxation Times in Biofilms. *Phys. Rev. Lett.* **2004**, *93*, 098102.

(30) Towler, B. W.; Rupp, C. J.; Cunningham, A. L. B.; Stoodley, P. Viscoelastic Properties of a Mixed Culture Biofilm from Rheometer Creep Analysis. *Biofouling* **2003**, *19*, 279-285.

(31) McMillan, D. E. Chapter 4: Hemorheology: Principles and Concepts. **2008**, *Levin and O'Neal's the diabetic foot*, 75-88.

(32) Howden, L.; Giddings, D.; Power, H.; Aroussi, A.; Vloeberghs, M.; Garnett, M.; Walker, D. Three-dimensional cerebrospinal fluid flow within the human ventricular system. *Computer methods in biomechanics and biomedical engineering* **2008**, *11*, 123-133.

(33) Lykoudis, P. S.; Roos, R. The fluid mechanics of the ureter from a lubrication theory point of view. *Journal of Fluid Mechanics* **1970**, *43*, 661-674.

(34) Christensen, G. D.; Simpson, W. A.; Anglen, J. O.; Gainor, B. J. Methods for Evaluating Attached Bacteria and Biofilms. **2000**, *Handbook of bacterial adhesion: principles, methods, and applications*, 213-233.

(35) Dobinsky, S.; Kiel, K.; Rohde, H.; Bartscht, K.; Knobloch, J. K.-M.; Horstkotte, M. A.; Mack, D. Glucose-Related Dissociation between icaADBC Transcription and Biofilm Expression by Staphylococcus epidermidis: Evidence for an Additional Factor Required for Polysaccharide Intercellular Adhesin Synthesis. *Journal of Bacteriology* **2003**, *185*, 2879-2886.

(36) Stepanović, S.; Vuković, D.; Hola, V.; Bonadventura, G. D.; Djukić, S.; Ćirković, I.; Ruzicka, F. Quantification of biofilm in microtiter plates: overview of testing conditions and practical recommendations for assessment of biofilm production by staphylococci. *APMIS* **2007**, *115*, 891-899.

(37) Rachid, S.; Ohlsen, K.; Witte, W.; Hacker, J.; Ziebuhr, W. Effect of subinhibitory antibiotic concentrations on polysaccharide intercellular adhesin expression in biofilm-forming Staphylococcus epidermidis. *Antimicrobial agents and chemotherapy* **2000**, *44*, 3357.

(38) Conlon, K. M.; Humphreys, H.; O'Gara, J. P. icaR encodes a transcriptional repressor involved in environmental regulation of ica operon expression and biofilm formation in Staphylococcus epidermidis. *Journal of bacteriology* **2002**, *184*, 4400.

(39) Polonio, R. E.; Mermel, L. A.; Paquette, G. E.; Sperry, J. F. Eradication of biofilm-forming Staphylococcus epidermidis (RP62A) by a combination of sodium salicylate and vancomycin. *Antimicrobial agents and chemotherapy* **2001**, *45*, 3262.

(40) Kogan, M.; Dibble, C. J.; Rogers, R. E.; Solomon, M. J. Viscous solvent colloidal system for direct visualization of suspension structure, dynamics and rheology. *Journal of Colloid and Interface Science* **2008**, *318*, 252-263.

(41) Lu, P. J.; Zaccarelli, E.; Ciulla, F.; Schofield, A. B.; Sciortino, F.; Weitz, D. A. Gelation of particles with short-range attraction. *Nature* **2008**, *453*, 499-503.

(42) Allen, M. P.; Tildesley, D. J. *Computer Simulation of Liquids;* Oxford University Press: 1989.

(43) Ganesan, M.; Stewart, E. J.; Szafranski, J.; Satorius, A.; Younger, J. G.; Solomon, M. J. Molar mass, entanglement and associations of the biofilm polysaccharide of Staphylococcus epidermidis. *Biomacromolecules* **2013**, *14*, 1474-1481.

(44) Dinsmore, A. D.; Prasad, V.; Wong, I. Y.; Weitz, D. A. Microscopic Structure and Elasticity of Weakly Aggregated Colloidal Gels. *Phys. Rev. Lett.* **2006**, *96*, 185502.

(45) Lattuada, M.; Wu, H.; Hasmy, A.; Morbidelli, M. Estimation of Fractal Dimension in Colloidal Gels. *Langmuir* **2003**, *19*, 6312-6316.

(46) Blaaderen, A. v.; Wiltzius, P. Real-Space Structure of Colloidal Hard-Sphere Glasses. *Science New Series* **1995**, *270*, 1177-1179.

(47) Dinsmore, A. D.; Weeks, E. R.; Prasad, V.; Levitt, A. C.; Weitz, D. A. Three-Dimensional Confocal Microscopy of Colloids. *Appl. Opt.* **2001**, *40*, 4152–4159.

(48) Lin, M. Y.; Lindsay, H. M.; Weitz, D. A.; Ball, R. C.; Klein, R.; Meakin, P. Universality in colloid aggregation. *Nature* **1989**, *339*, 360-362.

(49) Potanin, A. A. On the Computer Simulation of the Deformation and Breakup of Colloidal Aggregates in Shear Flow. *Journal of Colloid and Interface Science* **1993**, *157*, 399 - 410.

(50) Hsiao, L. C.; Newman, R. S.; Glotzer, S. C.; Solomon, M. J. Role of isostaticity and load-bearing microstructure in the elasticity of yielded colloidal gels. *Proceedings of the National Academy of Sciences* **2012**, *109*, 16029-16034.

(51) Russel, W. B.; Saville, D. A.; Schowalter, W. R. *Colloidal dispersions*; Cambridge University Press: 1992.

(52) Carpineti, M.; Giglio, M. Spinodal-type dynamics in fractal aggregation of colloidal clusters. *Physical Review Letters Phys. Rev. Lett. PRL* **1992**, *68*, 3327-3330.

(53) Krall, A. H.; Weitz, D. A. Internal Dynamics and Elasticity of Fractal Colloidal Gels. *Phys. Rev. Lett.* **1998**, *80*, 778-781.

(54) Hammond, J. F.; Stewart, E. J.; Younger, J. G.; Solomon, M. J.; Bortz, D. M. Spatially Heterogeneous Biofilm Simulations using an Immersed Boundary Method with Lagrangian Nodes Defined by Bacterial Locations. *J arXiv preprint arXiv:1302.3663* **2013**.

(55) Mitri, S.; Xavier, J. B.; Foster, K. R. Social evolution in multispecies biofilms. *Proceedings of the National Academy of Sciences* **2011**, *108*, 10839–10846.

Chapter 3

Bacterial-chitosan constructs establish the role of physical self-assembly in biofilm formation[‡§]

3.1 Abstract

Bacterial constructs with biofilm-like microstructural and mechanical properties were self-assembled by exploiting interactions that were exclusively physicochemical – rather than genetically constitutive – in origin. Bacterial biofilms are viscoelastic, structured communities of bacteria; they possess heterogeneous microstructure, local pH gradients, and an extracellular polymeric substance (EPS) comprised predominantly of polysaccharides along with proteins and DNA. Although the genetic pathways of EPS synthesis, the microstructure and the rheology of biofilms have been previously probed, how the cells and the extracellular matrix materials generate the biofilm morphology and mechanics is not understood. Here, we find that physical interactions drive the self-assembly of EPS components and bacterial cells into viscoelastic, structured communities. Specifically, pH conditions that induce phase instability of polysaccharide solutions yield artificial biofilms whose microstructures and mechanics match

[‡] This work has been submitted for publication by [E.J. Stewart, M. Ganesan, J.G. Younger, & M.J. Solomon].
[§] E.J. Stewart and M. Ganesan co-authored this work.

those of natural biofilms. Thus, during the biofilm lifecycle, genetic regulation triggers the synthesis of EPS, but physical self-assembly generates the morphology and viscoelasticity of the biofilm. An implication of the results is that pH-induced solubilization of the EPS polysaccharide triggers biofilm disassembly and dispersion, a result significant for biofilm control in medical devices, biofouling, and dental plaques.

3.2 Introduction

Bacterial biofilms are viscoelastic multi-cellular structured communities encapsulated in an extracellular polymeric substance (EPS) of polysaccharides, proteins, and DNA [1, 2]. Their viscoelasticity prevents fragmentation [3,4] and promotes resilience against shear [4,5,6]. Biofilms display structural and physicochemical heterogeneity across multiple spatial scales [7-10] and pH microenvironments [11]. This heterogeneity mediates nutrient and antimicrobial transport [2,12], mechanics [13,14], and sociobiology [15].

The formation of biofilms is commonly viewed as the consequence of genetically controlled synthesis and export of EPS components [16]. However, there remains a profound gap between our understanding of the effect of these synthesis and export operations on biofilm formation and the complex microstructure and rheology that is achieved by mature biofilms. Bridging this gap has implications for large-scale mechanics of biofilm streamers [17] and strain hardening [18]. The idea of depletion-mediated aggregation of bacteria contributing towards biofilm formation has been previously introduced [19,20].

Here we show that the purely physical self-assembly of cellular and polymeric components can, in the absence of any bacterial regulatory control, produce the morphology and

mechanics of *S. epidermidis* biofilms. The essential role of self-assembly in the formation of biofilms suggests strategies for their control and mechanical remediation.

3.3 Materials and Methods

3.3.1 Bacterial strains and culture conditions

S. epidermidis RP62A (ATCC 35984) was grown in 50 mL tryptic soy broth (TSB) with 1% added glucose at 200 RPM in an overnight culture in a 250 mL Erlenmeyer flask. 1 mL of the overnight culture was added to 50 mL TSB with 1 wt. % added glucose and was grown to OD_{600}= 0.5, 1.0, or 1.4. Bacteria were stained with 2.5 μM Syto9 for 30 minutes. The cellular concentration at each optical density was measured using a Neubauer improved hemocytometer (INCYTO, Korea). Three replicates were performed at each OD and the average and standard error of the mean (SEM) were computed. The OD_{600} measurements and concentrations are summarized in Table 3-1.

S. aureus SH1000 colonies were cultured on Tryptic Soy Agar (TSA) for the 18-hour *S. aureus* biofilm experiments.

Table 3-1: Conversion of optical densities to cell concentrations. This table is reprinted from the submitted paper of [E.J. Stewart, M. Ganesan, J.G. Younger, & M.J. Solomon].

OD_{600}	Cell Concentration (cells/ mL)
0.5	2.4E8 ± 0.3E8
1.0	5.1E8 ± 1E8
1.4	9.7E8 ± 0.5E8

3.3.2 Extraction and quantification of biofilm polymers

S. epidermidis batch biofilms were cultured and the extracellular polymeric substances (EPS) and high purity polysaccharide intercellular adhesin (PIA) isolates were obtained

following the protocol of refs [21, 22]. The concentration of glucosaminoglycans in EPS and PIA isolates was measured using the Smith Gilkerson assay [23]. Proteins and nucleic acids in the EPS were quantified using the BCA and PicoGreen assay respectively. The concentrations of PIA, protein, and nucleic acids within *S. epidermidis* biofilms were calculated by obtaining the total concentration of EPS polymers per biofilm cell (the latter is quantified as total cell density per culture using a hemocytometer), computing the average extracellular volume available per biofilm cell (from measurements of *in situ* cell number density of Stewart et al., [9]) and dividing the two to obtain the total average extracellular concentration of PIA, protein and nucleic acids *in situ* as done earlier [21]. The calculated values are averaged over at least 10 different batch cultures and are reported in Table 3-2.

Table 3-2: Average extracellular concentrations, as defined by Ganesan et al. (28) of PIA, protein and DNA within *S. epidermidis* biofilms. This table is reprinted from the submitted paper of [E.J. Stewart, M. Ganesan, J.G. Younger, & M.J. Solomon]. This table was created by Mahesh Ganesan.

Component	Concentration (g/mL) x 10^2
PIA	2.0 ± 0.5
Total Protein	1.0 ± 0.4
Total DNA	0.1 ± 0.07

3.3.3 Particle tracking microrheology using diffusing wave spectroscopy (DWS)

DWS was carried out as per ref [24]. The probes used were 0.5 μm sulfate latex beads (Invitrogen, Eugene, OR) at suitable concentrations to ensure multiple scattering [24]. Biofilms were cultured directly in 1 mm thick rectangular cuvettes by using *S. epidermidis* colonies to inoculate the growth media; the probes were added during inoculation. Stability of probes in growth media was confirmed using zeta potential measurements. The mean squared

displacement (MSD) of probes in PIA, EPS and biofilm was computed from their normalized intensity autocorrelation function, $g_2(t) = \langle I(0)I(t)\rangle/\langle I(t)\rangle^2$, where I(t) is the scattering intensity at time t and $\langle\ \rangle$ is the time average operator, as per ref [24]. The material storage, G'(ω) and loss, G"(ω) modulus were obtained using the generalized Stokes Einstein relation (GSER) as per [25]. Zero shear viscosity, η_0, and creep, J(t), was calculated from MSD following [24, 26]. A probe size and surface chemistry study on PIA and EPS solutions indicated no local heterogeneity and no probe-polymer interaction, therefore validating the use of the GSER. Biofilm DWS however exhibited strong probe size dependence. Probes larger than the size of *S. epidermidis* cells (> 0.5 μm) exhibited nonergodic dynamics, as characterized by a $g_2(t)$ intercept << 1 [27], presumably because of entrapment within or between biofilm clusters and were therefore not analyzed further. Probes of size equivalent to that of the bacterial cells – 0.5 μm diameter – exhibited decay in $g_2(t)$ that was consistent with thermally induced random motion. The $g_2(t)$ of probes smaller than the cellular diameter (< 0.5 μm) did decay to zero at infinite time; this behavior is indicative of restricted concentration fluctuations (i.e. localization), because of entrapment of the smaller probes within biofilm clusters. The biofilm J(t) as a function of probe size is shown in Fig. 3-1. We found that the short time response ($t < 10^{-3}$s) was independent of probe size while the cross over into the viscoelastic regime was found to be strongly dependent on probe size. Probes of size 0.5 μm – a dimension equivalent to the size of a *S. epidermidis* bacterial cell – resulted in a biofilm J(t) that matched the mechanical rheometry [6].

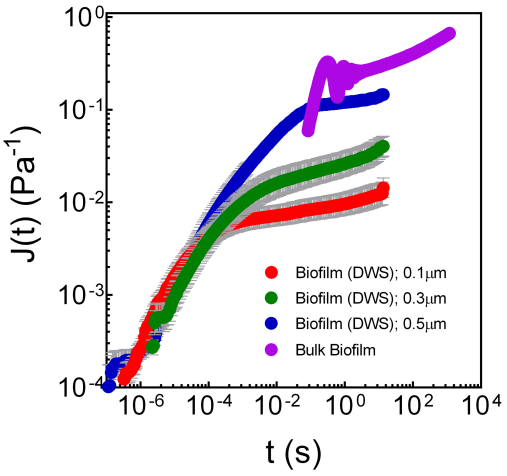

Figure 3-1: Creep compliance, J(t) of biofilms obtained from DWS microrheology using probes of size 0.1 μm, 0.2 μm and 0.5 μm and from the bulk biofilm mechanical rheometry [6]. The concentration of probes was chosen to ensure multiple scattering following [24]. This figure is reprinted from the submitted paper of [E.J. Stewart, M. Ganesan, J.G. Younger, & M.J. Solomon]. This figure was created by Mahesh Ganesan.

The probe surface chemistry study using confocal microscopy showed that 0.5 μm carboxylate and amine probes strongly associated with the biofilms (fraction of aggregated or stuck probes > 70%), while 0.5 μm sulfate probes showed much weaker association of < 15%. Using the theory of multiple scattering in binary suspensions [28] and the structure factor formulation for aggregates [29], we found that the impact of this association caused < 1 % change on the transport mean free path of multiply scattered light and a < 6 % change in the calculated MSD [30].

3.3.4 Construct matrix materials: chitosan, bovine serum albumin and DNA

Stock solutions of 1 wt. % chitosan, with manufacturer reported molar mass of 190 – 300 kDa and a degree of deacetylation of ~75-85 % (Sigma Aldrich, St. Louis, MO), were solubilized in 0.3 M Acetic Acid (pH = 3.0). PIA and chitosan solution properties such as molar mass, self-associations at acidic pH [21, 31] are nearly equivalent and both complex with proteins

and nucleic acids [21, 32]. For confocal laser scanning microscopy imaging, chitosan was labeled using 10 μg/mL Wheat Germ Agglutinin (WGA), AlexaFluor® 633 (Life Technologies, Grand Island, NY). Artificial EPS was prepared in the tryptic soy broth media by mixing together chitosan, BSA (Sigma Aldrich, St. Louis, MO) and λ DNA (Invitrogen, Eugene, OR) as per refs [21, 33] according to their *in situ* stoichiometry as reported in Table 3-2.

3.3.5 Bacterial-chitosan constructs

To simulate the biofilm solvent environment discussed in most reports on staphylococcal biofilms, tryptic soy broth media supplemented with 1 wt. % glucose was used as the solvent for making the constructs [22]. We probed six different chitosan concentrations and three different cellular optical densities. For each *S. epidermidis* cellular OD_{600} value (0.5, 1.0, 1.4), we created bacterial constructs with chitosan concentrations of 0, 0.05, 0.1, 0.2, 0.25, and 0.3 wt. %. The pH of these construct solutions varies as per Table S3. High cellular density constructs in Figure 2 and 3 correspond to samples made with OD_{600} = 1.4 and 0.3 wt. % chitosan, while low cellular density constructs in Figure 2 and 3 were made from cells with OD_{600} = 1.0 and 0.05 wt. % chitosan. Chitosan was added to 200 μL *S. epidermidis* cells. Constructs equilibrated for two hours prior to imaging. We decreased the pH of the low-density bacterial constructs (0.05 wt. % chitosan, pH=5.3±0.1) to pH = 4.4 by adding 40 μL 0.3 M Acetic Acid. We increased the pH of the high-density bacterial constructs (0.3 wt. % chitosan, pH=4.3 ± 0.02) to 7.3 by adding 18 μL 1 M KOH. We waited 3 hours after the pH was changed before imaging the constructs. Separately, the phase stability of chitosan and *S. epidermidis* EPS in growth media was studied by tracking changes in absorbance at 600 nm (GENESYS 20, Thermo Scientific, Madison, WI) with pH. The transition from a stable to an unstable phase was marked at the pH where a five-

fold increase in absorbance was first observed. The pH range of 4.5 and 6.7 studied here are within the reported pH range of *in situ S. epidermidis* biofilms (4.5-7.5)[34,35,36].

Table 3-3.

Table 3-3: pH of bacterial constructs at each OD_{600} and chitosan concentration. This table is reprinted from the submitted paper of [E.J. Stewart, M. Ganesan, J.G. Younger, & M.J. Solomon].

Chitosan (wt.%)	OD_{600} (Cell Concentration- cells/mL)		
	0.5 (2.4E8±0.3E8)	1.0 (5.1E8±1E8)	1.4 (9.7E8±0.5E8)
0	6.7 ± 0.03	6.3 ± 0.05	5.5 ± 0.2
0.05	5.7 ± 0.03	5.4 ± 0.04	4.9 ± 0.1
0.1	5.1 ± 0.003	5.1 ± 0.2	4.7 ± 0.04
0.2	4.6 ± 0.02	4.6 ± 0.02	4.5 ± 0.03
0.25	4.5 ± 0.01	4.5 ± 0.02	4.4 ± 0.02
0.3	4.4 ± 0.003	4.4 ± 0.01	4.3 ± 0.02

3.3.6 Biofilm growth conditions

Unstressed biofilms with heterogeneous density phenotypes were grown by passing TSB with 1 wt. % glucose added through a flow cell with a shear stress of 0.01 Pa, as per ref [9]. *S. epidermidis* RP62A and *S. aureus* SH1000 biofilms used to investigate the effect of pH changes on biofilm mobility and mechanics were grown in Nunc™ Lab-Tek™ II Chambered Coverglass dishes (Thermo Scientific, USA) for 18 hours at 60 RPM at 37°C. Each well contained a single bacterial colony and 400 µL TSB with 1% glucose added. After the biofilm containing dishes were removed from the incubator they were stained with LIVE/DEAD (Molecular Probes, Inc., Eugene, OR). Concentrations of 4 µM Syto9 and 25 µM Propidium Iodide were used. To induce pH changes to the naturally occurring biofilms, the growth media was replaced with 400 µL TSB with 1 wt. % glucose added with a pH adjusted to 3, 7, or 10. pH was adjusted using 0.3 M acetic acid or 1 M KOH. Media was allowed to incubate with the biofilm at room

temperature for 4 hours before imaging occurred. The final pH values within pH-modified constructs are found in Table 3-4.

Table 3-4: Final pH of pH-modified biofilms. This table is reprinted from the submitted paper of [E.J. Stewart, M. Ganesan, J.G. Younger, & M.J. Solomon].

	S. epidermidis	*S. aureus*
Naturally occurring biofilm	5.0 ± 0.1	4.55 ± 0.01
4 hours after pH 3 media is added	4.1 ± 0.1	3.8 ± 0.1
4 hours after pH 7.1 media is added	6.10 ± 0.04	5.9 ± 0.2
4 hours after pH 10 media is added	7.3 ± 0.1	6.9 ± 0.3

3.3.7 CLSM imaging and analysis

Bacterial constructs and biofilms were imaged using a Nikon A1Rsi confocal laser scanning microscope with a 100x, 1.45 NA, oil immersion objective lens. The excitation wavelength was 488 nm for the Syto9 and 633 nm for the AlexaFluor 633 WGA. Three-dimensional image volumes of size 31 x 31 x 5-23 μm^3 and time series of 150 two-dimensional images with size 31 x 31 μm^2 were collected at 15 frames per second. Local number densities, radial distribution functions, and mean squared displacements were computed from bacterial centroids identified by image analysis [37]. Bacterial centroids were resolved to within ± 35 nm in the object plane and ±45 nm in the axial plane [38]. For the characterization of the MSD, we found the lower limit of the instrument sensitivity to be $\langle \Delta x^2(\Delta t) \rangle_{min} = 4.5 \times 10^{-4}$ μm^2 by tracking fully immobilized bacteria at the coverslip of an arrested sample. There is a small abundance of initially flocculated bacteria in some of the samples. These flocs are not indicative of the dynamics that determine the construct microrheology. We account for the presence of flocs in two ways. First, the 1% of trajectories that are most immobilized at each condition probed were discarded from further analysis. Second, the error in the average $\langle \Delta x^2(\Delta t) \rangle$ due to the flocs within the initial cultures was estimated. To determine this error, we resolved the van Hove self-

correlation function of displacement into initially flocculated (slow) and bulk bacterial (fast) contributions. We performed this operation for ten different time points of three samples, one from each optical density, as per the methods of [39]. From the Gaussian distributions of flocculated and bulk bacterial populations, we estimated $<\Delta x^2(\Delta t)>$ for each population. The bulk bacterial subpopulation $<\Delta x^2(\Delta t)>$ was plotted in Fig. 3*A*, 4*C*, and 4*E*. As a control measurement: the removal of the flocculated bacteria from the average free bacteria $<\Delta x^2(\Delta t)>$ only increased the $<\Delta x^2(\Delta t)>$ by a factor of 4, while the $<\Delta x^2(\Delta t)>$ of the flocculated population was 15 times less than the average. Thus, the average $<\Delta x^2(\Delta t)>$ within all samples is representative of the bulk (fast) bacteria.

3.4 Results and Discussion

We first assessed the mechanical properties of the primary components of a naturally occurring biofilm. Figure 3-2 reports the mechanical properties of biofilms formed by the commonly isolated opportunistic, nosocomial pathogen *Staphylococcus epidermidis* [40]. *S. epidermidis* biofilm EPS consists predominantly of the polysaccharide intercellular adhesin (PIA)–an EPS component known to mediate the virulence, resistance, dissemination and eradication of *S. epidermidis* biofilms [41]. *The* creep compliance, J(t), of a mature *S. epidermidis* biofilm is characteristic of a viscoelastic solid (Fig. 3-2*A*). The extracellular polymers synthesized by *S. epidermidis* – either polysaccharide intercellular adhesin (PIA) or the entire acellular EPS [41] – show only a viscous response at their *in situ* stoichiometry, contrary to the idea that exopolymers determine biofilm mechanics [42, 43]. Other measures, such as the viscosity (Fig. 3-2*B*) and the storage and loss moduli (Fig. 3-2*C*, 3-2*D*) confirm that neither PIA nor EPS exhibit the rheology of a mature biofilm. Thus, there is, presumably, a phenomena that then mediates an interaction between these secreted polymers and the multi-cellular microbial

communities, that results in an viscoelastic composite as seen from both the DWS and shear rheometry data in Fig. 3-2. Traditional biofilm experiments are limited in understanding this phenomena mediating the interactions of biofilm components due the limited ability to control concentrations of both cells and matrix materials.

Self-assembly is the process by which individual constituents organize into structures as a result of their physical interactions. We hypothesize that biofilm viscoelasticity emerges from the physical self-assembly of its constituent cellular and polymeric components. This self-assembly – independent of genetic control – induces self-organization of volumes containing thousands of cells. Biofilm morphology and viscoelasticity are then the consequence of processes akin to those of attractive colloids, whose self-organization yields heterogeneous, viscoelastic structures [42,44].

To test this, planktonic bacterial cells and abacterial proxies for the polysaccharides, proteins, and DNA that comprise the EPS were mixed at *in situ* stoichiometry (Table 3-2) to create artificial biofilms (Fig. 3-2*E*) in tryptic soy broth with 1wt. % glucose. Crucially, the abacterial proxies eliminated genetic regulation as an explanation of the artificial biofilm morphology and mechanics. Additionally, self-assembly experiments allowed for control of cellular and matrix components as well as the solvent environment. Specifically, in place of PIA, we used the N-acetylglucosamine glycan chitosan that is a product from crustacean shells, which differs from PIA only in glycosidic linkages [21, 45]. We varied chitosan concentration between 0.05 and 0.3 wt. %, representative of *in situ* PIA; this step also introduced pH variation. Similarly, bovine serum albumin (BSA) derived from cows and λ-DNA derived from lambda phage virus replaced biofilm extracellular proteins and DNA, as the corresponding abacterial proxies (Fig. 3-3).

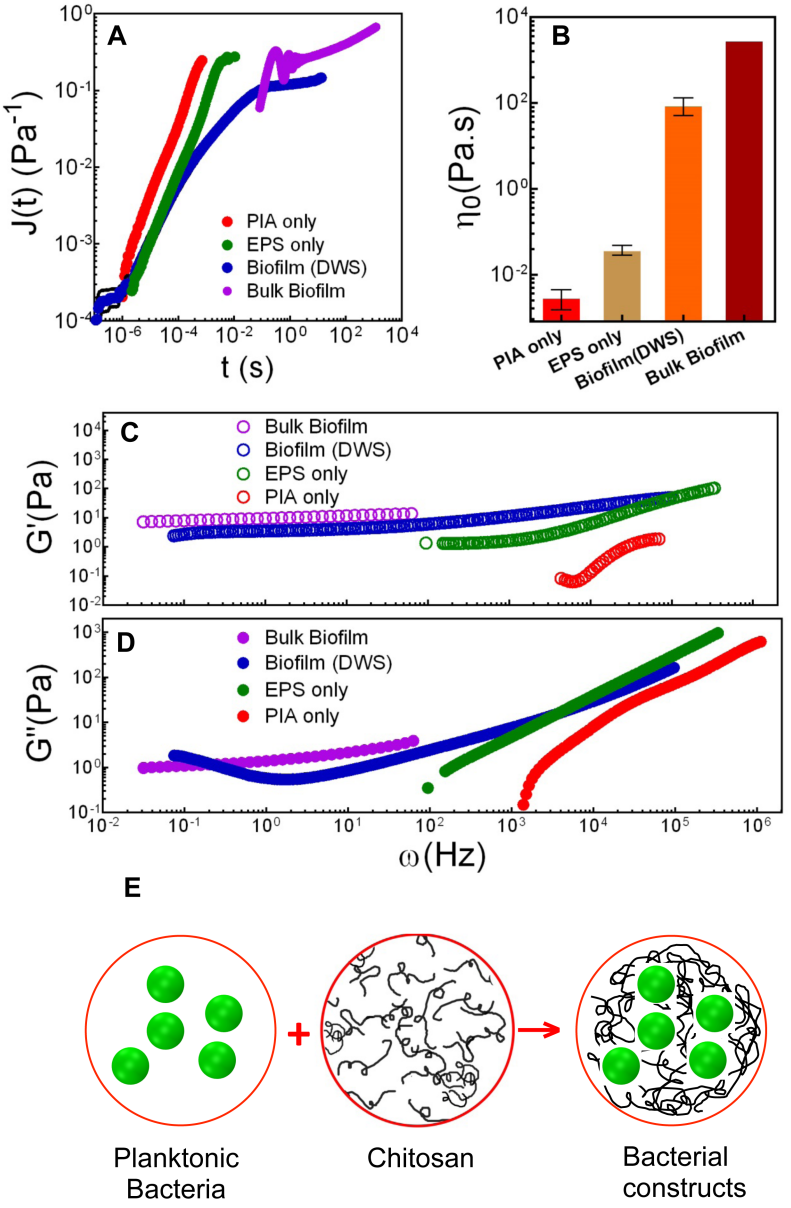

Figure 3-2: Mechanical properties of *S. epidermidis* biofilms and its constituent polymers. (A to D) Creep compliance, J(t) (A), viscosity, η_0, (B), storage modulus, G', (C) and loss modulus, G", (D) of PIA(0.016 g/mL), EPS (containing PIA at 0.016 g/mL) and cultured *S. epidermidis* biofilms. Bulk biofilm data are from [6] (E) Process to create biofilm-like bacterial constructs. This figure is reprinted from the submitted paper of [E.J. Stewart, M. Ganesan, J.G. Younger, & M.J. Solomon]. This figure was created by Mahesh Ganesan.

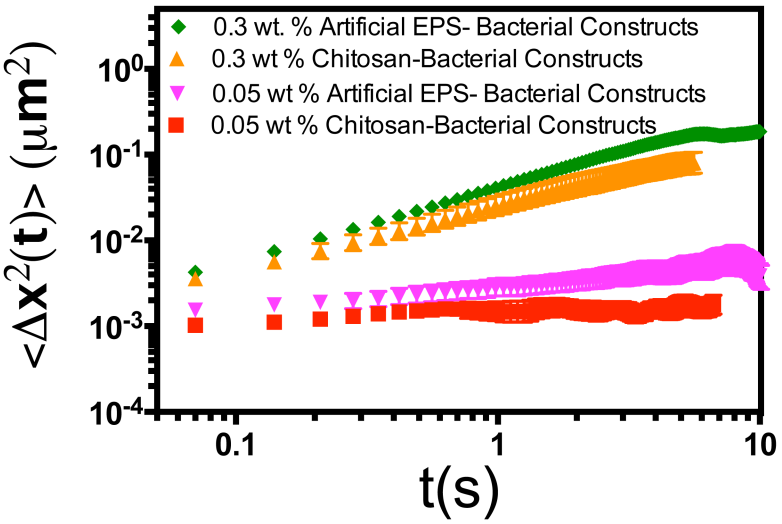

Figure 3-3: MSD of artificial EPS Constructs. The $\langle \Delta x^2(\Delta t) \rangle$ of the constructs with 0.3 wt. % chitosan and the 0.3 wt. % chitosan with λ-DNA and BSA or artificial EPS constructs are similar to one another as is the case with the 0.05 wt.% chitosan and 0.05 wt. % artificial EPS. Thus, the effects of the λ-DNA and BSA are small compared to that of the chitosan. This figure is reprinted from the submitted paper of [E.J. Stewart, M. Ganesan, J.G. Younger, & M.J. Solomon].

Artificial high cellular density biofilms were self-assembled using an initially dilute suspension of cells and chitosan at 0.3 wt. % and pH=4.3 ± 0.02 (Fig. 3-4*A*, Fig. 3-4*B*). The number density of cells was 0.162 ± 0.001 cells/μm^3, similar to the naturally occurring high-density phenotype of *S. epidermidis* (0.2 cells/ μm^3 or greater) [9]. A 3D confocal laser scanning microscopy (CLSM) rendering of bacterial centroids within the artificial biofilm shows that the cells span the volume heterogeneously, like natural biofilms[7,8] (compare Fig. 3-4*A* to 3-4*D*, Fig. 3-4*B* to 3-4*E*, and Fig. 3-4*C* to 3-4*F*).

The cellular radial distribution function, g(r) – the probability of finding a cell at a distance r from a reference bacterium – quantifies the microscale morphology [9]. The high-density construct g(r) is characteristic of a densely packed, disordered microstructure (Fig. 3-4*G*). The peak at r = 0.5 μm is due to cell division while the peak at r = 1.0 μm matches the primary g(r) peak of natural biofilms of the equivalent density phenotype (Fig. 3-4*H*).

Artificial low cellular density biofilms (local number density = 0.017 ± 0.002 cells/ μm^3) were created from initially dilute planktonic cells and chitosan at 0.05 wt. % and pH = 5.3 ± 0.1. These constructs were qualitatively more clustered than high density constructs, and had cellular densities that matched natural low-density phenotype biofilms (0.06 cells/μm^3 or less). They displayed open structures (Fig. 3-4*I*, 3-4*J*) and were spatially heterogeneous (Fig. 3-4*K*) like their natural equivalents (Fig. 3-4*L*, 3-4*M*, 3-4*N*). The g(r) peak values of 14 for the constructs and 18 for the natural system confirm their similarity (Fig. 3-4*O*, 3-4*P*).

Thus, Fig. 3-4 shows that the microstructure of bacterial biofilms is not necessarily mediated through genetic processes alone, as shown by using self-assembly of an abacterial polymeric component and cells to create microstructures that match natural biofilms. Previous work on biofilms has not accounted for self-assembly as a factor dictating observed structures.

The mean squared displacement, $\langle \Delta x^2(t) \rangle$, of cells in the bacterial-chitosan construct characterizes its rheology [46]. Cells of the high density construct are less mobile than planktonic cells but the near-linear increase in $\langle \Delta x^2(t) \rangle$ indicates viscous behavior (Fig. 3-5*A*). Natural biofilms however exhibit a plateau in $\langle \Delta x^2(t) \rangle$ (Fig. 3-5*A*), characteristic of elastic behavior.

Cells in the low density construct show nearly time independent $\langle \Delta x^2(t) \rangle$, consistent with an elastic modulus ~ 2.6 Pa (Fig. 3-5*A*). Native *S. epidermidis* biofilms have an elastic modulus

of ~ 3.7 Pa, as inferred from the plateau in Fig. 3-2*A*. This difference between construct and biofilm modulus is small compared to the ~ 10^4 variability reported for natural biofilms [4].

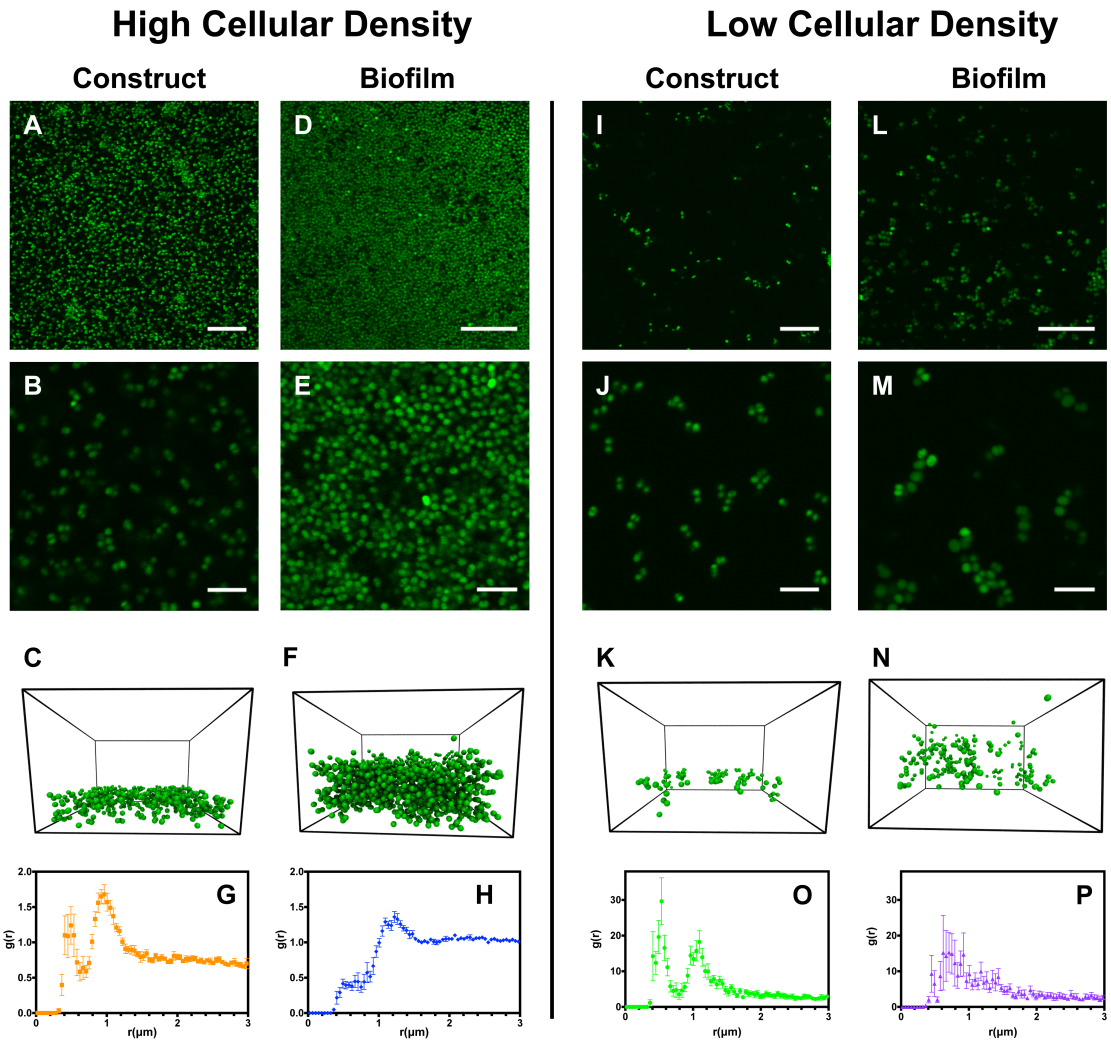

Figure 3-4: Microstructure of high and low cellular density *S. epidermidis*-chitosan constructs and biofilms. Left half compares high cellular density constructs (pH = 4.3) and high-density biofilms; right half compares low cellular density constructs (pH = 5.3) and low-density biofilms. First and second rows: CLSM images of (A and B) high cellular density bacteria-chitosan constructs; (D and E) high-density biofilms, (I and J) low cellular density constructs, and (L and M) low-density biofilms. Third row (C, F, K, and N): volume renderings of bacterial positions. Fourth row: g(r) of (G) high cellular density constructs, (H) high-density *S. epidermidis* biofilms, (O) low cellular density constructs, and (P) low-density *S. epidermidis* biofilms. Scale bars, 20 μm (A, D, I, and L) and 5 μm (B, E, J, and M). This figure is reprinted from the submitted paper of [E.J. Stewart, M. Ganesan, J.G. Younger, & M.J. Solomon].

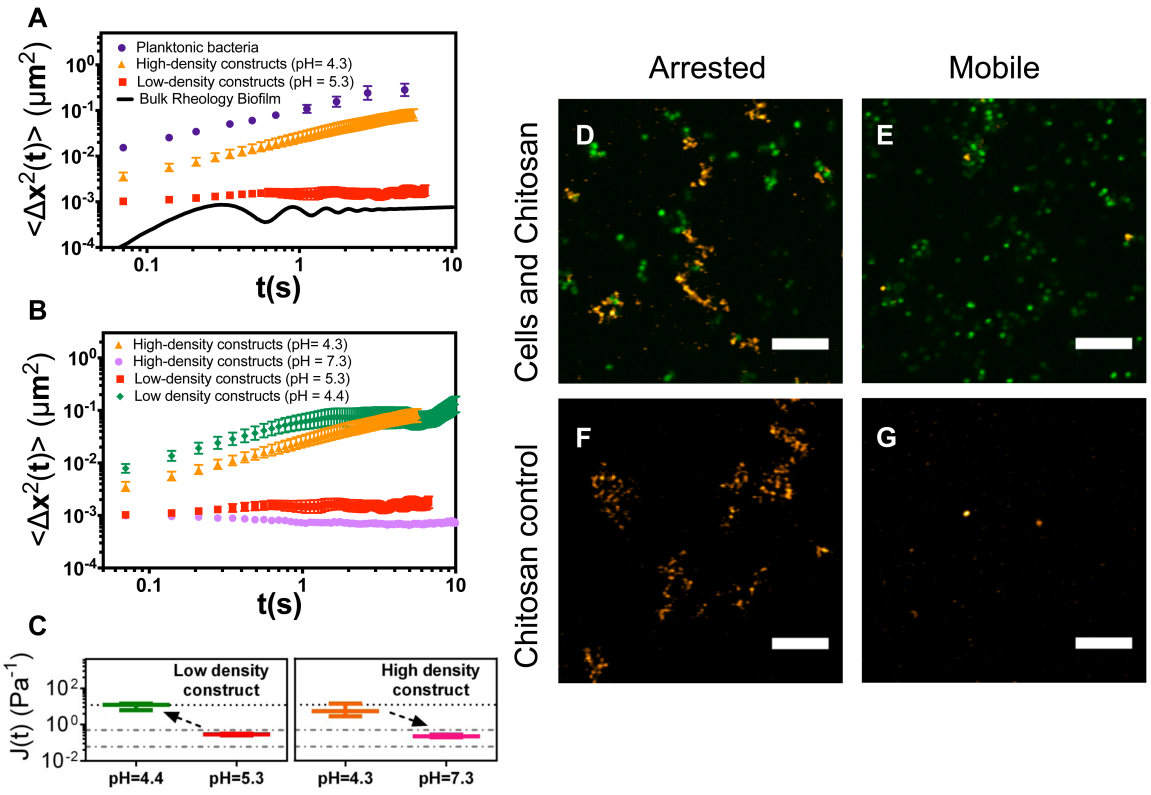

Figure 3-5: Effect of pH on dynamics of high and low cellular density bacterial constructs and chitosan. (A) $\langle \Delta x^2(t) \rangle$, of planktonic bacteria and bacteria in high (pH = 4.3) and low (pH = 5.3) cellular density constructs compared with biofilm $\langle \Delta x^2(t) \rangle$ inferred from ref [6]. (B) $\langle \Delta x^2(t) \rangle$ of high cellular density constructs before (pH = 4.3) and after (pH = 7.3) pH is increased, and low cellular density constructs before (pH = 5.3) and after (pH = 4.4) pH is decreased. (C) J(t) of high and low-density constructs before and after pH changes; arrows indicate the direction of pH change. The upper dotted line is J(t) of planktonic cells. The dotted dashed lines bound the J(t) observed for *S. epidermidis* biofilms [6]. (D) CLSM image of cells and 0.05 wt. % chitosan at pH = 5.3. (E) CLSM image of cells and 0.3 wt. % chitosan at pH = 4.3. (F) 0.05 wt. % chitosan in tryptic soy broth (TSB) with 1 wt. % added glucose. (G) 0.3 wt. % chitosan in TSB with 1 wt. % added glucose. Scale bars, 10 μm (D, E, F, and G). This figure is reprinted from the submitted paper of [E.J. Stewart, M. Ganesan, J.G. Younger, & M.J. Solomon]. Panel C was created by Mahesh Ganesan.

It is remarkable that the cells in the low-density construct (0.05 wt. % chitosan) are localized, consistent with a viscoelastic biofilm, while cells in the high-density construct (3.0 wt. % chitosan) are not localized. There is no indication of this dynamical difference in the microstructure reported in Fig. 3-4. Thus, cellular localization and elasticity of the bacterial-

chitosan constructs are correlated neither with increased cell density nor chitosan concentration (Fig. 3-6).

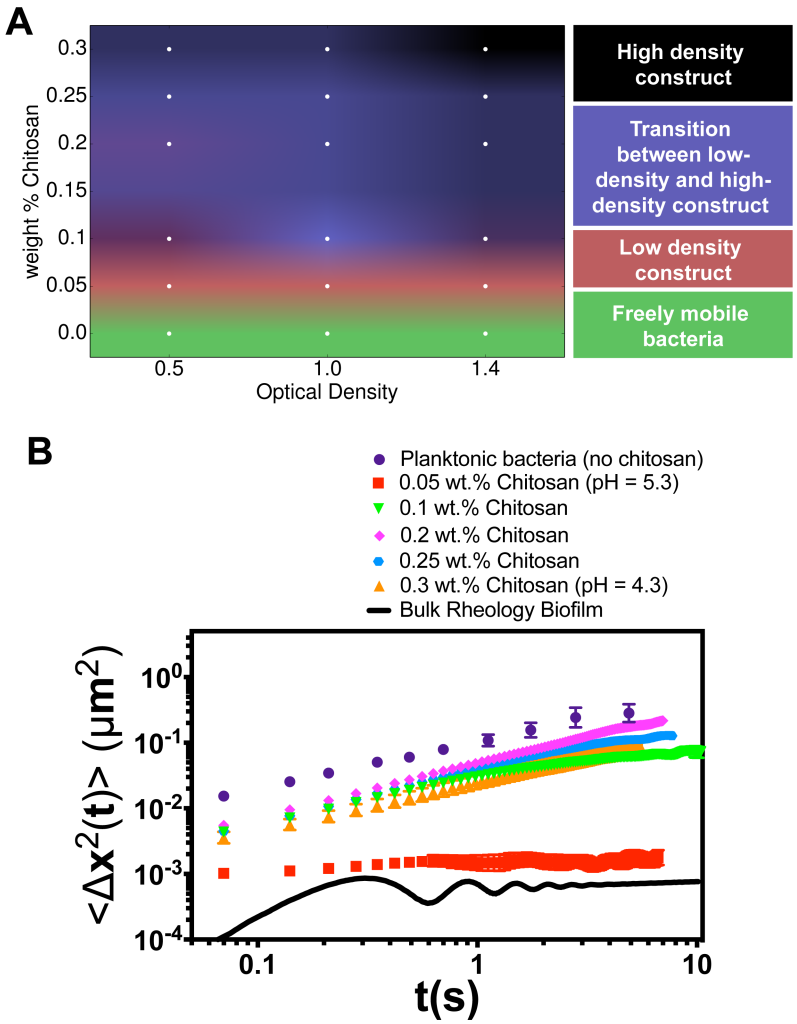

Figure 3-6: Dynamics of other bacteria and chitosan concentrations probed. (A) Phase diagram of construct mobility, per visual observation, in which three dynamical regimes exist. The first regime is that of fully mobile planktonic bacteria; the second is the arrested state of the 0.05 wt. % chitosan constructs; the third is a slowed state, present between 0.1 and 0.25 wt. % in which dynamics are intermediate to the planktonic and arrested states. (B) $\langle \Delta x^2(\Delta t) \rangle$ of constructs with all chitosan concentrations probed. There is a transition region between the arrested state of the 0.05 wt. % chitosan constructs and the 0.3 wt. % chitosan where the mobility increases to nearly that of the planktonic cells before decreasing to the slowed state of the 0.3 wt. % chitosan constructs. This figure is reprinted from the submitted paper of [E.J. Stewart, M. Ganesan, J.G. Younger, & M.J. Solomon].

Instead, pH of the artificial biofilm controls whether it is viscous or elastic. When pH of the high cellular density construct was increased from 4.3 to 7.3, the cellular $\langle \Delta x^2(t) \rangle$ transitioned from viscous diffusion to elastic localization (Fig. 3-5*B*). Analogously, when pH of the low-density bacterial construct was decreased from 5.3 to 4.4, the mobility of cells increased and approached that of free bacteria (Fig. 3-5*B*). J(t) of both high and low-density constructs at a pH= 4.4 was just below that of free bacteria (Fig. 3-5*C*). When the pH is 5.3 and 7.4 for the low- and high-density constructs, respectively, J(t) approximates that of native biofilms (Fig. 3-5*C*).

Visualization of chitosan within the arrested and mobile constructs reveals the effect of pH (Fig. 3-5*D*, 3-5*E*). At pH = 5.3, chitosan formed a stringy network between the bacterial cells that visibly spanned the image volume (Fig. 3-5*D*). However, at pH=4.3, the stringy chitosan network was absent, due to the molecular-level dispersion of chitosan (Fig. 3-5*E*). Control experiments without cells (Fig. 3-5*F*, 3-5*G*) confirmed the pH effect. Thus, at low pH (4.3), the polymer is stable and uniformly dispersed. At high pH (5.3) the polymer is unstable and present as an aggregated, stringy network.

Figures 3-4 and 3-5 support the central role of self-assembly in producing biofilm structure and dynamics. Specifically, the solvent pH mediated chitosan phase instability yields polymer aggregation (Fig. 3-5*D*) that then dynamically arrests the *S. epidermidis* cells, and generates biofilm-like viscoelasticity.

If chitosan phase instability is critical to the bacterial construct viscoelasticity, then EPS phase instability might also control the viscoelasticity of naturally occurring biofilms. Figures 3-7*A*, 3-7*B* compare the pH dependent absorbance of chitosan and *S. epidermidis* EPS. Consistent with the results of Fig 3-5*D*-*G*, chitosan showed a significant increase in turbidity, as measured by the absorbance at pH ~ 7, marking a transition from a stable phase at low pH to an unstable

phase at high pH. In the *S. epidermidis* EPS, the effect of pH on stability is reversed; the EPS is stable at high pH and unstable at low pH, with a transition at pH ~ 7. This reversal generates a non-trivial prediction for *S. epidermidis* biofilm viscoelasticity, namely, that a change in natural biofilm pH from low to high will result in a loss of biofilm viscoelasticity.

Figure 3-7*C*, 3-7*D* tests this prediction. When the pH of a natural *S. epidermidis* biofilm was increased from 5.0 to 6.1, the biofilm bacteria remained arrested (Fig. 3-7*C*); however, at a pH of 7.3, mobility increased and approached that of planktonic bacteria (Fig. 3-7*C*). This change in biofilm mechanics occurs at a pH where the EPS absorbance is low, consistent with thermodynamic stability of the EPS.

A matrix of 0.3 wt. % chitosan becomes unstable at pH = 7.1, consistent with the transition from a mobile to an arrested construct between pH = 5.6 – 7.3 (Fig. 3-7*D*). When EPS is the matrix, it transitions between stable and unstable phases at pH 7. High-density *S. epidermidis* biofilms transition from their native arrested state to a viscous mobile state between pH= 6.2 - 7.0. The antipodal pH dependence of the artificial constructs and natural biofilms is conserved in both their matrix stability (as measured by absorbance) and their mechanics (as measured by $\langle \Delta x^2(t) \rangle$).

Staphylococcus aureus biofilms secrete the same EPS polysaccharide as *S. epidermidis*[47]. When *S. aureus* biofilm pH was increased from 4.6 to 6.9, the $\langle \Delta x^2(t) \rangle$ increased by a factor of four (Fig. 3-7*E*). This increased mobility indicates a weakening of the biofilm (Fig. 3-7*F*), just as for *S. epidermidis*, which shows that our finding holds true in multiple species of biofilms.

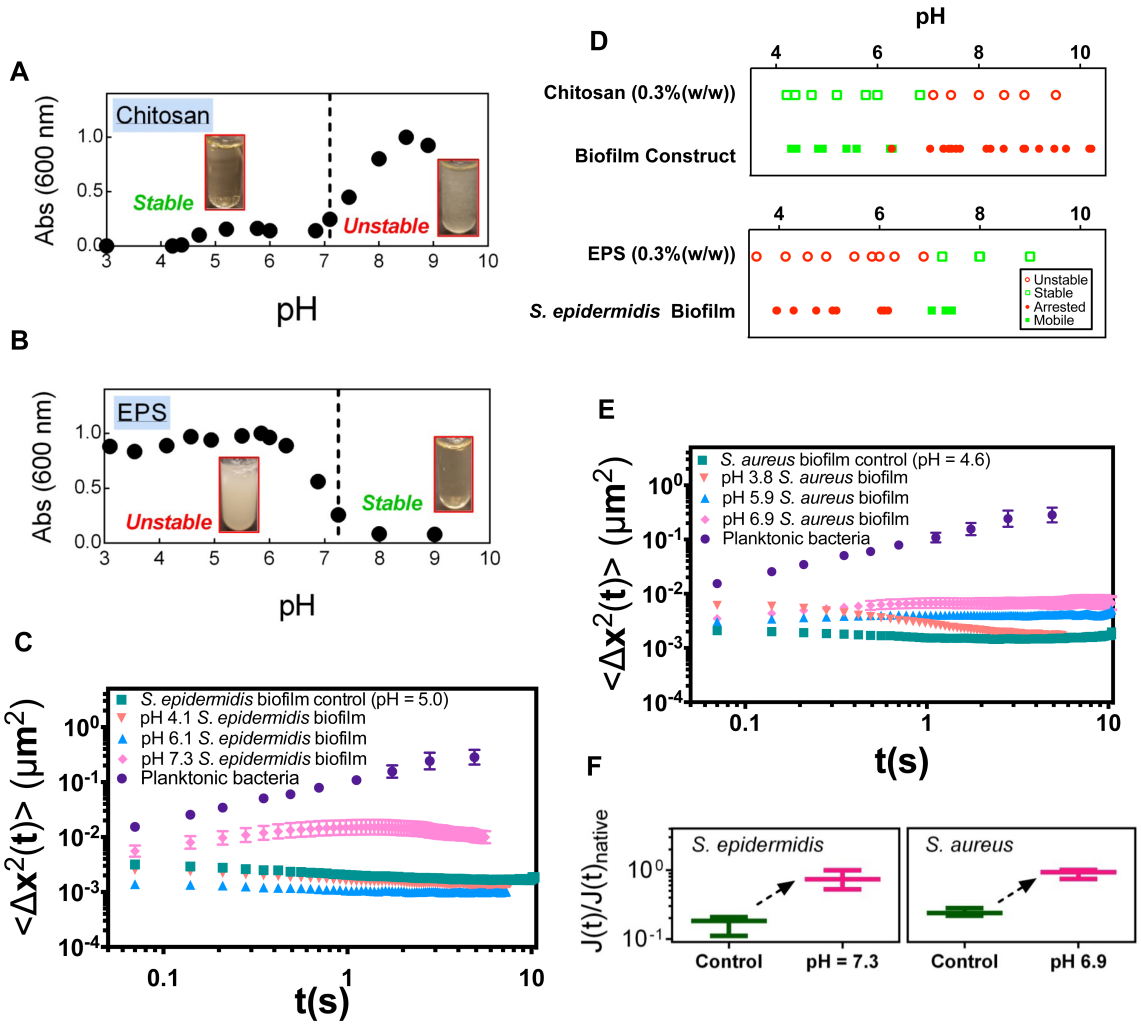

Figure 3-7: Effect of pH on the stability/mobility of chitosan, EPS, and natural biofilms. Absorbance versus pH of 0.3 wt. % chitosan (A) and 0.3 wt.% *Staphylococcal* biofilm EPS (B) in TSB. (C) $\langle \Delta x^2(t) \rangle$ of *S. epidermidis* planktonic bacteria, 18-hour biofilm, and 18-hour biofilms with pH adjusted to 4.1, 6.1, and 7.3. (D) Comparison of 0.3 wt. % chitosan stability and the mobility of 0.3 wt. % bacterial-chitosan constructs, as well as the stability of 0.3 wt. % EPS and the mobility of 18-hour *S. epidermidis* biofilms at pH 4-10. (E) $\langle \Delta x^2(t) \rangle$ of planktonic cells, *S. aureus* 18-hour biofilm, and 18-hour biofilms with pH adjusted to 3.8, 5.8, and 6.9. (F) Normalized J(t) of *S. epidermidis* and *S. aureus* biofilms at their native growth condition and after increasing the pH to 7.3 and 6.9, respectively. This figure is reprinted from the submitted paper of [E.J. Stewart, M. Ganesan, J.G. Younger, & M.J. Solomon]. Panels A, B, F and parts of D were created by Mahesh Ganesan.

Therefore, the Fig. 3-7 findings introduce self-assembly as a factor in both biofilm formation and dispersal. First, the correlation between the EPS phase stability and the mechanics of the construct indicates that the viscoelasticity of biofilms is not just an additive effect of the individual mechanics of polymers and cells, but instead includes cross contributions generated by associations between polymeric species that are mediated by the state of the solvent environment. The presence of pH microenvironments within biofilms [11] and the self-association of PIA at low pH [21] indicate that bacteria produce polymers that exhibit poor solvent behavior in their growth environment. Second, the presence of high and low density phenotypes that span viscous to elastic mechanics depending on local pH offers a possible explanation for the recently observed spatial variation of the compliance within bacterial biofilms [14]. Particularly, the presence of pH microenvironments and the connection of pH to EPS phase stability, could facilitate microbial survival by promoting either the formation or breakdown of biofilm elasticity. pH variation within the biofilm can be a consequence of metabolism; the role of pH in mediating biofilm elasticity presents an interesting coupling between metabolism and mechanical properties.

The finding that EPS phase stability controls biofilm morphology and mechanics therefore has both scientific and practical implications. Scientifically, the presence of pH microenvironments in biofilms raises the interesting possibility of a relationship to the pH-dependent stability of the biofilm EPS. pH dependent EPS phase stability may also have implications for biofilm disassembly and dispersion—a poorly understood but broadly recognized phenomena of the biofilm lifecycle. Finally, practically, the correlation between EPS stability and biofilm softening suggests a biofilm control strategy in which EPS solubilization is induced by pH change.

3.5 References

(1) Costerton, J. W.; Stewart, P. S.; Greenberg, E. P. *Science* **1999**, *284*, 1318; Vlamakis, H.; Chai, Y.; Beauregard, P.; Losick, R.; Kolter, R. *Nature Reviews Microbiology* **2013**, *11*, 157-168.

(2) Hall-Stoodley, L.; Costerton, J. W.; Stoodley, P. *Nature Reviews Microbiology* **2004**, *2*, 95-108.

(3) Shaw, T.; Winston, M.; Rupp, C. J.; Klapper, I.; Stoodley, P. *Physical Review Letters* **2004**, *93*, 098102.

(4) Böl, M.; Ehret, A. E.; Bolea Albero, A.; Hellriegel, J.; Krull, R. *Critical Reviews in Biotechnology* **2013**, *33*, 145-171.

(5) Guélon, T.; Mathias, J.-D.; Stoodley, P. **2011**, *Biofilm Highlights*, 111-139.

(6) Pavlovsky, L.; Younger, J. G.; Solomon, M. J. *Soft Matter* **2013**, *9*, 122-131.

(7) Xavier, J. B.; White, D. C.; Almeida, J. S. *Water Science & Technology* **2003**, *47*, 31-37; Beyenal, H.; Donovan, C.; Lewandowski, Z.; Harkin, G. *Journal of Microbiological Methods* **2004**, *59*, 395-413.

(8) Bridier, A.; Dubois-Brissonnet, F.; Boubetra, A.; Thomas, V.; Briandet, R. *Journal of Microbiological Methods* **2010**, *82*, 64-70.

(9) Stewart, E. J.; Satorius, A. E.; Younger, J. G.; Solomon, M. J. *Langmuir* **2013**, *29*, 7017-7024.

(10) Berk, V.; Fong, J. C. N.; Dempsey, G. T.; Develioglu, O. N.; Zhuang, X.; Liphardt, J.; Yildiz, F. H.; Chu, S. *Science* **2012**, *337*, 236-239.

(11) Hidalgo, G.; Burns, A.; Herz, E.; Hay, A. G.; Houston, P. L.; Wiesner, U.; Lion, L. W. *Applied and Environmental Microbiology* **2009**, *75*, 7426-7435.

(12) Stewart, P. S.; Franklin, M. J. *Nature Reviews Microbiology* **2008**, *6*, 199-210.

(13) Birjiniuk, A.; Billings, N.; Nance, E.; Hanes, J.; Ribbeck, K.; Doyle, P. S. *New Journal of Physics* **2014**, *16*, 85014.

(14) Galy, O.; Latour-Lambert, P.; Zrelli, K.; Ghigo, J.-M.; Beloin, C.; Henry, N. *Biophysical Journal* **2012**, *103*, 1400-1408.

(15) Xavier, J. B.; Martinez-Garcia, E.; Foster, K. R. *The American Naturalist* **2009**, *174*, 1-12.

(16) Flemming, H.-C.; Wingender, J. *Nature Reviews Microbiology* **2010**, *8*, 623-633.

(17) Kim, M. K.; Drescher, K.; Pak, O. S.; Bassler, B. L.; Stone, H. A. *New Journal of Physics* **2014**, *16*.

(18) Hohne, D. N.; Younger, J. G.; Solomon, M. J. *Langmuir* **2009**, *25*, 7743-7751.

(19) Dorken, G.; Ferguson, G. P.; French, C. E.; Poon, W. C. K. *Journal of The Royal Society Interface* **2012**, *9*, 3490-3502.

(20) Schwarz-Linek, J.; Winkler, A.; Wilson, L. G.; Pham, N. T.; Schilling, T.; Poon, W. C. K. *Soft Matter* **2010**, *6*, 4540-4549.

(21) Ganesan, M.; Stewart, E. J.; Szafranski, J.; Satorius, A. E.; Younger, J. G.; Solomon, M. J. *Biomacromolecules* **2013**, *14*, 1474-1481.

(22) Sadovskaya, I.; Vinogradov, E.; Flahaut, S.; Kogan, G.; Jabbouri, S. *Infection and Immunity* **2005**, *73*, 3007-3017.

(23) Smith, R. L.; Gilkerson, E. *Analytical biochemistry* **1979**, *98*, 478-480.

(24) Lu, Q.; Solomon, M. J. *Physical Review E* **2002**, *66*, 061504.

(25) Dasgupta, B. R.; Tee, S.-Y.; Crocker, J. C.; Frisken, B. J.; Weitz, D. A. *Physical Review E* **2002**, *65*, 051505.

(26) Xu, J.; Viasnoff, V.; Wirtz, D. *Rheologica Acta* **1998**, *37*, 387-398.

(27) Scheffold, F.; Skipetrov, S. E.; Romer, S.; Schurtenberger, P. *Physical Review E* **2001**, *63*, 061404.

(28) Pine, D. J.; Weitz, D. A.; Maret, G.; Wolf, P. E.; Herbolzheimer, E.; Chaikin, P. M. *Series on Directions in Condensed Matter Physics* **1990**, *Scattering and Localization of Classical Waves in Random Media*, 312-372.

(29) Sinha, S. K.; Freltoft, T.; Kjems, J. *Kinetics of Aggregation and Gelation* **1984**, *Kinetics of Aggregation and Gelation*, 87-90.

(30) Kaplan, P. D.; Yodh, A. G.; Pine, D. J. *Physical Review Letters* **1992**, *68*, 393.

(31) Anthonsen, M. W.; Vårum, K. M.; Hermansson, A. M.; Smidsrød, O.; Brant, D. A. *Carbohydrate polymers* **1994**, *25*, 13-23.

(32) Il'ina, A. V.; Varlamov, V. P. *Applied Biochemistry and Microbiology* **2005**, *41*, 5-11.

(33) Mao, H.-Q.; Roy, K.; Troung-Le, V. L.; Janes, K. A.; Lin, K. Y.; Wang, Y.; August, J. T.; Leong, K. W. *Journal of Controlled Release* **2001**, *70*, 399-421.

(34) Cerca, F.; Andrade, F.; França, Â.; Andrade, E. B.; Ribeiro, A.; Almeida, A. A.; Cerca, N.; Pier, G.; Azeredo, J.; Vilanova, M. *Journal of Medical Microbiology* **2011**, *60*, 1717-1724.

(35) Lindgren, J. K.; Thomas, V. C.; Olson, M. E.; Chaudhari, S. S.; Nuxoll, A. S.; Schaeffer, C. R.; Lindgren, K. E.; Jones, J.; Zimmerman, M. C.; Dunman, P. M. *Journal of Bacteriology* **2014**, *196*, 2277-2289.

(36) Wang, F.; Raval, Y.; Chen, H.; Tzeng, T. J.; DesJardins, J. D.; Anker, J. N. *Advanced Healthcare Materials* **2014**, *3*, 197-204.

(37) Crocker, J. C.; Grier, D. G. *Journal of Colloid and Interface Science* **1996**, *179*, 298-310.

(38) Dibble, C. J.; Kogan, M.; Solomon, M. J. *Physical Review E* **2006**, *74*, 041403.

(39) Hsiao, L. C.; Kang, H.; Ahn, K. H.; Solomon, M. J. *Soft Matter* **2014**, *10*, 9254-9259.

(40) Otto, M. *Nature Reviews Microbiology* **2009**, *7*, 555-567.

(41) Rohde, H.; Frankenberger, S.; Zähringer, U.; Mack, D. *European Journal of Cell Biology* **2010**, *89*, 103-111.

(42) Wilking, J. N.; Angelini, T. E.; Seminara, A.; Brenner, M. P.; Weitz, D. A. *MRS Bulletin* **2011**, *36*, 385-391.

(43) Sutherland, I. W. *Microbiology* **2001**, *147*, 3-9.

(44) Zaccarelli, E. *Journal of Physics: Condensed Matter* **2007**, *19*, 323101.

(45) Rinaudo, M. *Progress in Polymer Science* **2006**, *31*, 603-632.

(46) Squires, T. M.; Mason, T. G. *Annual Review of Fluid Mechanics* **2009**, *42*, 413.

(47) Joyce, J. G.; Abeygunawardana, C.; Xu, Q.; Cook, J. C.; Hepler, R.; Przysiecki, C. T.; Grimm, K. M.; Roper, K.; Ip, C. C. Y.; Cope, L. *Carbohydrate research* **2003**, *338*, 903-922.

Chapter 4

Effect of antimicrobial and physical treatments on growth of multispecies *Staphylococcal* biofilms[**]

4.1 Abstract

The prevalence and structure of *Staphylococcus aureus* and *Staphylococcus epidermidis* within their multispecies biofilms was found to vary depending on both the physical and antimicrobial environment. Although these species commonly infect similar orthopedic infection sites, little is know about how they compete or cooperate with one another, particularly during treatment. We find that *S. aureus* is much more prevalent than *S. epidermidis w*hen grown in common, unstressed, growth conditions—tryptic soy broth with 1% glucose at 37°C at neutral pH. However, growth at higher temperature (45°C) resulted in an environment where *S. aureus* became more porous. This porosity allowed *S. epidermidis* to colonize more of the surface. Alternatively, variations in the pH environment resulted in increased prevalence of *S. epidermidis* at low pH (5, 6), while *S. aureus* remained the dominant species at high pH (8, 9). Application of different vancomycin dosages generated variable behaviors: *S. epidermidis* is the more prevalent species at 1.0 μg/mL vancomycin, but reduced growth of both species occurs at

[**] This chapter is in preparation for publication by [E.J. Stewart, D.E. Payne, B.R. Boles, J.G. Younger, & M.J. Solomon].

1.9 μg/mL vancomycin. This variability is consistent with the different minimum inhibitory concentrations (MIC) of *S. aureus* and of *S. epidermidis*. This work establishes the structural variability of multispecies staphylococcal biofilms as they undergo physical and antimicrobial treatments. It therefore provides a basis for understanding the structures communities of these species may form at orthopedic infection sites.

4.2 Introduction

Staphylococci are a prominent cause of acute and chronic infections. 79% of orthopedic implant-associated infections are from staphylococcal species. *Staphylococcus aureus* is responsible for 34% of these infections while *Staphylococcus epidermidis* accounts for 32% of them[1]. Both *S. aureus* and and *S. epidermidis* are non-motile, gram-positive cocci of the genus *Staphylococcus*. Both species are capable of forming biofilms—structured communities of cells that are encapsulated in a matrix of polysaccharides, proteins, and DNA. Biofilms have been shown to impact the persistence of chronic infections[2]. Though *S. aureus* is considered to be more virulent than *S. epidermidis,* treatment of biofilms formed by both species is difficult due to the resistance of their biofilm phenotypes to antimicrobials or other treatment methods [2].

Although biofilms formed from *S. aureus* and *S. epidermidis* are responsible for the majority of prosthetic joint infections [3,4], the species may be introduced to the infection site at different times, since the onset of prosthetic joint infections varies from one patient to another. When a prosthetic joint infection occurs less than 3 months postoperatively, it is referred to as an early infection; most early infections are caused by *S. aureus* [3,4]. Delayed infections of prosthetic joints occur between 3-24 months postoperatively, and are frequently caused by less virulent bacteria, such as *S. epidermidis* [3,4]. Late infections occur at times greater than 24 months postoperatively and are mainly caused by haematogenous seeding—where the bacteria

are introduced to the infection site via the bloodstream—or reoccurrence of inadequately treated early infections [3, 4]. Haematogenous seeding is especially high for patients with *S. aureus* bacteremia [5]. The occurrence of prosthetic joint infections breaks down in the following way: 29% are caused by early infection, 41% are caused by delayed infection, and 30% are caused by late infection [6]. The majority of these infections are culture positive for only one organism; however, 10-16% are classified as polymicrobial [1, 4], and 10-11% of these infections have no detected microorganisms [4].

In addition to being found at the same sites of prosthetic joint infections, *S. aureus* and *S. epidermidis* also colonize the human nares (nostrils) [7]. *S. aureus* persistently or intermittently resides in the nasal cavity of 50% of the population [7], and its presence in the nasal cavity has been linked to *S. aureus* bacteremia [8]. When compared to a healthy population, in-patient nasal microbiotas are enriched in *S. aureus* and *S. epidermidis* [7]. Within the in-patient population, the abundance of *S. aureus* was negatively correlated with the abundance of *S. epidermidis* [7]. When *S. epidermidis* was the dominant species within the in-patient nares, *S. epidermidis* was 43.7% of the microbiota and *S. aureus* was 0.1% of the microbiota [7]. When *S. aureus* was dominant in the in-patient population, it made up 46.1% of the microbiota and *S. epidermidis* was 8.2% of the nasal microbiota [7]. One study indicated that the excretion of serine protease Esp from a subset of *S. epidermidis* species inhibits biofilm formation and nasal colonization of *S. aureus* [9].

Polymicrobial biofilm communities are known as multispecies biofilms. Most studies of biofilms involve a single species; however, in many natural environments biofilms grow in structured multispecies communities[10, 11]. The presence of multiple species is able to impact the development and shape of the community [12]. The interactions between species within a multispecies biofilm can be competitive or cooperative [12, 13], and the spatial heterogeneity that

results from the interactions between species can impact the ability of cells to communicate with one another [12]. Multispecies biofilms are typically organized in one of three general ways. They can be organized into single species microcolonies where each species is clustered together [12]. The two species can co-aggregate and form a biofilm that has cells of each species located next to one another. Finally, layering can occur, where one species is found in the upper layers and another is found in the lower layers [12]. The structural behavior between the species has also been shown to be dependent not just on the presence of the additional species, but also on the environmental surroundings of the organisms [12]. Structures within multispecies biofilms have been analyzed through the use of COMSTAT—a computer program developed in MatLab to quantify biofilm structures such as thicknesses or biomass volumes [14]. Specific features that have been quantified within multispecies biofilms are the biomass volume of each bacterial population [15], the distribution of distances between the surfaces of microcolonies of different species [16], and the distribution of biomass at various depths within the sample [17].

Biofilms can be controlled through the use of a variety of treatment methods. Clinically, *S. aureus* and *S. epidermidis* biofilm infections are commonly treated using the antibiotic vancomycin [2]. Sub-lethal concentrations of vancomycin also produce *S. epidermidis* biofilms with open, porous structures [18]. High temperatures (45°C) have recently been reported as a potential treatment method for *S. aureus* and *S. epidermidis*[19], and temperature has been shown to have an effect on the mechanical properties of the biofilm [20]. Temperatures as high as 45°C have safely been used in hyperthermia treatment of cancer cells [21, 22]; thus, temperature treatment may be a viable treatment method for bacterial infections as well. Increased pH (> 7) has also been shown to soften the mechanical properties of *S. aureus* and *S. epidermidis* biofilms when used as

a treatment after biofilms have formed [23]. Low pH may be an opportune growth environment for *S. epidermidis* since it typically resides on the skin where pH is 4.0-7.0 [24].

In this work, we evaluate the spatial structure of *S. aureus* and *S. epidermidis* in multispecies biofilms grown in a variety of physical and antibiotic treatment conditions. Due to the prevalence of both species in prosthetic joint infections and the nares, there is ground to consider the degree to which each of these organisms impacts the growth and structure of the other when they form a multispecies community. We pose the following questions through our work: A) How are the structure and cellular growth kinetics of single species biofilms of *S. aureus* and *S. epidermidis* impacted by the introduction of an additional species? B) How do physical (temperature and pH) and sub-lethal antibiotic (vancomycin) treatments affect the typical organization of a *S. aureus* and *S. epidermidis* multispecies biofilm?

We find that *S. aureus* is the dominant species within multispecies biofilms grown in unstressed conditions; however varying the growth environment can significantly shift the *S. aureus* dominance. Understanding the general growth behavior of these multispecies communities with and without treatment creates a basis for understanding the effects – intended or not – that treatment methods may have on an infection site if more than one species of bacteria is present.

4.3 Materials and Methods

4.3.1 Bacterial strains

S. aureus SH 1000 (BB 386) [25] was used.. It is a commonly used model strain of *S. aureus* [26]. Colonies of *S. aureus* were cultured on tryptic soy agar (TSA).

S. epidermidis 1457/pCM29 (AH2982) was used as the *S. epidermidis* strain in our experiments (kindly provided by A. Horswill, University of Iowa). *S. epidermidis* 1457 transformed with pCM29 [27]—a green fluorescent protein(GFP) reporter with a *sarA* P1 promotor, which is maintained in tryptic soy broth(TSB) or TSA supplemented with 10 μg/mL chloramphenicol—was chosen due to its ability to constitutively express GFP. *S. epidermidis* 1457 is a commonly used biofilm forming strain of *S. epidermidis*. Colonies of *S. epidermidis* were cultured on TSA with 10 μg/mL chloramphenicol. We chose a strain of *S. epidermidis* with a fluorescent reporter in order to distinguish *S. epidermidis* cells from *S. aureus* cells within multispecies biofilms that were grown.

4.3.2 Single and multispecies biofilm growth conditions

Biofilms were grown in Nunc™ Lab-Tek™ II Chambered Coverglass dishes (Thermo Scientific, USA) for 18 hours at 60 RPM at 37°C, unless otherwise noted. We grew single species biofilms by inoculating a single colony of either *S. aureus* SH1000 or *S. epidermidis* 1457/pCM29 in 400 μL of tryptic soy broth with 1% glucose (TSB_G). For multispecies biofilms, we inoculated a single colony of *S. aureus* SH1000 and a single colony of *S. epidermidis* 1457/pCM29 in the growth media. After 18 hours, bacteria were stained with 5 μM Syto 59 (Molecular Probes, USA) for 30 minutes prior to imaging. Syto 59 was chosen for staining bacteria because the excitation and emission are 622 nm and 645 nm, respectively. These are much higher than the excitation and emission of GFP, which enables us to distinguish the *S. epidermidis* cells from the *S. aureus* cells in the multispecies biofilms. *S. epidermidis* is identified by the GFP and *S. aureus* is located by identifying regions where Syto59 is present, but GFP is not. Three replicates were performed for each growth condition.

4.3.3 Biofilm kinetics

Biofilm kinetic experiments were performed by growing single (*S. aureus* alone*; S. epidermidis* alone), and multispecies (*S. aureus* with *S. epidermidis*) biofilms for 1, 2, 4, 6, 12, and 18 hours in 400 µL of TSB_G. Three replicates were performed at each time point for each single and multispecies biofilm.

4.3.4 Temporal addition of species to biofilm

Multispecies biofilms were grown for which either *S. aureus* or *S. epidermidis* was given a lead time of 1, 2, 4, 6, 9, 12, or 15 hours before the second species of bacteria, *S. epidermidis* or *S. aureus,* respectively, was introduced through inoculation of a single colony in the supernatant of the biofilm well. These multispecies biofilms were grown for a total of 18 hours at 37°C in 400 µL TSB_G. Each experimental condition was performed in triplicate.

4.3.5 Sub-lethal antibiotic, temperature, and pH biofilm growth conditions

We considered single and multispecies growth in sub-lethal vancomycin growth conditions. We grew biofilms in both 1.0, and 1.9 µg/mL vancomycin to determine the effect of varying concentrations of sub-lethal vancomycin. Vancomycin is an antibiotic commonly used to treat both *S. aureus* and *S. epidermidis* infections [2].

Single (*S. aureus* alone*; S. epidermidis* alone), and multispecies (*S .aureus* and *S. epidermidis*) biofilms were grown in triplicate for 18 hours in TSB_G at 45°C and compared to biofilms grown at 37°C.

We grew single (*S. aureus* alone*; S. epidermidis* alone), and multispecies (*S. aureus* and *S. epidermidis*) biofilms for 18 hours at 37°C in TSB_G with a pH adjusted to pH = 5, 6, 8, or 9. pH was adjusted using 1 M HCl to lower the pH and 1 M NaOH to increase the pH. We probed

this range of pH values, because *S. epidermidis* biofilms have been found to grow at pH values ranging from 4.5-7.5 [28], and planktonic *S. aureus* growth has been shown to decrease as pH drops from 7 to 4.5 [29]. Additionally, staphylococcal biofilms treated with higher pH media have been shown to soften their mechanical properties at higher pH [23]. Three replicates were performed for each pH growth condition.

4.3.6 Confocal Laser Scanning Microscopy Imaging and Analysis

We imaged samples using a Nikon A1Rsi confocal laser scanning microscope with a 100x, 1.45 NA, oil immersion objective lens. The excitation wavelength was 488 nm for the GFP within the *S. epidermidis* samples, and 641 nm for the Syto59. The GFP channel was used for identifying *S. epidermidis,* while the Syto59 was used for identifying the total biomass since it stains both the *S. aureus* and the *S. epidermidis* cells. Three-dimensional image volumes of size 128 x 128 x ~3-15 μm^3 were collected for each biofilm grown and used to assess biofilm growth. Most biofilm volumes were 10-15 μm high. Volumes that were ~3 μm were only obtained when growth was sparse i.e.) at short times (< 4 hours) or in high stress growth conditions (1.9 μg/mL vancomycin). Total biomass of multispecies biofilms was assessed using Syto 59, which stains the eDNA of all cells present, and *S. epidermidis* biomass was evaluated by the presence of GFP.

Images were inspected visually to determine the trends within the data. Images representative of each condition are reported in the figures. For projections of representative CLSM biofilm volumes, the Z project tool is used in ImageJ to create a composite image where the sum of the pixels from all the slices is displayed. Biomass within image volumes was quantified using the computer program COMSTAT (a program developed in MatLab to quantify biofilm structures[14]). The average biomass from three samples and the standard error of the

mean are reported. Biomass was determined for the Syto 59 channel and the GFP channel of each image. The total biomass is reported using the Syto59 channel. *S. epidermidis* biomass is reported as the GFP channel. *S. aureus* biomass is approximated by subtracting the GFP channel from the Syto 59 channel.

4.4 Results and Discussion

Our results yield a comparison of the prevalence of *S. aureus* and *S. epidermidis* in multispecies biofilm grown at a variety of physical (T and pH) and antibiotic (vancomycin) growth conditions. We first conduct a kinetic study to determine the typical behavior of *S. aureus* and *S. epidermidis* in single and multispecies biofilms grown in an unstressed growth environment (37°C, pH =7). We then consider multispecies biofilm growth at sub-lethal vancomycin concentrations (1.0, 1.9 μg/mL), an elevated temperature (45°C), and increased and decreased pH values (pH = 5, 6, 8, 9). Using the results from the unstressed condition, we assess the deviations from the norm that occur at the physical and antibiotic treatment conditions.

4.4.1 Kinetics of single and multispecies growth

To provide a baseline for studying multispecies biofilms, we considered the kinetic growth of *S. aureus* and *S. epidermidis* single species biofilms and compared this kinetics with the growth of multispecies biofilms consisting of *S. aureus* and *S. epidermidis*. Based on the planktonic growth curves of *S. aureus* and *S. epidermidis* (Fig. 4-1A), we expected that *S. aureus* biofilm development would be faster than *S. epidermidis* biofilm development. We found that it took *S. aureus* ~ 4 hours to colonize the majority of the substrate surface (Fig. 4-1B), while *S. epidermidis* took ~8 hours to form a contiguous biofilm (Fig. 4-1C). Thus, our hypothesis based on the growth rates of the planktonic species was validated. This aligned with previous work

showing that *S. aureus* colonizes surfaces more rapidly than *S. epidermidis* on different surfaces[30].

After 18 hours both *S. aureus* and *S. epidermidis* biofilms were structurally similar with densely packed and space-spanning structures similar to those previously observed in unstressed biofilms that were grown in flow cells [18] (Fig. 4-1D, 4-1E). The 18 hour *S. aureus* and *S. epidermidis* biofilms had similar biomasses, where *S. aureus* had a biomass of 6.7±0.6 $\mu m^3/\mu m^2$ and *S. epidermidis* had a biomass of 6.2±1.3 $\mu m^3/\mu m^2$ (Fig 4-1H).

In the multispecies biofilm that consisted of both *S. aureus* and *S. epidermidis*, substrate coverage was obtained at ~4 hours of growth (Fig. 4-1F), which was similar to the time for substrate coverage in *S. aureus* biofilms. After 18 hours the multispecies biofilm consisted mainly of *S. aureus* cells (Fig. 4-1G). The overall biomass was 5.69±0.98 $\mu m^3/\mu m^2$, which was similar to that of the single species biofilms (Fig. 4-1H). In 18 hour multispecies biofilms, *S. aureus* biomass was 5.66±0.98 $\mu m^3/\mu m^2$ and *S. epidermidis* growth was minimal with a biomass of 0.03±0.02 $\mu m^3/\mu m^2$ (Fig. 4-1H).

Figure 4-2 shows the kinetic development of single and multispecies *S. aureus* and *S. epidermidis* biofilms. The kinetics of the multispecies biofilm appeared to be the additive accumulation of the single species until ~4 hours of growth at which the majority of the surface was covered by *S. aureus*, and then the *S. aureus* dominated the growth (Fig. 4-2). Thus, in the common biofilm growth environment of tryptic soy broth with 1% glucose (TSB_G) at 37°C and a pH of 7, *S. aureus* is the dominant species, densely packed, and spans the imaged volume. In multispecies biofilms at this condition (TSB_G, 37°C, pH 7), *S. epidermidis* is in small clusters

that are not very connected to each other. The total biomass is space filling and densely packed without many large pores present within the volume.

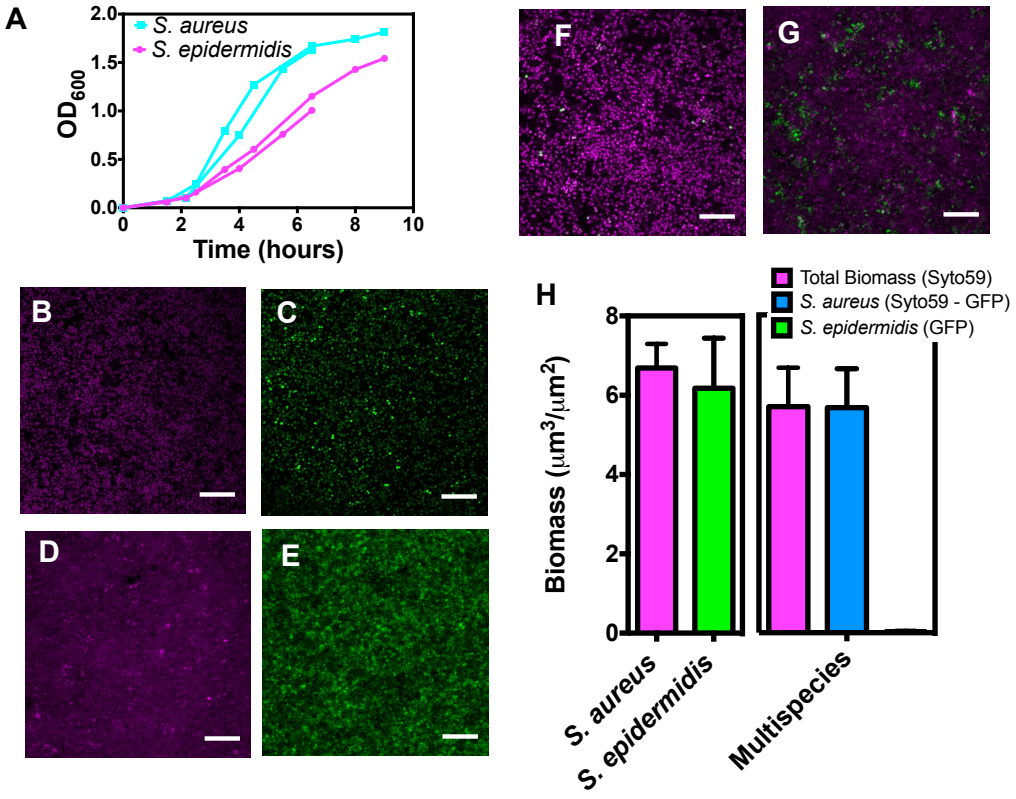

Figure 4-1: Typical planktonic and single and multispecies biofilm growth of *S. aureus* and *S. epidermidis*. (A) Growth curves of planktonic *S. aureus* and *S. epidermidis*. (B) CLSM image of *S. aureus* substrate surface coverage at 4 hours. (C) CLSM image of *S. epidermidis* surface coverage at 8 hours. Sum of intensities from a 3D image volumes of (D) an 18 hour *S. aureus* biofilm, (E) an 18 hour *S. epidermidis* biofilm. (F) CLSM image of *S. aureus* and *S. epidermidis* surface coverage in a multispecies biofilm at 4 hours. (G) Sum of intensities from a 3D image volume of an 18-hour multispecies biofilm. Scale bars: 20 μm. (H) Plot of average biomasses in 18 hour *S. aureus, S. epidermidis,* and multispecies biofilms. This figure is in preparation for publication by [E.J. Stewart, D.E. Payne, B.R. Boles, J.G. Younger, & M.J. Solomon].

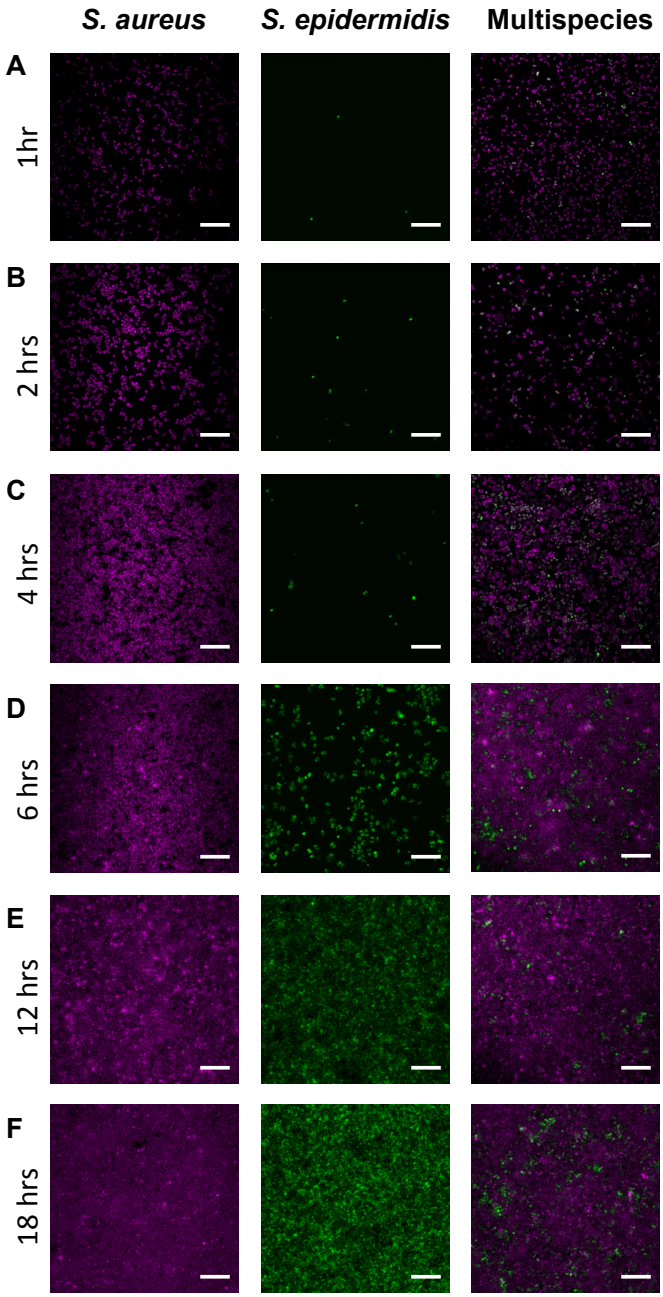

Figure 4-2: Kinetic growth of *S. aureus*, *S. epidermidis*, and multispecies biofilms from 1 to 18 hours. Sums of slices from confocal image volumes of representative *S. aureus* biofilms (left column), *S. epidermidis* biofilms (center column), and multispecies biofilms (right column) at the following time points: (A) 1 hr, (B) 2 hrs, (C) 4 hrs, (D) 6 hrs, (E) 12 hrs, and (F) 18 hrs, where each row is labeled with a letter. Scale bars: 20 µm. This figure is in preparation for publication by [E.J. Stewart, D.E. Payne, B.R. Boles, J.G. Younger, & M.J. Solomon].

4.4.2 Temporally variable addition of second species to a single species biofilm

Since *S. aureus* had a planktonic growth rate higher than that of *S. epidermidis*, it was not surprising that *S. aureus* was the dominant species within biofilms where both *S. epidermidis* and *S. aureus* were inoculated within the growth media at the same time. Because *S. epidermidis* took ~8 hours to achieve full surface coverage of the substrate in a single species biofilm (Fig. 4-1C), we hypothesized that *S. epidermidis* would require ~8 hours of lead-time to colonize the substrate of the biofilm, and allow *S. epidermidis* to be the dominant species within the multispecies biofilm.

Figure 4-3 shows the temporal addition of *S. epidermidis* to *S. aureus* biofilms after giving *S. aureus* an inoculation lead-time of 1, 2, 4, and 6 hours (Fig. 4-33 A-H) and the temporal addition of *S. aureus* to *S. epidermidis* biofilms after *S. epidermidis* has been given a lead-time of 1, 2, 4, and 6 hours (Fig. 4-3I-P). We found that *S. epidermidis* is able to become the dominant species within the biofilm if given a lead-time of 4-6 hours (Fig. 4-3K/O, 4-3L/P). It takes ~6 hours for the biofilm to be nearly all *S. epidermidis* (Fig. 4-3L/P), which is three times longer than the ~2 hours of lead-time necessary for *S. aureus* to nearly eliminate the population of *S. epidermidis* to only a few single cells (Fig. 4-3B/F). In addition to the immediate understanding of the impact of temporal addition of a second species within our system, this result is valuable clinically since pathogens are not guaranteed to colonize a surface at the same time. An example of this is haematogenous seeding at a previously infected site. Though the time scales of our experiments may not be the same as those found clinically, biofilm development may be slower at a prosthetic joint infection site as well and similar multispecies structures may be capable of developing at infection sites on different time scales. Our work

suggests that the order of bacteria seeding and lead-time for single species growth at an infection site impacts the structure of the multispecies community.

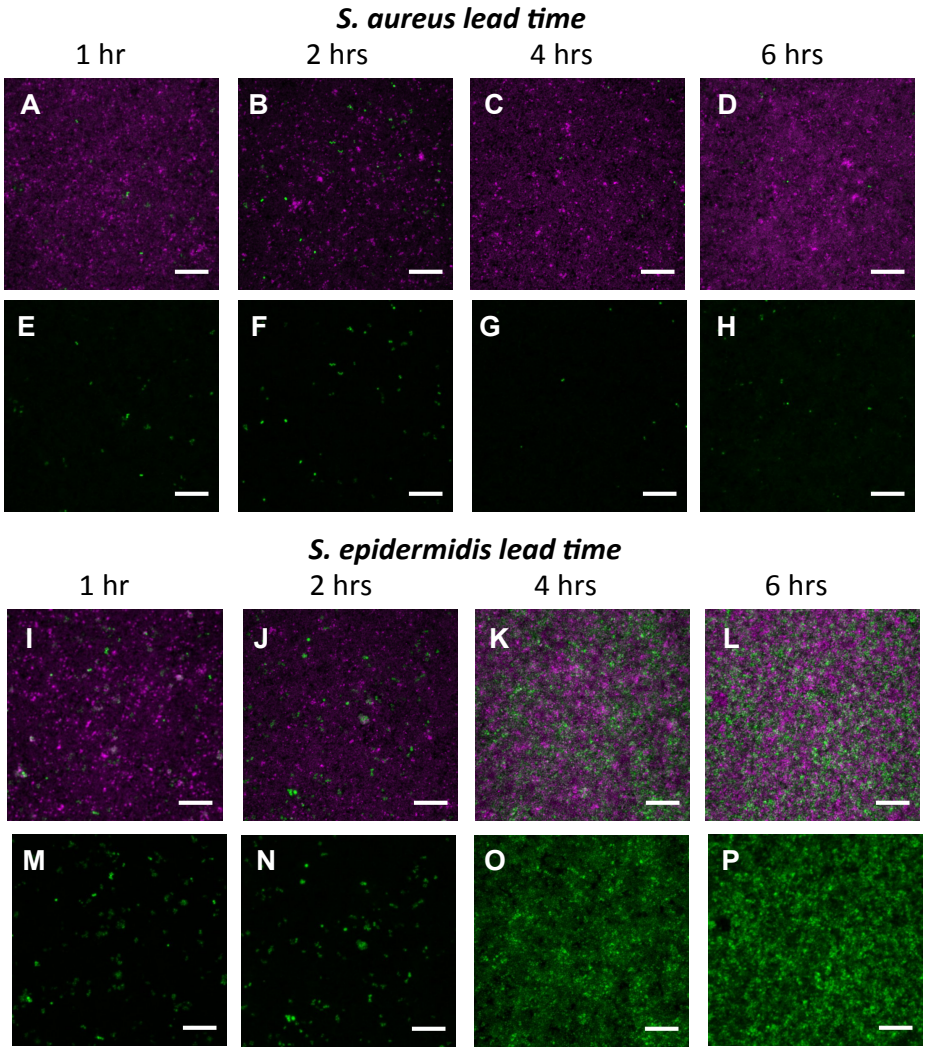

Figure 4-3: Temporal addition of second species to *S. aureus* and *S. epidermidis* multispecies biofilms. The top row shows multispecies biofilms where *S. aureus* has been given a lead-time of (A) 1 hour, (B) 2 hours, (C) 4 hours, and (D) 6 hours before *S. epidermidis* is introduced. (E-H) show the *S. epidermidis* growth (the GFP channel only) of the images immediately above them. The third row shows multispecies biofilms where *S. epidermidis* has been given a lead-time of (I) 1 hour, (J) 2 hours, (K) 4 hours, and (L) 6 hours before *S. aureus* is introduced. (M-P) show the *S. epidermidis* growth (the GFP channel only) of the images immediately above them. The total growth is 18 hours for all sums of slices from 3D image volumes. Scale bars: 20 µm. This figure is in preparation for publication by [E.J. Stewart, D.E. Payne, B.R. Boles, J.G. Younger, & M.J. Solomon].

4.4.3 Effect of sub-lethal vancomycin on multispecies biofilms

S. aureus and *S. epidermidis* infections are commonly treated with vancomycin [2]. Vancomycin is an antibiotic that inhibits the formation of the bacterial cell wall and interferes with peptidoglycan synthesis in gram-positive bacteria [3]. The minimum inhibitory concentration (MIC)—the lowest concentration of antibiotic required to inhibit visible bacterial growth after overnight culture—is different for *S. aureus* than for *S. epidermidis*. The MIC of vancomycin for *S. aureus* is ~ 1 μg/mL; for *S. epidermidis* it is ~ 2 μg/mL [31]. We therefore investigated two sub-lethal vancomycin concentrations: 1 μg/mL vancomycin, which is near the MIC of *S. aureus,* and 1.9 μg/mL, which is just under the MIC of *S. epidermidis*. Figure 4-4 shows the behavior of multispecies biofilms at each of these vancomycin concentrations.

When the concentration of vancomycin was 1.0 μg/mL, *S. epidermidis* was the dominant species. *S. epidermidis* grew a porous biofilm at this condition, but there were still regions of *S. aureus* within the volume (Fig. 4-4A). The regions of growth containing predominantly *S. aureus* seemed to have extracellular DNA present as indicated by the Syto59 not being localized to the interior of the cell, as shown by the bright pink regions within the image that are larger than regular cell size (Fig. 4-4B). The total biomass at 1.0 μg/mL was similar to that of multispecies biofilms without vancomycin, but *S. epidermidis* is the dominant species instead of *S. aureus* (Fig. 4-4A, 4-4G). This is consistent with our expectations since the vancomycin MIC for *S. aureus* is ~1 μg/mL and the vancomycin MIC for *S. epidermidis* is ~2 μg/mL [31].

When the concentration of vancomycin was 1.9 μg/mL, a concentration just below the vancomycin MIC of *S. epidermidis*, the total biomass of all organisms was reduced (Fig. 4-4G). However, the growth was heterogeneous at this concentration of vancomycin. In some cases

there was more *S. aureus* than *S. epidermidis* (Fig. 4C) and in others there was more *S. epidermidis* than *S. aureus* (Fig. 4D). To emphasize the prevalence of *S. epidermidis* in Fig. 4D, we show the *S. epidemidis* channel in Fig. 4E. The degree to which growth was decreased varied as well with some volumes containing extremely sparse growth (Fig. 4F) and some with larger clusters of cells (Fig. 4C, 4D).

The effectiveness of an antibiotic is dependent on the concentration. Lethal antibiotic concentrations vary from one species to another. Variations in the concentration of antibiotic reaching bacteria within a biofilm may prevent the growth of one species but allow another to prosper. This work shows that variation in the sub-lethal concentrations of vancomycin yields different growth behavior for each species within multispecies biofilm communities.

4.4.4 Effect of temperature on multispecies growth

The effect of antibiotics becomes limited when bacteria form their biofilm phenotype; thus, novel prophylactic and therapeutic solutions are necessary [5]. Recent work has shown that increased temperatures may disrupt mature *S. aureus* and *S. epidermidis* biofilms and their mechanical properties[19, 32]. Given this work for single species biofilms, we here investigate the effect of temperature on their multispecies biofilms.

We found that when multispecies biofilms consisting of *S. aureus* and *S. epidermidis* were grown at 45°C, the biofilm that formed was more porous than multispecies staphylococcal biofilms grown at 37°C (compare Fig. 4-5A and 4-5B). This increase in porosity corresponded with a decrease in the total biomass of the biofilm(Fig. 5C). In particular, the *S. aureus* formed a less continuous structure at 45°C in comparison to the biofilms formed at 37°C. The porous nature of the *S. aureus* biofilm at the substrate surface allowed for an increase *S. epidermidis* at

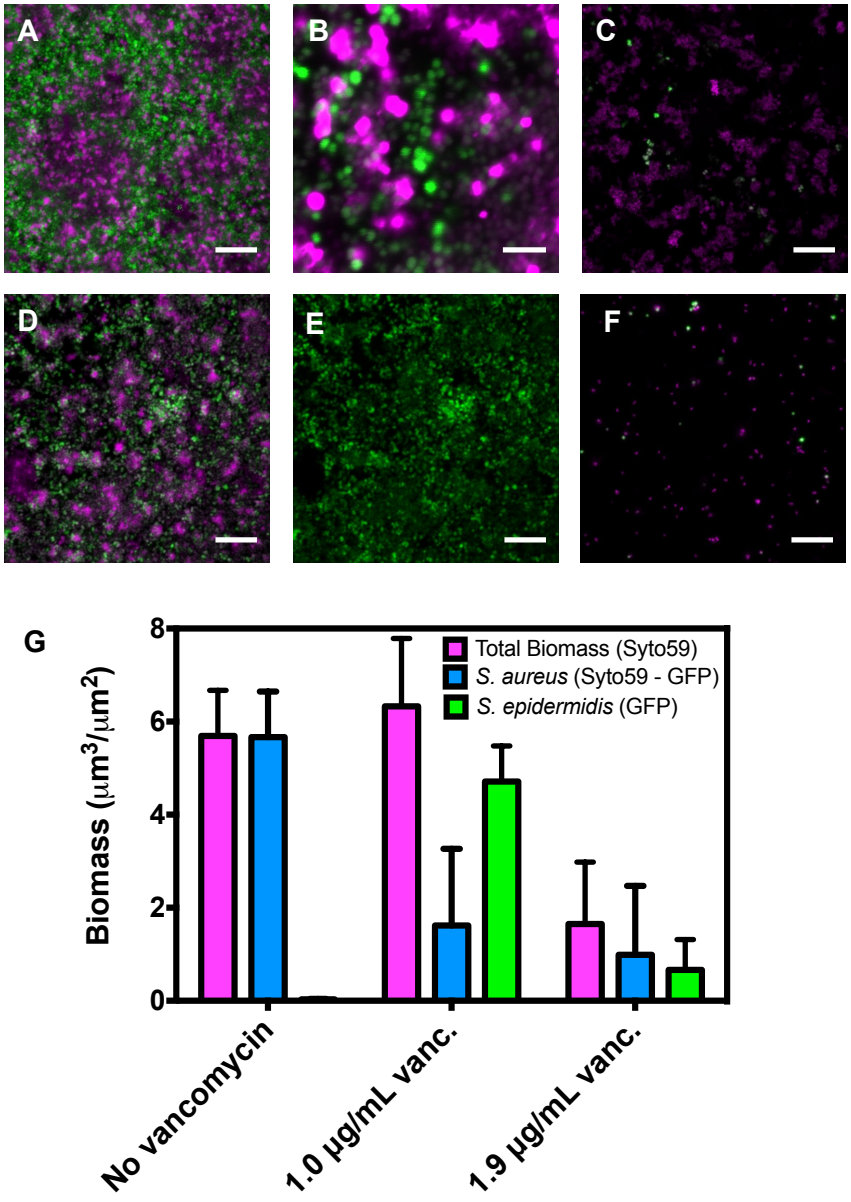

Figure 4-4: Effect of sub-lethal vancomycin on multispecies biofilms. (A) Sum of intensities from a CLSM volume of a multispecies biofilm grown in 1.0 μg/mL vancomycin (Volume height: 8.5 μm). Scale bar: 20 μm. (B) Image of potential eDNA within multispecies biofilm grown in 1.0 μg/mL vancomycin. The bright pink regions that are much larger than regular cell size are presumable eDNA. Scale bar: 5 μm. Sum of intensities from a CLSM image volume of a multispecies biofilm grown in 1.9 μg/mL vancomycin, where (C) *S. aureus* has outgrown *S. epidermidis* (Volume height: 9.3 μm), (D) *S. epidermidis* has outgrown *S. aureus* (the *S. epidermidis* channel of this image is shown in panel E), (Volume height: 6.0 μm), and (F) growth is sparse in both species(Volume height: 6.3 μm). Scale bars: 20 μm. (G) Plot of changes in total, *S. aureus* and *S. epidermidis* biomasses with vancomycin concentrations of 0, 1.0, and 1.9 μg/mL. This figure is in preparation for publication by [E.J. Stewart, D.E. Payne, B.R. Boles, J.G. Younger, & M.J. Solomon].

the substrate surface. This increase of *S. epidermidis* at the substrate surface is consistent with the increase in *S. epidermidis* biomass (Fig. 4-5C).

Increased temperatures have been used in hyperthermia treatment of cancer cells [33]. Our result shows that hyperthermia treatments may also be a viable treatment for disrupting multispecies biofilm infections; however, this treatment would need to be augmented with an additional treatment approach.

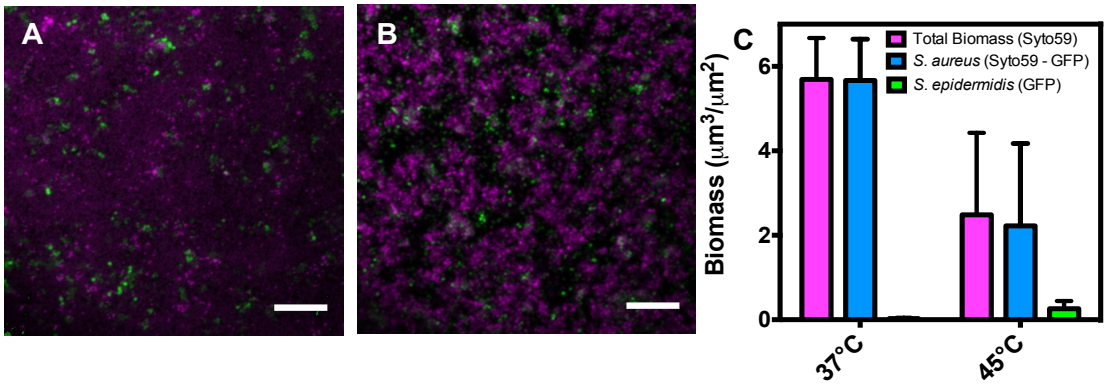

Figure 4-5: Effect of increased temperature on multispecies biofilms. Sum of intensities of CLSM volumes of multispecies biofilms grown for 18 hours at (A) 37°C and (B) 45°C. Scale bars: 20 μm. (C) Plot of changes in total, *S. aureus* and *S. epidermidis* biomasses with temperature in multispecies biofilms. This figure is in preparation for publication by [E.J. Stewart, D.E. Payne, B.R. Boles, J.G. Younger, & M.J. Solomon].

4.4.5 Multispecies growth in varying pH conditions

Another potential approach for disrupting biofilms is pH treatment of biofilms. Recently, both *S. aureus* and *S. epidermidis* biofilms mechanical properties have been softened through increasing the pH environment of the biofilm. Adjustment of biofilm pH to greater than 7 was suggested as a potential treatment method for disrupting biofilms and softening their mechanical properties [23]. *S. epidermidis* survives in the low pH conditions of the skin, which ranges from pH

4.0-7.0 [24]. Thus, at low pH *S. epidermidis* may be capable of being the prevalent species and at high pH we may expect for the biofilm to be more sparsely populated due to the weakening of the biofilm mechanical properties at high pH [23]. *S. aureus* may be less densely populated at lower pH, since planktonic *S. aureus* growth has been shown to decrease as pH drops from 7 to 4.5 [29].

We found that *S. epidermidis* dominates growth when multispecies biofilms are grown at lower pH conditions. At pH 5, the biofilm became predominantly *S. epidermidis* (Fig. 4-6A, 4-6F); additionally, the overall biomass was reduced compared to the biofilms observed at pH 7 (Fig. 4-6C, 4-6F). At pH 6, there was more *S. epidermidis* than in the control at pH 7; however, there were still large regions containing *S. aureus* (Fig. 4-6B, 4-6F). The dominant behavior of *S. epidermidis* at low pH can be understood as a consequence of the *S. epidermidis* fitness for the low pH environment of the skin.

When multispecies biofilms were grown at higher pH values, we found that *S. epidermidis* does not incorporate into the biofilm very well and remains predominantly in the planktonic form with *S. aureus* as the dominant organism. Specifically, at pH 8, the biofilm behaves similarly to the multispecies biofilm grown at pH 7, where there are large regions of *S. aureus* with small clusters of *S. epidermidis* throughout the biofilm (Fig. 4-6D, 4-6F). At pH 9, *S. aureus* remains the dominant species in the biofilm (Fig. 4-6E, 4-6F).

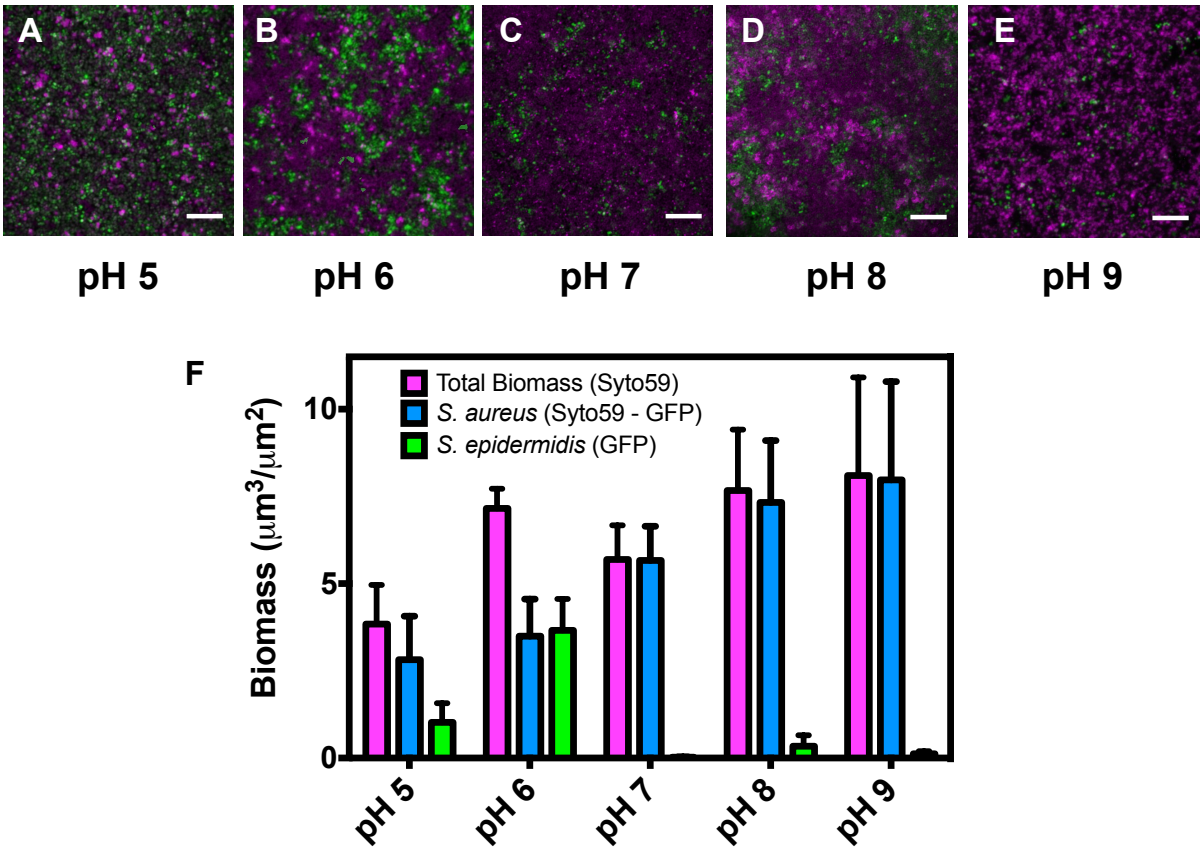

Figure 4-6: Effect of pH on multispecies biofilms. *S. aureus* and *S. epidermidis* multispecies biofilms grown at: (A) pH 5, (B) pH 6, (C) pH 7, (D) pH 8, and (E) pH 9. Images are sums of all images in a CLSM image volume. Scale bars: 20 μm. (F) Plot of changes in total, *S. aureus* and *S. epidermidis* biomasses with pH. This figure is in preparation for publication by [E.J. Stewart, D.E. Payne, B.R. Boles, J.G. Younger, & M.J. Solomon].

4.5 Conclusions

This work shows that the behavior of multispecies *S. aureus* and *S. epidermidis* biofilms varies greatly from one environmental growth condition to another. In common unstressed growth conditions (37°C, pH 7) *S. aureus* is the dominant species. *S. aureus* also outgrows *S. epidermidis* in conditions of high pH (8, 9) and high temperature (45°C). *S. epidermidis* was the

dominant species at low pH (5) and low concentrations of vancomycin (1.0 μg/mL). In a vancomycin concentration near the MIC of *S. epidermidis* (1.9 μg/mL), the overall biomass decreased; however, the species dominance varied and produced behaviors where sometimes the *S. aureus* grew more than *S. epidermidis* and vice versa. Understanding the general behavior of multispecies communities with and without treatment allows for understanding the unintended effects treatment methods may have on an infection site with more than one species present.

Since *S. aureus* and *S. epidermidis* single and multispecies biofilms may form on a variety of substrate surfaces, it would also be of interest to determine if substrate surfaces impact the structures of the multispecies biofilms that form from *S. aureus* and *S. epidermidis*. Additionally, other species of bacteria are capable of infecting these sites and could be added to these multispecies biofilm to consider how a third bacterial species impacts the structures formed by these species.

Beyond adding virulent pathogens to these communities, non-virulent pathogens could be studied with *S. aureus, S. epidermidis* or *S. aureus* and *S. epidermidis* multispecies biofilms to aid in the development of probiotic treatments for preventing biofilm infections. Probiotic treatment to eliminate growth of virulent pathogens has been gaining traction as a strategy for eliminating biofilm infections, especially since probiotic treatments have successfully been used for treating altered bowel flora [34]. Our work shows that the seedtime and growth environment of the organism used to displace the pathogen is critical to the displacement of the organism. For example, a probiotic solution that grows at a low pH may be a viable solution to displace *S. aureus* biofilm growth; however, this will not be effective against preventing *S. epidermidis* growth. *S. aureus* and *S. epidermidis* can coexist within biofilms together and this work has

established a basis for further understanding the interactions between these two species in additional treatment conditions.

4.6 References

(1) Campoccia, D.; Montanaro, L.; Arciola, C. R. *Biomaterials* **2006**, *27*, 2331-2339.

(2) Kiedrowski, M. R.; Horswill, A. R. *Annals of the New York Academy of Sciences* **2011**, *1241*, 104-121.

(3) Gbejuade, H. O.; Lovering, A. M.; Webb, J. C. *Acta orthopaedica* **2014**, *85.*

(4) Zimmerli, W.; Trampuz, A.; Ochsner, P. E. *New England Journal of Medicine* **2004**, *351*, 1645-1654.

(5) Zimmerli, W. *Journal of internal medicine* **2014**, *276,* 111-119.

(6) Giulieri, S. G.; Graber, P.; Ochsner, P. E.; Zimmerli, W. *Infection* **2004**, *32*, 222-228.

(7) Frank, D. N.; Feazel, L. M.; Bessesen, M. T.; Price, C. S.; Janoff, E. N.; Pace, N. R. *PLoS One* **2010**, *5*, e10598.

(8) Von Eiff, C.; Becker, K.; Machka, K.; Stammer, H.; Peters, G. *New England Journal of Medicine* **2001**, *344*, 11-16.

(9) Iwase, T.; Uehara, Y.; Shinji, H.; Tajima, A.; Seo, H.; Takada, K.; Agata, T.; Mizunoe, Y. *Nature* **2010**, *465*, 346-349.

(10) O'Toole, G.; Kaplan, H. B.; Kolter, R. *Annual Reviews in Microbiology* **2000**, *54*, 49-79.

(11) Stoodley, P.; Sauer, K.; Davies, D. G.; Costerton, J. W. *Annual Reviews in Microbiology* **2002**, *56*, 187-209.

(12) Elias, S.; Banin, E. *FEMS microbiology reviews* **2012**, *36*, 990-1004.

(13) Rendueles, O.; Ghigo, J. *FEMS microbiology reviews* **2012**, *36*, 972-989.

(14) Heydorn, A.; Nielsen, A. T.; Hentzer, M.; Sternberg, C.; Givskov, M.; Ersbøll, B. K.; Molin, S. *Microbiology* **2000**, *146*, 2395-2407.

(15) Hansen, S. K.; Rainey, P. B.; Haagensen, J. A. J.; Molin, S. *Nature* **2007**, *445*, 533-536.

(16) Hansen, S. K.; Haagensen, J. A. J.; Gjermansen, M.; Jørgensen, T. M.; Tolker-Nielsen, T.; Molin, S. *Journal of bacteriology* **2007**, *189*, 4932-4943.

(17) An, D.; Danhorn, T.; Fuqua, C.; Parsek, M. R. *Proceedings of the National Academy of Sciences of the United States of America* **2006**, *103*, 3828-3833.

(18) Stewart, E. J.; Satorius, A. E.; Younger, J. G.; Solomon, M. J. *Langmuir* **2013**, *29*, 7017-7024.

(19) Sturtevant, R. A.; Sharma, P.; Pavlovsky, L.; Solomon, M. J.; Younger, J. G. **2014**, Submitted.

(20) Pavlovsky, L.; Younger, J. G.; Solomon, M. J. *Soft Matter* **2013**, *9*, 122-131.

(21) Henle, K. J.; Leeper, D. B. *Radiology* **1976**, *121*, 451-454.

(22) Joshi, D. S.; Jung, H. *European Journal of Cancer (1965)* **1979**, *15*, 345-350.

(23) Stewart, E. J.; Ganesan, M.; Younger, J. G.; Solomon, M. J. Submitted.

(24) Lambers, H.; Piessens, S.; Bloem, A.; Pronk, H.; Finkel, P. *International journal of cosmetic science* **2006**, *28*, 359-370.

(25) Payne, D. E.; Martin, N. R.; Parzych, K. R.; Rickard, A. H.; Underwood, A.; Boles, B. R. *Infection and immunity* **2013**, *81*, 496-504.

(26) O'Neill, A. J. *Letters in applied microbiology* **2010**, *51*, 358-361.

(27) Pang, Y. Y.; Schwartz, J.; Thoendel, M.; Ackermann, L. W.; Horswill, A. R.; Nauseef, W. M. *Journal of innate immunity* **2010**, *2*, 546-559.

(28) Cerca, F.; Andrade, F.; França, Â.; Andrade, E. B.; Ribeiro, A.; Almeida, A. A.; Cerca, N.; Pier, G.; Azeredo, J.; Vilanova, M. *Journal of Medical Microbiology* **2011**, *60*, 1717-1724.

(29) Buchanan, R. L.; Smith, J. L.; McColgan, C.; Marmer, B. S.; Golden, M.; Dell, B. *Journal of food safety* **1993**, *13*, 159-175.

(30) Barth, E.; Myrvik, Q. M.; Wagner, W.; Gristina, A. G. *Biomaterials* **1989**, *10*, 325-328.

(31) Infectious Disease Management Program at UCSF. http://idmp.ucsf.edu/vancomycin-minimum-inhibitory-concentrations-against-staphylococcus-aureus/ (accessed Dec 16, 2014).

(32) Pavlovsky, L.; Younger, J. G.; Solomon, M. J. *Soft Matter* **2013**, *9*, 122-131.

(33) van der Zee, J. *Annals of oncology* **2002**, *13*, 1173-1184.

(34) Vuotto, C.; Longo, F.; Donelli, G. *International journal of oral science* **2014**, *6,* 189-194.

Chapter 5

Role of sample thickness in label-free visualization of *Staphylococcus epidermidis* biofilm microstructure with confocal Raman microscopy

5.1 Abstract

We found that label-free detection of *Staphylococcus epidermidis* biofilm cellular microstructure using confocal Raman microscopy is possible provided that specimens are thin and not more than a few cell layers thick. Confocal Raman microscopy allowed for label-free detection of cellular related material, as indicated by $-CH_3$ peaks within a biofilm sample. Confocal Raman mapping was compared to bright field microscopy images to qualitatively evaluate the effectiveness of the mapping. We identified that basis analysis of the Raman signal can be used to improve the clarity of biofilm-rich regions in thin biofilm samples.

5.2 Introduction

Bacterial biofilms are structured communities of cells embedded in a matrix comprised of polysaccharides, proteins and DNA [1]. *Staphylococcus epidermidis* is a gram-positive bacterial species, which is a common member of the human skin flora [2]. *S. epidermidis* is one of the most

isolated bacterial pathogens involved in nosocomial (hospital-acquired) infections[2]. The primary component of the *S. epidermidis* matrix is polysaccharide intercellular adhesion (PIA) [3]. Biofilm structure is important for mediating the transport of nutrients and antibiotics to the biofilm [4,5] as well as for mediating the mechanical properties of the biofilm, which have been shown to promote the resilience of biofilms [6,7]. Biofilm structure and heterogeneity have primarily been studied using fluorescence and confocal laser scanning microscopy [8,9,10,11]. However, imaging biofilms in this manner requires the use of fluorescent stains that bind to different components of the biofilm. A common biofilm staining technique involves using the LIVE/DEAD® Bacterial Viability Kit for microscopy (Life Technologies, USA), where bacterial DNA is stained with Syto9 in live bacteria and stained with propidium iodide in dead bacteria. Propidium iodide can also be used for visualizing the extracellular DNA (eDNA) of the biofilm[12]. The polysaccharide matrix has been observed using wheat germ agglutinin tagged with a fluorophore[13]. These fluorescence based imaging techniques allow for identification of specific features of the biofilm based on the ability of the stain to tag that feature. Chemical information is only available if the stain is designed to selectively identify particular chemical moieties.

Confocal Raman microscopy is a method that allows for chemical imaging of samples with spatial resolution [14]. Confocal Raman detects chemical signals at every pixel within an image, and resolution is determined by the optics of the microscope objectives[14]. Raman spectroscopy is used to detect the vibrational modes of a system by detecting shifts in the inelastic scattering of photons [15]. The Raman spectra provides a chemical fingerprint of the sample with each peak representing different chemical components of the system. The major advantages of Raman confocal are that it is a label-free, non-destructive microscopy technique that does not require sample preparation prior to imaging[14], and that the presence of water does

not hinder its applicability[16]. A constraint of Confocal Raman microscopy is the long time required for acquiring images.

Confocal Raman has been used to map and identify individual bacteria. For example, the single cell spectra of a variety of staphylococcal species have been reported [17], and individual cells of three different species were mapped using cellular peaks from samples of planktonic bacteria [18].

Characterizing the matrix materials of biofilms using Raman spectroscopy has also been of interest. Raman spectroscopy has begun to be used to conduct a chemical analysis of biofilm matrix materials [19, 20]. Raman spectra of individual points where filamentous matrix materials were presumed to be located within a bright field image of a sample have been reported [20]. The Raman spectra of common polysaccharides and alginates have been reported to identify potential chemical peaks that may be present in biofilm matrix materials[19].

Mapping of biofilm-rich and water-rich regions of biofilms has been performed using confocal Raman microscopy, where the biomass is identified by a $-CH_3$ stretching band at 2950 cm^{-1} and water-rich regions were identified by the –OH stretching vibration band at 3450 cm^{-1} [21,22]. *Pseudomonas aeruginosa* biofilms, which were five or more days old, were used in these studies, [21,22]. No cellular level resolution of the samples was achieved in these studies.

In the present study, we use confocal Raman microscopy to map *S. epidermidis* biofilms at early (6 hour) and late (24 hour) growth times. Specifically, we seek to answer the following questions: 1) Can we chemically identify and map biofilm microstructure using confocal Raman microscopy? 2) How do biofilm composition and heterogeneity affect the ability to map structures?

5.3 Materials and Methods

5.3.1 Bacterial strains and growth conditions

S. epidermidis RP62A obtained from American Type Culture Collection (ATCC 35984) was used as the model organism within our study. Biofilms were grown in flow cells (IBI Scientific, Peosta, IA) with dimensions of 40 mm x 4 mm x 1 mm. Flow cell experiments were performed in the manner reported in [23]. Briefly, *S. epidermidis* RP62A was cultured overnight in tryptic soy broth with 1% added glucose (TSB_G) at 37°C. A volume of 1 mL of overnight culture was diluted in 9 mL of TSB_G. The diluted culture was injected into the flow cell and incubated at 37°C without flow. Growth media was then flowed through the flow cell at 0.5 mL/min to induce a shear stress of 0.01 Pa along the wall of the flow cell for either 6 hours or 24 hours to create biofilms of different thicknesses.

To obtain Raman spectra of the *S. epidermidis* RP62A, planktonic cells from an overnight culture were centrifuged at 10,000 g to create a bacterial pellet. The supernatant was removed. The remaining pellet was placed on a coverslip and imaged using the confocal Raman microscope.

We obtained the Raman spectra of purified polysaccharide intercellular adhesion (PIA). PIA was purified using the ethylenediaminetetraacetic acid (EDTA) protocol described by [24]. Briefly, *S. epidermidis* RP62A flask-adherent biofilms were collected via centrifugation at 4500 g for 25 minutes at 4°C. The supernatant was discarded and the bacterial cell pellet was resuspended and washed in 100 mL DI water. 0.5 M EDTA was heated to 100°C and the bacterial cell pellet was added for 5 minutes to extract the PIA from the pellet. The solution was centrifuged at 6000 g for 20 minutes and the supernatant containing the PIA was retained. The

PIA was filter sterilized and concentrated using a Amicon Ultra-15, centrifugal filter with a 10 kDa cut-off membrane (Millipore). A droplet of the concentrated PIA solution was placed on a glass slide for confocal Raman imaging to obtain the Raman spectra of the PIA.

5.3.2 Confocal Raman Microscopy Imaging and Analysis

The confocal Raman microscopy was performed on a WITec alpha300R Confocal Raman Microscope equipped with a 20x objective (WITec, Ulm, Germany). A 532 nm laser was used for obtaining the Raman spectra. Spectra were acquired using an integration time of 0.5 seconds per pixel. Images were taken near the coverslip and in a 2D plane parallel to the coverslip. Pixels were 500 nm x 500 nm and scans were 25-43 μm x 25-40 μm depending on the size of the biofilm features being imaged.

Biomass-rich regions of the confocal Raman image were mapped using the $-CH_3$ peak at 2950 cm^{-1}. Basis analysis was performed using the method described in the WITec Project Data Evaluation Software User Manual, Chapter 6. The basis analysis allows for an image to be generated by assigning weights to unique Raman spectra of different materials within the image. The basis spectra were obtained from a biomass-rich region where cells were located and a biomass-poor region where there were no cells. An algorithm then fits spectra at each pixel with a linear combination of the two basis spectra using the least squares method. The weights of these were then used to generate a new image that weights the scattering intensity of the biomass-rich regions and the biomass-poor regions.

5.4 Results

Figure 5-1 reports the Raman spectra from the two primary components of *S. epidermidis* biofilms, cells and PIA, as well as the Raman spectra of a biofilm. The cells and PIA are imaged

as baseline measurements, since the biofilm consists of both of these components. Figure 5-1A shows that the signal from the biofilm spectra is low compared to the spectra of the cells and the PIA. The concentration of the cells and PIA is much higher in the pure samples than it is at points within a biofilm. The biofilm Raman signal is particularly low in the region from 800-1800 cm^{-1}. Thus, as was done by Sandt et al. [21,22], we focused our analysis on the biofilm-rich and water rich regions of the image, which were indicated by the $–CH_3$ and –OH peaks at 2950 and 3450 cm^{-1}, respectively. The spectra for cells, PIA and a flow cell biofilm in the region from 2500-4000 cm^{-1} are shown in Fig. 5-1B, while the spectra of the biofilm alone in this region is shown in Fig. 5-1C.

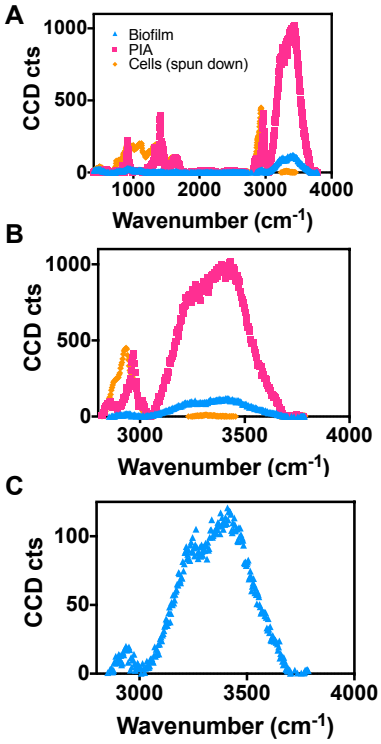

Figure 5-1: (A) Typical Raman spectra of a *S. epidermidis* RP62A flow cell biofilm, PIA, and planktonic cells. (B) The $–CH_3$ stretching band and –OH stretching band of a *S. epidermidis* RP62A flow cell biofilm, PIA, and planktonic cells. (C) Typical $–CH^3$ and –OH stretching bands from a flow cell biofilm.

When imaging flow cell biofilms, we found that the thickness of the biofilm impacted the ability to map the cells within the biofilm. *S. epidermidis* biofilms grown for 24-hours have heterogeneous structure. Bright field images that could be used to verify structures observed with Raman mapping could only be focused if there was contrast in the image due to pores within the biofilm. We found that $-CH_3$ mapping was clearer on thin sections of biofilm on the edge of an image where individual cells could be identified within the bright field image and biofilms were not more than a few cell layers thick, as shown in Fig. 5-2A and 5-2B. However, cells within thicker regions of 24-hour biofilms, where cells were not clearly distinguishable using bright field microscopy and the biofilm visibly filled much of the 1 mm thick channel, were not clearly mapped using $-CH_3$ mapping of the Raman signal, as seen in Fig. 5-2C and 5-2D.

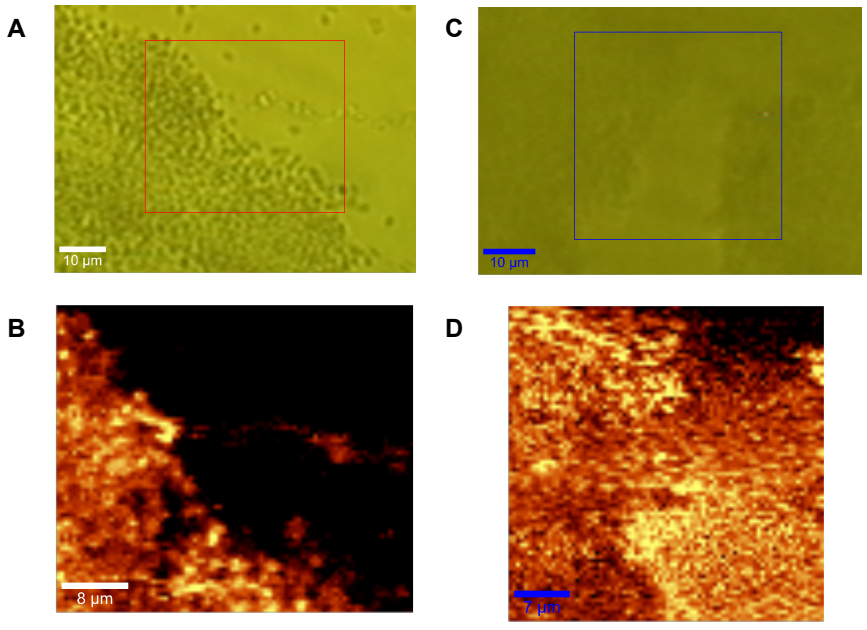

Figure 5-2: (A) Bright field image of biofilm region on the edge of a 24-hour biofilm. (B) Confocal Raman mapping of the $-CH_3$ stretching band in the box on the image shown in panel A. (C) Bright field image of a thick 24-hour biofilm imaged using confocal Raman (D) Confocal Raman mapping of the $-CH^3$ stretching band within the boxed region of the biofilm in panel C.

We performed a basis analysis on spectra from thin biofilm samples grown for 6-hours (Fig. 5-3A) and the edge of a biofilm grown for 24-hours (Fig. 5-3F) to determine if a basis analysis would allow for clearer identification of the cells within the spectra. We found that the basis analysis improved the visualization of the biomass contributions within a thin biofilm (compare Fig. 5-3B and 5-3C with Fig. 5-3D and 5-3E). The basis analysis did not further improve the visualization of the biomass within the thicker *S. epidermidis* biofilm samples (compare Fig. 5-3G and 5-3H with Fig. 5-3I and 5-3J).

5.5 Discussion

We found that the cellular microstructure of thin biofilms was more readily mapped in thin *S. epidermidis* biofilms than in thick *S. epidermidis* biofilms using confocal Raman microscopy. Biofilms contain heterogeneous structures, and cellular level microstructural features were not identified clearly in confocal Raman microscopy images in thick samples. We found that basis analysis can be used to further resolve structure of the biomass within thin *S. epidermidis* biofilms. The basis analysis may not improve the cellular resolution of the cells in thick biofilms due to the presence of the matrix materials between the cells in these images. However, since the Raman spectra of the *S. epidermidis* biofilm had such a low signal and high amount of noise in the region where the peaks of the matrix materials are located (from 800-1800 $cm^{-}1$), we are not able to verify if this lack of cellular resolution is due to an increased presence of matrix materials or not.

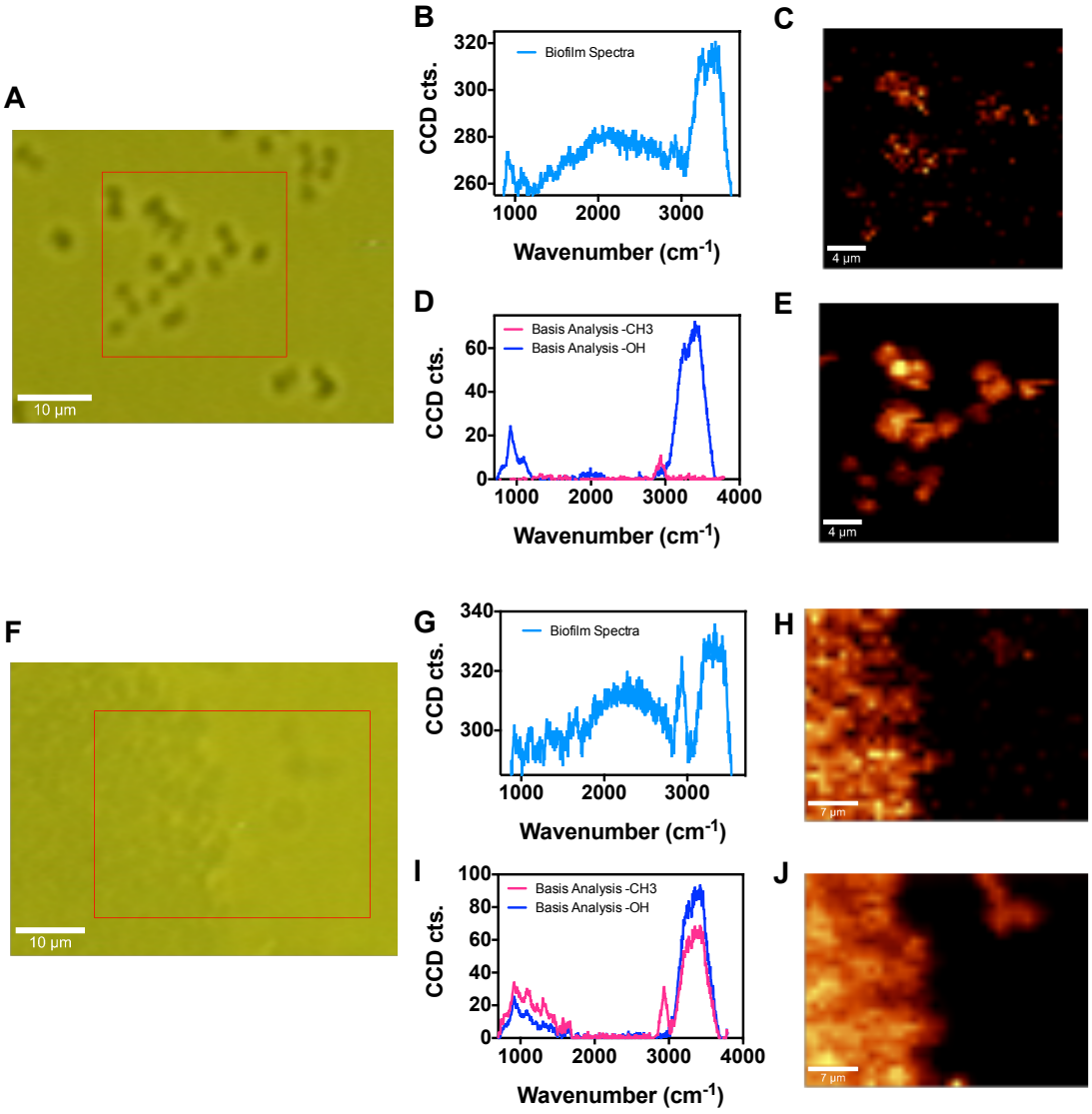

Figure 5-3: (A) Bright field image of a 6-hour biofilm. (B) Typical biofilm Raman spectra from cells in panel A. (C) Raman mapping of the –CH^3 stretching band within the box shown in panel A. (D) Basis spectra of biofilm-rich and water-rich regions used in basis analysis. (E) Raman mapping of the image shown in panel A using the weighted fits of biofilm-rich and water-rich regions at each pixel found through basis analysis. (F) Bright field image of a 24-hour biofilm. (G) Typical biofilm Raman spectra from cells in panel F. (H) Raman mapping of the –CH^3 stretching band of the biofilm shown in panel F. (I) Basis spectra of the biofilm-rich and water-rich regions used in basis analysis of F. (J) Raman mapping of the biofilm shown in panel F using basis analysis.

Previous studies have reported spectra of single cells[18] or small cell clusters in thin samples[20]. Confocal Raman has also been performed on biofilms that were 5 days or older [21,22]. The bright field imaging as well as the Raman mapping in these images did not resolve cellular level structures in these older, more developed biofilms. These biofilms grown for 5 days or longer were presumably very thick, which could have been the main limitation in visibly mapping the Raman spectra of the cells. These studies did not indicate that sample thickness was a key limitation for mapping the cellular level microstructure of biofilms.

Our work shows that biofilm thickness is a key parameter for both the mapping and verification of the mapping of cellular level structures. This work indicates that future studies for label-free mapping of biofilm cellular level structures using confocal Raman microscopy should focus on problems related to thin biofilms or the early stages of biofilm development due to the limitations of Raman microscopy in mapping cellular level microstructure of thick biofilms.

5.6 References

(1) Costerton, J. W.; Stewart, P. S.; Greenberg, E. P. *Science* **1999**, *284*, 1318.

(2) Vuong, C.; Otto, M. *Microbes and infection* **2002**, *4*, 481-489.

(3) Rohde, H.; Frankenberger, S.; Zähringer, U.; Mack, D. *European journal of cell biology* **2010**, *89*, 103-111.

(4) Hall-Stoodley, L.; Costerton, J. W.; Stoodley, P. *Nature Reviews Microbiology* **2004**, *2*, 95-108.

(5) Stewart, P. S.; Franklin, M. J. *Nature Reviews Microbiology* **2008**, *6*, 199-210.

(6) Böl, M.; Ehret, A. E.; Bolea Albero, A.; Hellriegel, J.; Krull, R. *Critical Reviews in Biotechnology* **2013**, *33*, 145-171.

(7) Guélon, T.; Mathias, J.-D.; Stoodley, P. **2011**, *Biofilm Highlights*, 111-139.

(8) Xavier, J. B.; White, D. C.; Almeida, J. S. *Water Science & Technology* **2003**, *47*, 31-37.

(9) Beyenal, H.; Donovan, C.; Lewandowski, Z.; Harkin, G. *Journal of microbiological methods* **2004**, *59*, 395-413.

(10) Heydorn, A.; Nielsen, A. T.; Hentzer, M.; Sternberg, C.; Givskov, M.; Ersbøll, B. K.; Molin, S. *Microbiology* **2000**, *146*, 2395-2407.

(11) McLean, J. S.; Ona, O. N.; Majors, P. D. *The ISME journal* **2007**, *2*, 121-131.

(12) Chiang, W.-C.; Nilsson, M.; Jensen, P. Ø.; Høiby, N.; Nielsen, T. E.; Givskov, M.; Tolker-Nielsen, T. *Antimicrobial agents and chemotherapy* **2013**, *57*, 2352-2361.

(13) Pintens, V.; Massonet, C.; Merckx, R.; Vandecasteele, S.; Peetermans, W. E.; Knobloch, J. K.-M.; Van Eldere, J. *Microbiology* **2008**, *154*, 2827-2836.

(14) Everall, N. J. *Analyst* **2010**, *135*, 2512-2522.

(15) Schrader, B.; Bougeard, D. **1995**, *Infrared and Raman spectroscopy: Methods and Applications*, 7-61.

(16) Dietzek, B.; Cialla, D.; Schmitt, M.; Popp, J. **2011**, *Confocal Raman Microscopy*, 21-42.

(17) Harz, M.; Rösch, P.; Peschke, K.-D.; Ronneberger, O.; Burkhardt, H.; Popp, J. *Analyst* **2005**, *130*, 1543-1550.

(18) Hermelink, A.; Brauer, A.; Lasch, P.; Naumann, D. *Analyst* **2009**, *134*, 1149-1153.

(19) Ivleva, N. P.; Wagner, M.; Horn, H.; Niessner, R.; Haisch, C. *Analytical and bioanalytical chemistry* **2009**, *393*, 197-206.

(20) Wagner, M.; Ivleva, N. P.; Haisch, C.; Niessner, R.; Horn, H. *Water research* **2009**, *43*, 63-76.

(21) Sandt, C.; Smith Palmer, T.; Pink, J.; Pink, D. *Journal of microbiological methods* **2008**, *75*, 148-152.

(22) Sandt, C.; Smith-Palmer, T.; Comeau, J.; Pink, D. *Applied microbiology and biotechnology* **2009**, *83*, 1171-1182.

(23) Stewart, E. J.; Satorius, A. E.; Younger, J. G.; Solomon, M. J. *Langmuir* **2013**, *29*, 7017-7024.

(24) Vuong, C.; Kocianova, S.; Voyich, J. M.; Yao, Y.; Fischer, E. R.; DeLeo, F. R.; Otto, M. *Journal of Biological Chemistry* **2004**, *279*, 54881-54886.

Chapter 6

Assessment of Interdisciplinary Learning in Graduate Elective Coursework[††]

6.1 Abstract

Because engineers are required to solve challenges at the interface of multiple disciplines, educational training to address problems that incorporate multiple disciplinary perspectives is increasingly important. The number of interdisciplinary graduate programs has been increasing; however, little has been done to assess the effectiveness of the components of these programs, including interdisciplinary elective coursework. Our purpose was to assess changes in interdisciplinary learning outcomes and interdisciplinary fluency of students throughout a single semester graduate interdisciplinary elective course. We used a mixed-methods approach to assess changes in interdisciplinary learning. We conducted three surveys to assess changes in student self-perception of interdisciplinary learning outcomes and coded language within open-ended homework assignments to assess interdisciplinary fluency throughout the semester. We

[††] This chapter is in preparation for publication by [E.J. Stewart, S.R. Daly, J.G. Younger, & M.J. Solomon].

found increases in student self-perception of learning outcomes related to recognizing disciplinary perspectives and teamwork skills as well as increases in the interdisciplinary fluency of students from the beginning to the end of the term. We did not find changes in student self-perception of learning outcomes related to interdisciplinary skills or reflective behavior. This study found that a single semester interdisciplinary elective was able to increase interdisciplinary learning in the graduate classroom. This work should be implemented in additional graduate courses to establish if similar increases in learning are achieved or if the methods should be further improved for assessing interdisciplinary learning. The techniques used in this study could be used to assess the effectiveness of interdisciplinary curricular components within graduate programs beyond coursework as well.

6.2 Introduction

The need to create graduate students with interdisciplinary skillsets is increasingly necessary as research challenges become more complex and fall outside the disciplinary constructs of established fields. Interdisciplinary skills are furthermore desired within academia, government and industry. As a result, interdisciplinary graduate programs and interdisciplinary research funding are becoming more prevalent. A search of the active research funding opportunities at the National Science Foundation (NSF) in December 2013 revealed that ~40% (166/416) of programs with active funding emphasize or encourage interdisciplinary work[1]. Many schools offer specific graduate degree programs with an emphasis on a particular interdisciplinary area or supplement single graduate degrees with training in an additional field of study through dual degree or certificate programs. Some schools are internally supporting the expansion of interdisciplinary research by creating internal funding competitions for researchers who collaborate with other colleges or departments within the university. One program that

specifically supported interdisciplinarity in graduate student training was the NSF's Integrative Graduate Education Research Training (IGERT) Program to fund the training of graduate students. In 2010, Borrego et al. analyzed 94 IGERT awards and found that 80% (75/94) of the programs proposed an interdisciplinary graduate course as a primary means to achieve interdisciplinary learning outcomes for students, other common components of interdisciplinary curriculum include seminars, retreats, and workshops[2].

Beyond new specific interdisciplinary funding opportunities or graduate programs, equipping engineering students with interdisciplinary skills creates students that are ready to solve problems in new or emerging fields where the understanding must extend beyond preexisting disciplinary boundaries—a valued skillset for engineers and scientists regardless of if they are enrolled in interdisciplinary graduate programs [3,4]. While faculty may agree that interdisciplinary training would help in approaching complex problems that involve many disciplines, much of the university is structured around specific departments, schools, and colleges, and faculty are seldom encouraged to develop pedagogies related to interdisciplinary learning [5]. Even in interdisciplinary graduate programs, the curriculum is framed around program level goals or requirements as opposed to assessable interdisciplinary metrics or specific student learning outcomes [2]. Little has been done to determine if interdisciplinary graduate elective courses or other curricular components impact the interdisciplinarity of students. Methods of assessing the impact of different aspects of interdisciplinary graduate programs are required to evaluate both the effectiveness and necessity of program components.

The goal of our work was to develop and implement a strategy for assessing changes in interdisciplinary graduate student learning. We applied our assessment method in a graduate elective course on a subject at the interface of microbiology and engineering to measure

changes in student interdisciplinary learning. We assessed student learning through monitoring changes in: a) student self-perception of learning outcomes as evaluated through three surveys, and b) student interdisciplinary fluency as measured through coding responses to open-ended homework assignments at different points during the course. The course contained graduate students from chemical engineering, civil and environmental engineering, and microbiology and immunology. The interdisciplinarity of the enrolled students within the course was compared to the general population within each of their departments to assess if enrolled students were representative of the student body within their respective programs. Our research shows that in one semester, students readily incorporated concepts from multiple disciplines into written work and increased their teamwork skills and appreciation for different disciplines' perspectives. We also found that the course did not increase student self-perception of learning outcomes related to interdisciplinary skills or reflective behavior. The tools and strategy for assessing student learning from this study can be further used to measure the effectiveness of other courses or interdisciplinary graduate curriculum components.

6.3 Background

6.3.1 Defining Interdisciplinarity

Interdisciplinarity can be defined as a way of solving problems that integrate knowledge from two or more disciplines to provide a holistic understanding that would be unlikely using single methods or approaches alone [6, 7,8]. Some researchers distinguish multidisciplinarity and transdisiciplinarity from interdisciplinarity, where multidisciplinary is a less integrative combination of disciplines, and transdisciplinarity focuses on theories that transcend traditional disciplines[7]. Here we do not distinguish interdisciplinarity from multidisciplinarity or

transdisciplinarity. That is, as has been done previously, we define interdisciplinarity as behaviors which are interdisciplinary, multidisciplinary or transdisciplinary [7].

6.3.2 Interdisciplinarity in Science and Engineering

In science and engineering, interdisciplinary problems are often approached by collaborative teams[7]. As a result, scientists and engineers often operationalize interdisciplinarity as teamwork[7]. Thus, much of the literature from engineering education related to interdisciplinarity has focused on interdisciplinary teams. Research has been done to assess interdisciplinary identities[5], self-efficacy [9], and communication, trust, and respect [10] within interdisciplinary engineering teams. However, interdisciplinarity in science and engineering extends beyond teamwork, so we must consider aspects of interdisciplinarity beyond teamwork when assessing student learning.

6.3.3 Interdisciplinary Learning in Science and Engineering Graduate Education

Although research on graduate interdisciplinary learning is increasing, studies have predominately focused on the curriculum, or other program level assessments. For example, research has found that interdisciplinary programs facilitating engagement through supporting diversity, participation, and interactive teaching and learning are well received by students [11]. Research has also shown that semi-structured learning communities with a student-centered approach create opportunities that promote community building and research centered discussions[12]. One key challenge to interdisciplinary research that has been identified through this educational research on semi-structured learning communities is differences in the terminology used by individuals from different disciplines [12]. Thus, interdisciplinary fluency is a key attribute of interdisciplinary learners. Though these program level objectives creating

inclusive learning communities are important, they do not assess student learning within the program.

There has been limited research on assessment and efficacy of interdisciplinary graduate coursework. Available research on interdisciplinary graduate coursework has described the content of the course, or aspects of the course that could be considered as interdisciplinary components of a course. For example, a nanotechnology course was described that included interdisciplinary group work, and assignments that were intentional about making students think about different disciplines[13], and an interdisciplinary business course for science graduate students contained students from a variety of disciplines and considered student perceptions of the course[14]. To our knowledge there has been no research to assess interdisciplinary learning outcomes and interdisciplinary fluency of students within an interdisciplinary graduate course or other curricular component of an interdisciplinary graduate program.

6.3.4 Interdisciplinary Learning Outcomes for Graduate Education

Research has been done to distinguish elements of interdisciplinarity that can be assessed and in turn measured. Categories of learning outcomes for assessing interdisciplinary graduate education have been identified as follows: grounding in traditional disciplines, integration and broad perspective, teamwork, interdisciplinary communication, and critical awareness [7]. In 2011, Lattuca et al. assessed interdisciplinary learning in a large population of undergraduates through the use of a survey that evaluated four categories of learning outcomes related to interdisciplinarity: interdisciplinary skills, recognizing disciplinary perspectives, reflective behavior, and teamwork skills [8]. These four categories overlapped similarly with the learning outcomes identified as being key for assessing interdisciplinary graduate education in [7]. The learning outcome of interdisciplinary skills overlaps some with interdisciplinary communication.

Recognizing disciplinary perspectives relates to integration and broad perspective. Reflective behavior relates to critical awareness, and teamwork skills align with teamwork. However, in the learning outcomes for graduate education grounding in traditional disciplines was also emphasized. Due to the similarity of the learning outcomes, this survey could be broadly used to assess interdisciplinary learning in elements of a graduate program.

6.4 Research Design

6.4.1 Research Questions

In the current work, we develop and implement a strategy for assessing interdisciplinary learning in elective graduate coursework. The context of our study is a graduate course in bacterial biofilms—a topic that is at the boundaries of microbiology and engineering. Through our study, we specifically addressed the following research questions: A) How does a single graduate elective course impact student interdisciplinary learning? B) Does a graduate elective that is designed to be interdisciplinary change student self-perception of interdisciplinary learning outcomes? C) Do graduate students increase their usage of language from disciplines outside of their own and in turn their interdisciplinary fluency during a single semester elective course?

6.4.2 Participants

There were two populations of students that were involved in our study: the students enrolled in the graduate elective course on bacterial biofilms and the students from the home departments of the enrolled students. We included the students from the home departments of the enrolled students to look at the interdisciplinarity of the enrolled students in comparison to the general populations within their home departments.

Students were recruited to enroll in the course by standard posting of the course description and through personal communications between the course faculty and graduate program directors within both the College of Engineering and the life science components of the Medical School, School of Public Health and College of Literature, Sciences, and Arts at the University of Michigan. There were 11 students enrolled in the course from the following disciplines: chemical engineering, civil and environmental engineering, and microbiology and immunology. There were also 3 students auditing the course that did not complete course assignments, but completed the surveys. The demographics of the enrolled and auditing students are summarized in the first two columns of Table 6-1.

Graduate students from chemical engineering, civil and environmental engineering, and microbiology and immunology were invited to participate in the survey used in the study. There were 120 students in the chemical engineering graduate program, 68 students in the civil and environmental engineering program, and 43 students in the microbiology and immunology program at the time the survey was distributed. This data is presented in the third column of Table 6-1.

Administration of the surveys to the general population in chemical engineering, civil and environmental engineering, and microbiology and immunology and to the students within the course was IRB-approved. Collection of the assignments from students that were coded for analysis was also IRB-approved.

Table 6-1: Student population by major. This table is in preparation for publication by [E.J. Stewart, S.R. Daly, J.G. Younger, & M.J. Solomon].

Department	All students in course* N=14	Students enrolled in course N=11	Students in department (Total N=231)
Chemical Engineering	7	6	120
Civil and Environmental Engineering	4	3	68
Microbiology and Immunology	3	2	43

*Four post-doctoral students audited the course and participated in surveys, but not course assignments.

6.4.3 Course Description

We used a graduate level elective course listed in the chemical engineering department as a pilot study to advance the understanding of interdisciplinary learning. The course consisted of subject matter related to understanding bacterial biofilms, a topic at the interface of engineering and microbiology. Bacterial biofilms are multicellular structures responsible for the contamination and failure of many engineered systems and also play a central role in infectious diseases for humans, animals, and plants. In motivating the course, the instructors argued that advancing the understanding of bacterial biofilms in engineered and biological contexts benefits from knowledge of the physical forces and fluid dynamics of the growth environment as well as the genetic pathways that lead to the production of biofilm matrix materials. Neither a traditional engineering view of the physics involved nor a life science view of the cell biology involved was argued to be sufficient for developing new strategies for mitigation and remediation of fouling by biofilms.

The aim of the course was to provide students with skills to understand, analyze, and interpret research and technologies associated with bacterial biofilms that could be encountered in both research and industry. Topics covered in the class included relevant fundamentals from microbiology, fluid dynamics, and material science. In addition to the interdisciplinarity of the

course content, the course instructors included elements to increase interdisciplinary exposure. The class was co-taught by a faculty member from the College of Engineering and a faculty member from the Medical School. The course consisted of two segments. The first segment (weeks 1-9) was made up of lectures and in-class problems, alternating between the two disciplinary perspectives, and the second segment (weeks 10-14) synthesized the understanding from the two disciplines through real world examples of the material highlighted by three external speakers as well as a required course project by each student. Students were regularly encouraged to discuss topics within the course and ask questions.

6.4.4 Timeline of data collection

Survey data was collected three times from students within the bacterial biofilm class. Surveys were administered during weeks 1, 9, and 14. Open-ended homework assignments used for assessing interdisciplinary fluency were given during weeks 4 and 14. To ensure confidentiality of students, students were de-identified from their responses before presenting the data. Additionally, any data used in the study from student coursework was analyzed after the course had concluded. A schematic of the timeline of data collection during the course is shown in Figure 6-1.

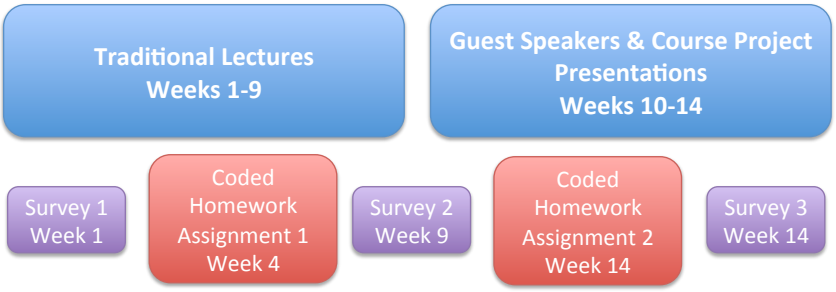

Figure 6-1: Timeline of course segments and student data sampling. This figure is in preparation for publication by [E.J. Stewart, S.R. Daly, J.G. Younger, & M.J. Solomon].

6.4.5 Survey Data Collection and Analysis

Students were invited to participate in an IRB-approved online survey via email to evaluate differences and similarities in student-perception of learning outcomes. The surveys were administered to the students taking the class at the following three time points: (1) during the first week of class, (2) at the conclusion of the lecture portion of the class (week 9), and (3) at the end of the semester (week 14). The survey was administered to all graduate students in chemical engineering, civil and environmental engineering, and microbiology and immunology at one time point to enable assessment of the interdisciplinarity of the general population within each department.

The survey was used to assess student self-perception of interdisciplinary learning and consisted of elements of an instrument created by Lattuca et al. in 2011[8]. This instrument was initially used in a study to assess student learning outcomes related to interdisciplinarity in a nationally representative sample population of undergraduate engineering students [8]. The survey contained questions associated with interdisciplinary learning outcomes to establish if students' self-perception within any of four domains: interdisciplinary skills, recognizing disciplinary perspectives, reflective behavior or teamwork skills changed over the duration of the course.

The interdisciplinary skills section of the survey included questions on the self-perceived extent that students do the following: value reading about topics outside of their field; enjoy thinking about how different fields approach problems; think about if problems have non-technical solutions; seek information from experts in other fields; figure out ideas that are appropriate for solving a problem; see connections between ideas in their field and ideas in other fields; take ideas from outside of their field and synthesize them to solve a problem; and use ideas from another field to solve a new problem. The recognizing disciplinary perspectives

domain includes questions on the extent students recognize the kinds of evidence that different fields rely on, identify the kinds of knowledge and ideas that are distinctive to different fields of study, and are good at figuring out what experts in different fields have missed in explaining a problem or proposing a solution. Reflective behavior contains questions on the degree to which students stop to think about where they are going right or wrong with a problem solution, and step back to reflect on what they are thinking to determine whether they may be missing something. Students also rated teamwork skills based on their self-perceived ability to do the following: work in teams of people with a variety of skills and backgrounds, work with others to accomplish group goals, work in teams where knowledge and ideas from multiple fields must be applied, work in teams that include people from fields outside of their field of study, and put aside differences within a design team to get work done. These four subsets of questions had previously been correlated to interdisciplinarity [8]. The specific survey elements used in this study are found in Figure 6-2.

Lattuca et al. developed the questions in each of these domains through a rigorous, two year process that included a thorough literature review, individual and focus-group interviews, and the use of the Cronbach's α as the indicator of the internal consistency reliability of the four subsets of interdisciplinary questions (all Cronbach's α values were greater than or equal to 0.69 [8]). The Cronbach's α is a measure of how closely related a set of items are as a group and ranges from 0 to 1; values greater than 0.7 are considered to have good internal consistency.

In the present study, survey items for interdisciplinary skill, recognizing disciplinary perspectives, reflective behavior, and teamwork were averaged across domain for each student. Baseline differences in these features were compared across student discipline (i.e., chemical engineering, civil and environmental engineering, and microbiology and immunology) using

one-way analysis of variance. Clustering between student types was further compared with principal component analysis. Changes in features over time were examined using linear mixed effects models assuming that the three survey times (baseline, mid-semester, final) were equally spaced in time and that any changes over time in student characteristics were linear. The mixed effects model included survey time point and student type and used student identity as the random, repeated effect. Analysis was performed using the base and NLME packages in R 2.13.2 [15, 16].

Do you agree or disagree with the following statements?
(1: Strongly disagree; 2: Disagree; 3: Neither agree nor disagree; 4: Agree; 5: Strongly agree)
Interdisciplinary Skills

1. I value reading about topics outside of my major field of study.
2. I enjoy thinking about how different fields approach the same problem in different ways.
3. Not all problems have purely technical solutions.
4. In solving problems, I often seek information from experts in other academic fields.
5. Given knowledge and ideas from different fields, I can figure out what is appropriate for solving a problem.
6. I see connections between ideas in my field of study and ideas in the humanities and social sciences.
7. I can take ideas from outside my field of study and synthesize them in ways to better understand a problem.
8. I can use what I have learned in one field in another setting or to solve a new problem.

Recognizing Disciplinary Perspectives

1. I recognize the kinds of evidence that different fields of study rely on.
2. If asked, I could identify the kinds of knowledge and ideas that are distinctive to different fields of study.
3. I'm good at figuring out what experts in different fields have missed in explaining a problem or proposing a solution

Reflective Behavior

1. I frequently stop to think about where I might be going wrong or right with a problem solution.
2. I often step back and reflect on what I am thinking to determine whether I might be missing something.

Teamwork Skills
Please rate your ability to:
(1: Weak/None; 2: Fair; 3: Good; 4: Very good; 5: Excellent)

1. Work in teams of people with a variety of skills and backgrounds.
2. Work with others to accomplish group goals.
3. Work in teams where knowledge and ideas from multiple fields must be applied.
4. Work in teams that include people from fields outside your field of study.
5. Put aside differences within a design team to get the work done.

Figure 6-2: Survey elements sub-divided by category of the interdisciplinary learning outcome. This figure is in preparation for publication by [E.J. Stewart, S.R. Daly, J.G. Younger, & M.J. Solomon].

6.4.6 Qualitative Data Collection and Analysis

We coded responses from two open-ended homework assignments collected during the term. The open-ended questions used were designed such that they could be graded as correct regardless of if the student provided a response grounded in engineering or a response grounded in microbiology.

The first assignment we coded was from the first segment of the course and on the topic of bacterial interactions and adhesions. The problem statement was: "Using what you have learned from this course, the literature, and/or prior knowledge, please explain how bacteria adhere to a surface". The problem could be answered with a response related to physical interactions between bacteria and the environment such as electrostatic or van der Waals interactions and/or with a response related to specific microbiological behaviors of the bacteria such as the production of matrix materials or quorum sensing molecules. Thus, words could be pulled from the assignment and coded as engineering or microbiology terms. Analysis of the number of engineering and microbiology codes could then be used to determine if the content related primarily to engineering or microbiology. If a word could be coded as engineering or microbiology it was included in the count for both categories.

The second coded assignment was a peer reflection on two of the oral course project presentations. For the course project presentations, three students worked independently and eight students worked in groups of two. Thus, three presentations were presented individually and four presentations were presented in pairs. Presentation topics were selected based on student interests and summarized in Table 6-2. In the peer reflection on the projects, the students were asked to describe the project, and propose an idea that could be used to extend the project. We coded the assignment in two ways. First, we coded the descriptions of the two projects

chosen for the assignment. We determined if the language used to describe each of the projects was predominantly related to engineering, microbiology or at the interface of the two for each assignment. Second, we coded the ideas students had to extend or continue projects that had been presented by their peers. We determined if the language used to describe the new ideas was interdisciplinary or related mainly to engineering or microbiology.

Table 6-2: Summary of project topics and group compositions. This table is in preparation for publication by [E.J. Stewart, S.R. Daly, J.G. Younger, & M.J. Solomon].

Project Title	Group Composition	Discipline of Project Topic
Forces governing motion, adhesion, and clearance of rod-shaped bacteria	1 ChE student	Engineering
DLVO analysis of the effect of surface material, geometry, and roughness on bacterial adhesion	1 ChE student	Engineering
COMSOL simulation of bacteria absorbing in a biofilm	1 ChE student & 1 CEE student	Engineering
Proteins in biofilms: a brief look at the biofilm-associated protein	1 Microbiology & Immunology student	Microbiology
Prevention and treatment of dental plaque	1 ChE student & 1 Microbiology & Immunology Student	Microbiology
Biofilm formation by methanotrophs	2 CEE students	Microbiology
An enhanced wastewater treatment system: optimizing cellulose digestion using ruminant fungi	2 ChE students	Interdisciplinary

We coded the assignments using grounded theory, where patterns and theory are grounded in observation and developed from the data collected. We began coding by performing open coding, where the whole body of data was read and words that captured key concepts were highlighted [17, 18, 19]. The highlighted concepts focused on clearly observable characteristics of the student responses [20]. We then used axial coding to reanalyze the results of the open coding and label general concepts or categories that were reflective of one or more of the initially identified key concepts [17, 19]. Finally, we used selective coding to link the open and axial codes

to central concepts or phenomena [17, 19]. In our case, the central concepts were trends in the responses related to engineering, microbiology, or the interdisciplinary intersection of the two fields. The coding process was iterated and student assignments were reread until no new codes emerged from the data[21].

After words were coded for each assignment, the number of words coded as engineering and microbiology were tabulated separately. A ratio of the number of engineering codes to the number of microbiology codes was then computed. If the ratio of engineering codes to microbiology codes was greater than 1.5, the assignment was labeled as engineering. If the ratio was less than 0.5 the assignment was labeled as microbiology. If the ratio was between 0.5 and 1.5, the assignment was considered interdisciplinary.

A single coder coded all assignments and a second coder coded approximately 50% of the assignments. Both coders performed open coding on the assignments and computed the ratio of engineering codes to microbiology codes for each assignment. Reliability of the coding scheme was verified through comparing if assignments were labeled as engineering, microbiology, or interdisciplinary responses by both coders. If the categories of the responses (primarily engineering, primarily microbiology, or interdisciplinary) were the same for both coders then agreement was reached. Based on initial coding of the two assignments, coders reached agreement on codes for 83% of the responses. For the cases where coders disagreed, they settled discrepancies by mutual agreement until 100% of the responses were agreed upon. As an example, a summary of the engineering and microbiology codes assigned for the first coded assignment is in Table 6-3.

After an assignment was determined to be engineering, microbiology, or interdisciplinary, the coded result was compared to the discipline of the student whose response had been coded. This comparison was used to assess if students were responding with language that was mainly related to their home discipline, at the interface of engineering and microbiology or that extended outside of their home discipline.

6.5 Findings

6.5.1 Survey Analysis

We surveyed the graduate student body within chemical engineering, civil and environmental engineering, and microbiology and immunology to determine a baseline of student self-perception of interdisciplinary learning outcomes in four categories: interdisciplinary skills, recognizing disciplinary perspectives, reflective behavior and teamwork. We received a 35% (42/120) response rate in chemical engineering, a 35% (24/68) response rate in civil and environmental engineering, and 40% (17/43) response rate in microbiology and immunology. Clustering within students from the same graduate program was analyzed using principle component analysis. The features that loaded most heavily into the two principle components were teamwork (component 1) and recognizing disciplinary perspectives (component 2). No significant clustering of students was found, indicating that the students at the baseline responded very similarly across disciplines, as shown by Figure 6-3.

For students within the course, we received 100% (14/14) response rate. We found that at the beginning of the course students enrolled in the course were no more or less interdisciplinary than the students within each of their respective departments, as plotted in Figure 6-3. Because the students in the course were no different than the average population

within their respective departments, the students enrolled in the course can be considered representative of the general student population.

Table 6-3: Summary of codes for assignment 1. This table is in preparation for publication by [E.J. Stewart, S.R. Daly, J.G. Younger, & M.J. Solomon].

Central Concept	Coded words
Engineering	a. Physical interaction i. van der Waals ii. Electrostatics/charge iii. Refractive Index iv. Gravity v. DLVO vi. Brownian motion vii. Cell-cell interaction viii. Surface charge ix. Surface roughness x. Depletion xi. Forces xii. Potential energy xiii. Hydrophobicity/ Hydrophobic/ Hydrophilic xiv. Hydrogen bonding xv. Steric effects xvi. Osmotic interactions xvii. Bacterial size xviii. Solvent properties b. Covalent bonding c. Fluid Dynamics i. Convection d. Motility* i. Random Walk ii. Swimming iii. Swarming
Microbiology	a. Matrix Materials i. Polysaccharides ii. Secreted polymers iii. Extracellular polymeric substances iv. Capsule v. eDNA vi. Proteins vii. Glycoproteins viii. Glycolipids ix. Components of clotting cascade b. Nutrient-limited environment c. Quorum Sensing d. Gene Expression e. Other adhesive organelles Pili, curli, and fimbriae f. Motility*

*Motility was coded as both engineering and microbiology. Coding depended on the use within the assignment.

We compared the baseline averages within each of the four categories from each department and determined that there were no significant differences in the baseline averages across student type as indicated by $p > 0.05$ between student group averages in all four categories of interdisciplinarity. The baseline data are tabulated in Table 6-4.

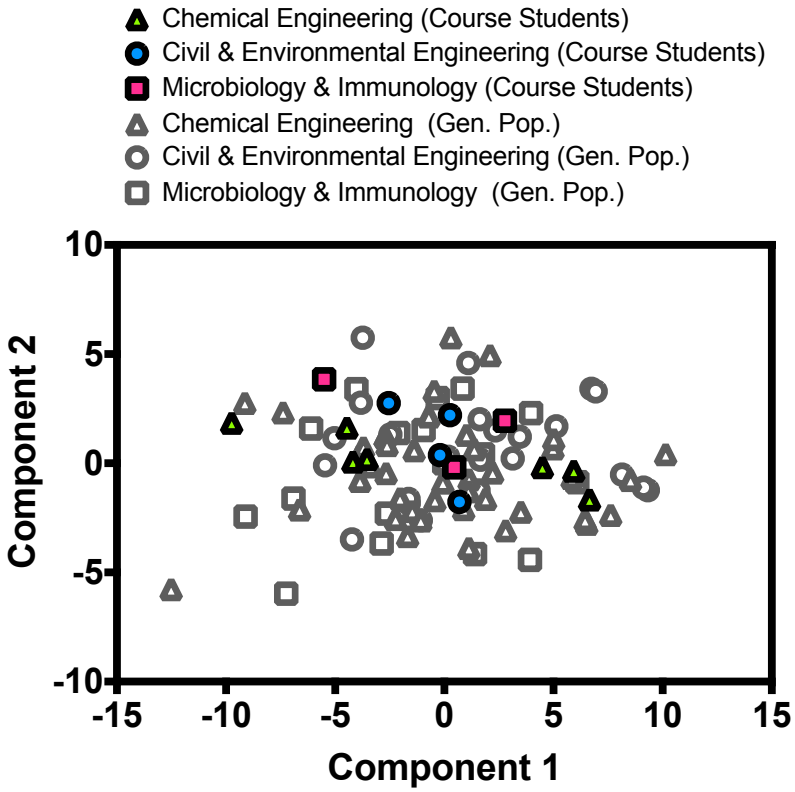

Figure 6-3: Principal component analysis of baseline interdisciplinary features in general and course populations within each department. Principal component analysis of student features shows that students in general were very similar across discipline, and no significant clustering was observed in the general population or the course population. Principal component 1 was teamwork and principal component 2 was recognizing disciplinary perspectives. This figure is in preparation for publication by [E.J. Stewart, S.R. Daly, J.G. Younger, & M.J. Solomon].

Through considering the shift in each of the four interdisciplinary features with time, we found that student self-perception of recognizing disciplinary perspectives ($p = 0.04$) and teamwork skills ($p = 0.03$) increased over the course of the semester for all student groups.

However, there was no significant increase in student self-perception of their interdisciplinary skills or reflective behavior, as shown in Figure 6-4.

Table 6-4: Baseline interdisciplinary features of students from the graduate elective course. This table is in preparation for publication by [E.J. Stewart, S.R. Daly, J.G. Younger, & M.J. Solomon].

	Chemical Engineering	Civil and Environmental Engineering	Microbiology and Immunology	P value (by ANOVA)
Interdisciplinary skills	3.6 (3.5, 4.3)*	3.9 (3.9, 4.0)	4.0 (3.8, 4.2)	0.82
Recognizing disciplinary perspectives	3.0 (2.4, 3.6)	3.5 (3.3, 3.7)	3.0 (2.7, 3.5)	0.53
Reflective behavior	4.0 (4.4, 4.5)	4.0 (3.8, 4.5)	3.5 (3.3, 3.8)	0.25
Teamwork skills	3.1 (2.8, 4.2)	3.4 (3.1, 3.6)	3.8 (2.9, 3.9)	0.97

* Presented as median and interquartile range.

6.5.2 Analysis of Coded Assignments

In addition to surveying students, we coded responses from two assignments during the semester. The first assignment was from the fourth week of class during the lecture-based portion of the course and between the first and the second survey. The second assignment was from the fourteenth week of the course after the project presentations, and between the second and the third survey.

We found that the majority of students did not have interdisciplinary fluency at the beginning of the course. Only 27% (3/11) of students gave responses that were labeled as either interdisciplinary or to a field outside of their own, while 73% (8/11) of students provided responses where the majority of the response was grounded in their primary discipline. However, 82% (9/11) of students began using some language from outside of their field to answer the question. 18% (2/11) of students, both of which were engineers, used information

solely from their field. 64% (7/11) of students gave responses related to engineering, 18% (2/11) of students gave responses related predominantly to biology, and 18% (2/11) of students gave interdisciplinary responses. These findings are reported in the first column of Table 6-5.

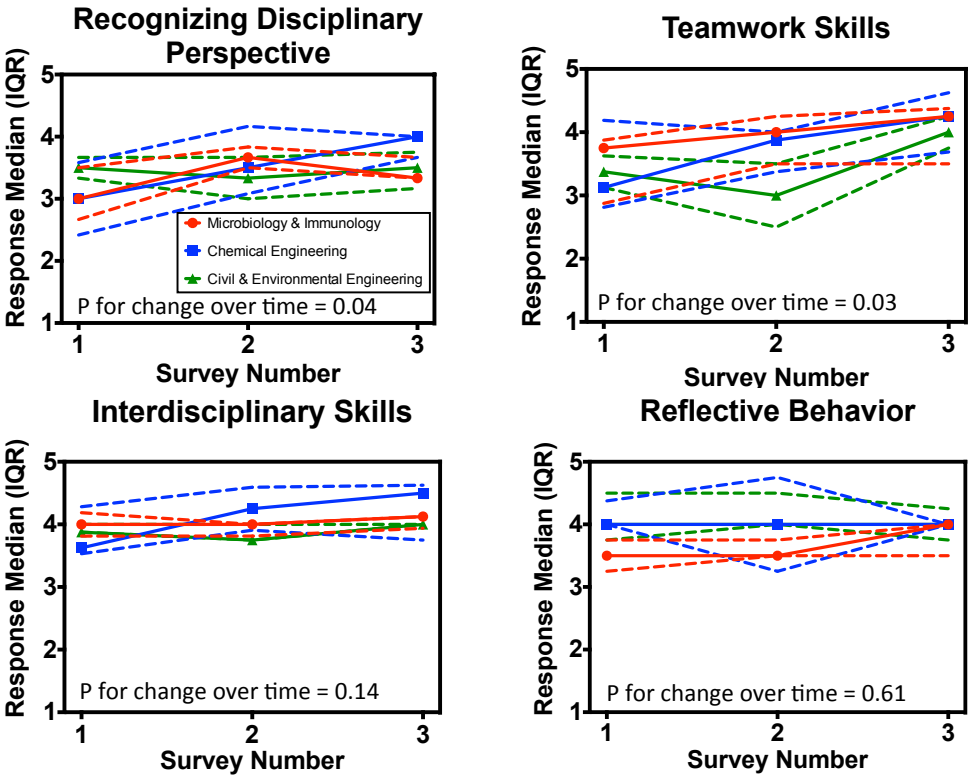

Figure 6-4: Changes in student characteristics over the course of the semester. Increases were seen over the semester in recognizing disciplinary perspectives and teamwork skills, both of which were statistically significant using linear mixed effects modeling. In no domain was student discipline statistically related to interdisciplinary skills or reflective behavior ($p > 0.05$ for each). Data expressed as mean (bold line) and upper and lower quartiles (dashed lines). This figure is in preparation for publication by [E.J. Stewart, S.R. Daly, J.G. Younger, & M.J. Solomon].

Table 6-5: Interdisciplinary fluency in students at beginning and end of the course. This table is in preparation for publication by [E.J. Stewart, S.R. Daly, J.G. Younger, & M.J. Solomon].

	Coded Assignment 1 (Bacterial adhesion)	Coded Assignment 2 (Project peer-reflection)
Response was either interdisciplinary or predominantly outside of discipline	27% (3/11 students)	64% (7/11 students)
Majority of response was grounded in major discipline	73% (8/11 students)	36% (4/11 students)

For the second coded assignment, the first portion of the assignment involved describing two of the seven oral project presentations that were given by students. In the project descriptions, 82% (9/11) of students used language predominantly relating to both engineering and microbiology or language from a discipline outside of their own to describe at least one project, indicating interdisciplinary responses to the assignment from the majority of the class when describing project presentations.

The second part of the assignment was to propose two ideas that extended upon the content of the project presentation. The responses to the second part of the assignment revealed that 64% (7/11) of students proposed at least one project extension labeled as interdisciplinary or outside of their discipline. However, since each student proposed 2 projects, only 41% (9/22) of all proposed project extensions involved ideas outside of the student's discipline. The results from both portions of the assignment reveal increases in interdisciplinary fluency within the student population when compared to the beginning of the semester. Thus, at least 64% (7/11) of students and possibly 82% (9/11) of students have achieved interdisciplinary fluency by the second half of the course, as assessed through coding the responses to the second open-ended homework assignment. These findings are reported in the second column of Table 5.

6.6 Discussion

By means of this research, we assessed increases in interdisciplinary learning that occurred in a graduate elective course on bacterial biofilms that was designed and offered with the intent of increasing interdisciplinary learning at the boundary of engineering and microbiology. The initial responses to survey questions were very similar across disciplines for all students in the course as well as the student population of the home departments of the enrolled students. Even though there were no significant differences between participants and the general population at baseline, there were still statistically significant changes in interdisciplinarity by the end of the course relative to that baseline.

When the survey data was analyzed with respect to time, the only categories of interdisciplinarity with significant increases were the dimensions of recognizing disciplinary perspectives and of teamwork. Categories not showing significant increases were interdisciplinary skills and reflective behavior. Interestingly, the categories with significant increases were the same features that loaded heavily into the two principle components. These areas also related to the categories of key learning outcomes for interdisciplinary learning [7]. Additionally, it is of interest that teamwork skills improved, since teamwork is often the means that scientists and engineers use to operationalize interdisciplinary work [7].

Interdisciplinary gains were made in the course as assessed through coding of assignments. Based on the assignment coded from the first half of the class only 27% of students gave interdisciplinary responses, while 64% of students gave interdisciplinary responses in the second half of the course. Since the population was only 11 students for this portion of the study, this was a gain of 36%, or rather four students, who were responding in an

interdisciplinary manner. Thus interdisciplinary gains were made, but there are still four students (36% of the class) that are not making these gains.

This work contributes to advancing the understanding and assessment of student learning in graduate education. It serves as a model for tracking changes in interdisciplinarity. It shows that a course intentionally designed to promote interdisciplinarity, with many attributes that would be commonly considered to promote interdisciplinarity, such as students drawn from multiple disciplines, instructors with different disciplinary perspectives, and assignments designed to promote collaboration across disciplines, yields gains in common measures of student interdisciplinarity.

6.6.1 Limitations and Future Work

The sample size for surveys of students in the course was 14, while the sample size for the coded assignments was 11 students. Though these students were determined to be similar to the general population within each of their respective departments, the sample size is still low. Determining if the findings from this single classroom of students hold true within classes with larger numbers of students as well as in different interdisciplinary classes is necessary to show if this approach for assessing interdisciplinary learning is appropriate in other contexts. However, this study does offer a preliminary look at the impact of a graduate elective course on interdisciplinary student learning.

Additionally, students in our course were not enrolled in an interdisciplinary program. Enrollment in an interdisciplinary program could impact the baseline interdisciplinarity of students. Students enrolled in the bacterial biofilm course may have taken the course because they were in need of an elective, interested in the particular course content, or because students

were from the research group or department of the instructors. Though we did observe increases in interdisciplinarity, the motivation and interests of the students within the course could impact the degree to which increases in interdisciplinary learning occur. Thus, performing similar research with a population of students enrolled in an interdisciplinary program may be valuable and could show how student motivation to transcend disciplines impacts their interdisciplinary learning.

Other metrics for assessing interdisciplinary learning could be developed. The students in the course may have been more interdisciplinary at the end of the course than the metrics were capable of assessing. For example, the survey instrument that was used was developed to assess interdisciplinary learning in a large population of undergraduate students. The survey may need to be changed further to fully assess interdisciplinary learning at the graduate level or within a smaller population of students.

In terms of assessing fluency, the specific questions that are asked could contribute to the degree of fluency that is evaluated through the coding. Open-ended questions that can be graded correctly with language from multiple disciplines may not be readily available for some interdisciplinary coursework, so other strategies may be necessary for assessing interdisciplinary fluency.

Expanding this study to multiple courses to see if the results from other courses are in agreement with our findings would allow for a more general understanding of the extent to which interdisciplinary courses are successful at creating interdisciplinary learners. Additionally, an investigation of the effect of using different methods to cover course material on interdisciplinary learning such as traditional lectures, commonly accepted methods that aim to

promote interdisciplinarity, or newly developed methods for interdisciplinary learning would be an excellent expansion of this study. Perhaps course instructors from multiple disciplines, bringing in external speakers or having project presentations, or some other component of the education experience is the most important aspect of interdisciplinary learning within the class we studied. Controlling the different elements within a course that is taught routinely or studying different courses that are taught using different techniques may yield an understanding of which components are critical for informing interdisciplinary learning. Furthermore, there is space to investigate differences between student learning in interdisciplinary courses and non-interdisciplinary courses with students from a variety of different majors.

This work served as the initial step for assessing interdisciplinary learning within graduate elective coursework. This strategy for measuring interdisciplinary learning could be easily translated to other common components of interdisciplinary programs, such as seminars, retreats, or workshops as well.

6.6.2 Implications

This research shows that a course with a student population from a variety of backgrounds, two course instructors, external speakers, and oral project presentations was able to increase interdisciplinary student learning. These elements specifically increased students ability to recognize kinds of evidence other fields rely on and identify the kinds of knowledge that are distinctive to different fields. These increases in recognizing disciplinary perspectives may have been related to the diversity of the students within the course, the different disciplines of the course instructors or the external speakers from different fields. The increases in teamwork skills could have been due to some students working in teams for their group projects or the relationship of the course instructors who frequently used examples from research that was

conducted collaboratively between the instructors. Fluency may have been increased due to both the content taught in the course as well as the questions asked by other students within the class with different backgrounds. Thus, the interdisciplinary elements of the course may have impacted the specific increases in interdisciplinarity that were observed, so these elements could be used to increase recognition of disciplinary perspectives, teamwork skills, and interdisciplinary fluency.

There are implications for improving the course related to the two categories that didn't change. To increase the number of opportunities for student reflection on interdisciplinary learning during the course, the instructors could add course content that is related to problem solving in situations that are at disciplinary boundaries. This would allow students more opportunities to stop and think about where they may be going wrong or reflect on areas where they may be missing something. Additionally, the instructors could be more intentional about including opportunities to enhance interdisciplinary skills. Specifically, instructors could have included readings that emphasized microbiological or engineering approaches to familiarize students with reading about topics outside of their field. Assignments where students were specifically told to integrate ideas from other fields and synthesize the information from both fields may have resulted in improvement in this interdisciplinary skill; a similar approach for creating opportunities for students to integrate ideas from multiple fields was taken in an interdisciplinary nanotechnology course[13]. Beyond these suggestions, achieving increases in student reflection and interdisciplinary skills may require non-course methods or longer time horizons.

6.7 Conclusions

This study found that increases in student interdisciplinary learning occurred in a graduate elective designed to promote interdisciplinarity, particularly in learning outcomes related to recognizing disciplinary perspectives and teamwork skills. Additionally, fluency increased across disciplinary boundaries during a single semester interdisciplinary elective course on bacterial biofilms. These increases in interdisciplinarity were measured using a mixed-methods approach including surveys and coding of language within open-ended assignments. This study served as a pilot study for this mixed-methods technique for assessing interdisciplinarity in graduate coursework. We hope that this work will be used as a basis for studying other interdisciplinary curricular components in the future.

6.8 References

(1) NSF Advanced Funding Search. Retrieved December 26, 2013 from http://www.nsf.gov/funding/advanced_funding_search.jsp. **2013**.

(2) Borrego, M.; Cutler, S. *Journal of Engineering Education* **2010**, *99*, 355-369.

(3) Clough, G. W. *National Academy of Engineering, Washington, DC* **2004**.

(4) Carney, J.; Neishi, K. *Abt Associates* **2010**.

(5) McNair, L. D.; Newswander, C.; Boden, D.; Borrego, M. *Journal of Engineering Education* **2011**, *100*, 374-396.

(6) Mansilla, V. B. *Change: The Magazine of Higher Learning* **2005**, *37*, 14-21.

(7) Borrego, M.; Newswander, L. K. *The Review of Higher Education* **2010**, *34*, 61-84.

(8) Lattuca, L. R.; Trautvetter, L. C.; Codd, S.; Knight, D. B. *Proceedings of the 118th Annual Conference of the American Society for Engineering Education, Vancouver, BC, Canada* **2011**.

(9) Schaffer, S. P.; Chen, X.; Zhu, X.; Oakes, W. C. *Journal of Engineering Education* **2012**, *101*, 82-94.

(10) Coso, A. E.; Bailey, R. **2011**, *American Society for Engineering Education*.

(11) Newswander, L. K.; Borrego, M. *Higher Education* **2009**, *58*, 551-562.

(12) Anthony, L. J.; Palius, M. F.; Maher, C. A.; Moghe, P. V. *Journal of Engineering Education* **2007**, *96*, 141-156.

(13) Hersam, M. C.; Luna, M.; Light, G. *Journal of Engineering Education* **2004**, *93*, 49-57.

(14) Flaherty, J.; von Massow, M. *Transformative Dialogues: Teaching & Learning Journal* **2013**, *6*.

(15) Team, R. D. C. **2011**.

(16) Pinheiro, J.; Bates, D.; DebRoy, S.; Sarkar, D.; Team, R. C. **2013**.

(17) Hsieh, H.-F.; Shannon, S. E. *Qualitative health research* **2005**, *15*, 1277-1288.

(18) Strauss, A.; Corbin, J. M. *Basics of qualitative research: Techniques and procedures for developing grounded theory*; Thousand Oaks: SAGE Publications, Inc.: USA, 1998.

(19) Babbie, E. *The basics of social research*; Wadsworth, Cengage Learning: Belmont, 2011.

(20) Bishop, B. A.; Anderson, C. W. *Journal of research in science teaching* **1990**, *27*, 415-427.

(21) Boeije, H. *Quality and quantity* **2002**, *36*, 391-409.

Chapter 7

Conclusions and Future Work

The overall goal of this dissertation was to determine the microstructural behavior of *S. epidermidis* biofilms in unstressed and stressed growth environments and apply this knowledge to investigate the role of self-assembly in determining biofilm mechanics, the structural changes that occur in multispecies *Staphylococcal* biofilms, and the effectiveness of label-free methods for imaging *S. epidermidis* biofilm microstructure.

In Chapter 2, we presented the effect of environmental stressors of NaCl and sub-lethal vancomycin on biofilm microstructure within flow cell grown biofilms. In unstressed and stressed growth environments, we found that biofilms achieved heterogeneous microstructures. In unstressed biofilms, bacteria formed low, medium and high cellular density biofilms, while in stressed conditions only low and medium density biofilms are formed. High cellular density bacterial biofilms have densely-packed, disordered microstructures. Low cellular density biofilms have open, tenuous structures. All biofilms contain clustering on length scales < 1 μm, which is a residual effect from cell division.

This work has been used to inform the development of a model of biofilm mechanics and fracture in fluid flow [1]. Additionally, it provided a metric for enhancing the understanding of

polysaccharide behavior [2]. This work could be further extended to investigate the microstructure of similar bacterial species, such as *S. aureus*, in various growth environments to determine if these findings hold true in other species of bacteria. Variations in microstructure with growth environment could also be probed in communities of rod-shaped bacteria, such as *Pseudomonas aeruginosa* or *Bacillus subtilis*.

In Chapter 3, we used the work on *S. epidermidis* biofilm microstructure from Chapter 2 to inform the development of bacterial-chitosan constructs with high- and low-density microstructures similar to those of naturally occurring *S. epidermidis* bacterial biofilms and mechanical properties that matched those of *S. epidermidis* biofilms. The construct mechanics matched natural biofilm mechanics at pH > 7, but were mobile at pH < 7. Chitosan is unstable at pH > 7. We compared the pH instability of chitosan with that of *S. epidermidis* biofilm matrix materials. Matrix materials were unstable at pH < 7. Based on the reverse behavior of these polysaccharides, we predicted that naturally occurring biofilms would become more mobile at pH > 7. We found that the material properties *S. epidermidis* biofilms softened after increasing the pH > 7. We applied this understanding to *S. aureus* biofilms and found that at pH > 7, *S. aureus* biofilms also softened.

Polysaccharide behavior in growth media should be modeled to determine the instability behavior of the chitosan and matrix materials in these various pH conditions. Computational modeling of the polysaccharide may reveal the mechanism of this instability. Additionally, it would be interesting to investigate the dependence of biofilm microstructure and mechanical behavior on natural pH gradients within a biofilm. To probe this a pH indicator could be used to identify regions of various pH values and then the microstructure and mechanics could be investigated using CLSM coupled with image processing in regions with different pH values.

In Chapter 4, we extended our understanding of *S. epidermidis* microstructure through investigating the structure of *S. epidermidis* and *S. aureus* in multispecies biofilms grown in various environmental conditions. We found that *S. aureus* dominates growth in multispecies biofilms grown in unstressed growth conditions of 37°C and pH 7. *S. aureus* also dominated growth high pH (8 and 9) as well as at high temperature (45°C). *S. epidermidis* biofilms dominated growth at low pH (5) and low concentrations of vancomycin (1.0 μg/mL).

This work could be furthered through investigating multispecies growth on different substrate materials. It has been found that *S. aureus* more readily colonizes metal surfaces and *S. epidermidis* more readily colonizes polymer surfaces [3]. Thus, it would be interesting to see if this behavior would shift when a second species of bacteria is present. Also, additional species of bacteria could be added to the multispecies community to see how the structural behavior of the multispecies community shifts. One could also add an additional virulent pathogen or a species that could be used as a probiotic treatment method, such as *Lactobacillus acidophilus* as suggested in [4].

In Chapter 5, we considered the label-free imaging of *S. epidermidis* biofilms using confocal Raman microscopy. We found that biofilm thickness impacted the ability to map cellular level structures of the bacteria using the chemical spectra of their biomass. This work could be extended by determining if thin samples are required for probing label-free cellular microstructure of other bacterial species, particularly species of bacteria that are electrochemically active, such as *Geobater,* since Cyt *c*—a ubiquitous component of extracellular electron transfer reactions in these bacteria—has a distinct and strong Raman signal[5]. One could also look at variations in the initial development of biofilms using confocal Raman microscopy, since biofilms in the initial stages of development are thin.

Finally, in Chapter 6 we used a course on bacterial biofilms to assess interdisciplinary learning within graduate students from chemical engineering, civil and environmental engineering, and microbiology and immunology. We found that students increased their self-perception of learning outcomes related to recognizing disciplinary perspectives and teamwork skills over the duration of a semester long course. Student interdisciplinary fluency also increased from the beginning to the end of the semester. We did not find significant changes in the areas of interdisciplinary skills or reflective behavior. This work served as a pilot study for assessing interdisciplinary learning in a graduate elective course. This work could be furthered though applying this method of assessing interdisciplinary learning to other interdisciplinary coursework or other programming intended to promote interdisciplinary learning such as seminars or workshops.

Overall, this dissertation has introduced a colloidal view of biofilm microstructure to advance the understanding of *Staphylococcal* biofilm growth in unstressed and stressed growth environments. Ultimately, this work will aid in the understanding of the origins of the mechanical properties of biofilms. This work can also be used to develop biofilm control strategies that could be used in clinical treatments of biofilms, or to create models of biofilm for understanding fundamental behaviors of biofilm mechanics and disassembly.

7.1 References

(1) Hammond, J. F.; Stewart, E. J.; Younger, J. G.; Solomon, M. J.; Bortz, D. M. *CMES: Computer Modeling in Engineering & Sciences* **2014**, *98*, 295-340.

(2) Ganesan, M.; Stewart, E. J.; Szafranski, J.; Satorius, A. E.; Younger, J. G.; Solomon, M. J. *Biomacromolecules* **2013**, *14*, 1474-1481.

(3) Barth, E.; Myrvik, Q. M.; Wagner, W.; Gristina, A. G. *Biomaterials* **1989**, *10*, 325-328.

(4) Vuotto, C.; Longo, F.; Donelli, G. *International journal of oral science* **2014**,

(5) Virdis, B.; Harnisch, F.; Batstone, D. J.; Rabaey, K.; Donose, B. C. *Energy & Environmental Science* **2012**, *5*, 7017-7024.